THE RADIO AND ELECTRONIC ENGINEER

The Journal of the Institution of Electronic and Radio Engineers

FOUNDED 1925 INCORPORATED BY ROYAL CHARTER 1961

"To promote the advancement of radio, electronics and kindred subjects by the exchange of information in these branches of engineering."

VOLUME 31 MARCH 1966 NUMBER 3

WHAT DOES R & D COST?

GOVERNMENTS as well as industry are continuously confronted with the problem of assessing the 'right' or 'optimum' level of resources which could be allocated to research and development (R & D), whether it be for individual projects or for entire sectors of the economy, or for the national activities as a whole. Statistics of the 'costs', including manpower, of R & D are thus essential.

Of considerable interest, therefore, is the experimental international comparison of research expenditures and manpower in the leading industrial countries of the world entitled 'The Research and Development Effort in Western Europe, North America and the Soviet Union'.* This was presented in January of this year at a meeting in Paris of Ministers responsible for science and technology in the Member countries of the Organization for Economic Co-operation and Development.

The report was produced by two members of the National Institute of Economic and Social Research in London and, taking the year 1962, it analyses three main areas roughly comparable in population and resources: the United States, the Soviet Union and Western Europe (in this instance Belgium, France, Germany, the Netherlands and the United Kingdom). It is pointed out that, considered in terms of total manpower employed, well over one million people are now engaged in R & D work in the U.S.A. and the U.S.S.R., while in Western Europe the figure is over half a million.

The simplest way of making an international comparison is to express each country's gross national expenditure on R & D in terms of a selected currency, such as U.S. dollars. On this basis, the U.S.A. spends about four times as much on research and development as Western Europe. Such a comparison does not, however, take into account the variation between countries in the cost of research inputs such as wages of scientists or prices of equipment, and a 'research exchange rate' has been calculated which indicates that total expenditure on research and development in the United States is only about two to three times that of Western Europe, while the Soviet expenditures were somewhat below that of the United States. The U.S.A. spends about one and half times as much as Western Europe on civil R & D, but four times as much on space and military research. (Soviet data are not available.)

Another way of comparing research expenditures is to relate them to Gross National Product in national currency. Although such comparisons may be affected by the relative cost of research within countries, they give an indication of how much a country can afford to spend on research and development, taking into account other claims on national resources. Thus the ratios were 3·1% for the United States and 1·6% for Western Europe. Within the latter group the ratio varied from 2·2% for the United Kingdom to 1·0% for Belgium.

The report then discusses manpower allocated to research and development and states that, related to total population, the figures are U.S.A. 6·2%, Western Europe 2·9% and U.S.S.R. 4·7–6·7%. Some interesting facts are also given regarding the 'technological balance of payments'—technical know-how, licences and patents—as an indication of the results of research.

The authors stress in their conclusions that the existence of a difference in scale between the resources devoted to research in Western Europe and in the U.S.A. (or U.S.S.R.) does not necessarily mean that the difference should be reduced or removed: this is a matter for science policy in each country or area. The report suggests however that, although difficult, a realizable long-term objective for civil research for some or all of the Western European countries would be to devote an amount of real resources *per capita* to R & D activity which is comparable with that of the U.S.A. But in the field of military and space research where the 'gap' is of the order of 4 to 1 or more, this is a far more difficult objective, even if the present ambitious plans for educational expansion are realized.

* An O.E.C.D. publication obtainable for H.M. Stationery Office, price 15s.

INSTITUTION NOTICES

Proposed Institution Section in Israel

At a meeting of members of the Institution in Israel held on 19th February and attended by the Secretary of the Institution, Mr. Graham D. Clifford, it was unanimously agreed to petition Council for permission to form a Section in Israel. The petition will be placed before the Council at its next meeting on 19th May; initially meetings will be held in Tel-Aviv.

Further information about the activities of the proposed section may be obtained from Mr. R. Danziger, M.I.E.R.E., P.O. Box 21045, Tel-Aviv.

I.E.R.E. Secretary Honoured

During his stay in Israel at the beginning of his tour of the Overseas Divisions and Sections of the Institution Mr. Graham D. Clifford was elected an Honorary Member of the Association of Engineers and Architects in Israel.

The Association comprises engineers of all disciplines and publishes a bi-monthly *Journal* as well as a brief digest of technical news, 'Technical Progress in Israel' which is sent monthly to overseas members. The Director General of the Association is Mr. E. Pelles, C.E., and its headquarters is at Engineers' House, 200 Dizengoff Street, Tel-Aviv.

New Zealand Electronics Conference

'Electronics in Action' is the theme for New Zealand's first National Electronics Conference, sponsored jointly by the New Zealand Electronics Institute Inc., and the New Zealand Section of the Institution of Electronic and Radio Engineers. It is to be held at the University of Auckland from 17th to 20th August, 1966. This will be the first opportunity for New Zealand engineers, scientists and technical personnel to attend a conference solely devoted to electronics.

The Conference will cover a wide range of topics under the following major sections; data handling; modern communications (radio and television); research electronics; industrial electronics; medical electronics; electronics in aviation and meteorology; nucleonics; electronics education. Additional activities will include a large scale trade exhibition, excursions, technical film showings and social events.

Enrolment forms and further information may be obtained on application to the Secretary, National Electronics Conference, P.O. Box 3325, Auckland, C.1 or to the Secretary of the Auckland Section of the I.E.R.E., Mr. C. W. Salmon, P.O. Box 3381, C.P.O., Auckland.

Presentation of Bose Premium

The Institution's Sir J. C. Bose Premium for 1964 was awarded to Dr. Y. N. Bapat, for his paper on 'Transistor Current-switching Circuits' which was published in the May 1964 issue of *The Radio and Electronic Engineer*. This Premium is awarded annually for the most outstanding paper by an Indian scientist or engineer published in the *Journal*.

Dr. Bapat, who is at the Indian Institute for Technology in Bombay, was not able to come to London to receive his prize from the President at the Annual General Meeting in December last. The Bombay Section of the Indian Division of the Institution, therefore, arranged for Dr. Bapat to receive his Premium at a meeting on 16th February, which was attended by Mr. G. D. Clifford, Secretary of the Institution, in the course of his tour of the Institution's overseas Divisions and Sections.

After Mr. Clifford had made the presentation and given a short address two papers were read: by Dr. Bapat on Digital Computers, and by Dr. B. V. Rao on Masers.

Achievement Award for Instrument Design

In order to recognize an outstanding achievement in instrumentation, particularly one which has been the result of an individual effort rather than that of a team or large organization, The Worshipful Company of Scientific Instrument Makers have instituted an annual Achievement Award. The Award for 1965 has been won by Professor Leslie Kay, Ph.D., C. Eng., (Member) for his Ultrasonic Blind Aid.

This Aid, developed by Dr. Kay whilst he was at the University of Birmingham, was described in a paper 'Auditory perception and its relation to ultrasonic blind guidance aids' which was published in the Institution's *Journal* in October 1962; the paper was awarded the Dr. V. K. Zworykin Premium for 1962 as the outstanding contribution of the year on medical and biological electronics. Professor Kay has recently been appointed to the Chair of Electrical Engineering at the University of Christchurch, New Zealand; he has been for the past four years Head of the Department of Electrical Engineering at Lanchester College of Technology, Coventry.

The Institution has been invited by The Worshipful Company to put forward suggestions for the Achievement Award for the current year. The Council will welcome comments by members which will assist it in reaching a decision on the names to be put forward in June, and these should reach the Secretary not later than 30th April.

U.D.C. 621.372.56: 621.382.23

Wideband Coaxial Variable Attenuators using p-i-n Diodes

By

J. R. JAMES, B.Sc., C.Eng.
(*Associate Member*) †

AND

Professor M. H. N. POTOK,
B.Sc., Ph.D., M.A., C.Eng.
(*Associate Member*) †

Reprinted from the Proceedings of the Joint I.E.R.E.–I.E.E. Symposium on 'Microwave Applications of Semiconductors' held in London from 30th June to 2nd July 1965.

Summary: Using a conventional equivalent circuit for a p–i–n diode, a computer program has been written which permits the compilation of data for use in designing a coaxial wide band variable attenuator.

Procedures are outlined leading to design of voltage controlled attenuators whose performance over an octave within 1 to 10 Gc/s compares very favourably with the best commercially available passive attenuators.

The procedures have been applied to specific cases and attenuators constructed. Their performance follows closely design data.

The compiled data can also be used to design strip line attenuators and levellers.

List of Symbols

n	number of p–i–n diodes
v	an integer $1 \leqslant v \leqslant n$
R_0	characteristic impedance of lossless transmission line
l_v	length of transmission line preceding vth p–i–n diode
f	frequency of wave in transmission line
y, z	real numbers $\geqslant 0$
f_0	normalizing frequency
$x = f/f_0$	
$\theta_v = (\pi/8)x[y+(v-1)z]$	
θ_v/l_v	phase constant for lossless line
L_p	p–i–n-diode post inductance
L_c	p–i–n-diode inductance due to capsule, etc.
$L = L_p+L_c$	
C	total capacitance appearing across p–i–n-diode junction
$X_c = (2\pi f_0 C R_0)^{-1}$	
$X_L = (2\pi f_0 L/R_0)$	
R_v	junction resistance of vth p–i–n diode
g'_v	conductance normalized by R_0, of combined diode and post network (L, C, R_v)
b_v	susceptance normalized by R_0, of combined diode and post network (L, C, R_v)
$g_v = (R_0/R_v)$	
$g = (R_0/R)$	when all p–i–n-diode junction resistances R_v are equal
f_R^v	frequency at which L, C, R_v are in series resonance
R'	resistance of compensation p–i–n diode in leveller
Y	an admittance
α	insertion loss
v.s.w.r.	voltage standing wave ratio
(A)	the A matrix (2×2) of a two-port network
(A_v)	the A matrix of the vth network
(B_v)	real part of (A_v)
(C_v)	imaginary part of (A_v)
a_{pq}	element in pth row and qth column of (A)
(ζ_i)	a 2×2 matrix, $i = 0, 1, 2, \ldots, n$.
$F_n(g)$	a polynomial of degree $2(n-1)$ in g
$(\zeta_i)_{pq}$	element in the pth row and qth column of (ζ_i)
Z_{in}	input impedance of attenuator, normalized by R_0

† Electronics Branch, Royal Military College of Science, Shrivenham, Swindon, Wiltshire.

1. Introduction

p–i–n diodes are now extensively used in levellers and narrow band switching devices but their application to wide-band high grade (i.e. low v.s.w.r. and flat attenuation characteristics) variable attenuators does not easily follow. This paper is concerned mainly with these latter applications. A p–i–n-diode attenuator is quite simple to construct in practice but the optimizing of the v.s.w.r. and attenuating

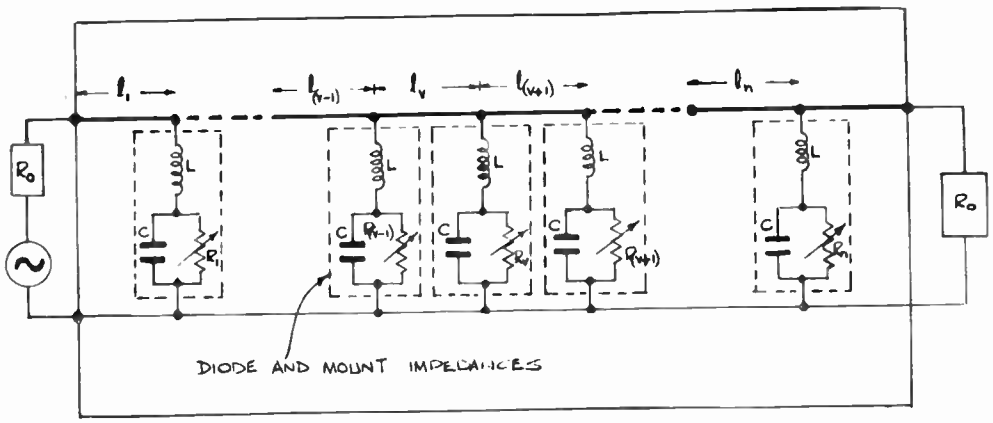

Fig. 1. Usual equivalent circuit for n p–i–n diodes placed across a matched transmission line. Each R_v is controlled by external bias.

characteristics over a wide band is very difficult because of the large number of possible variables and the tediousness of the measurements. Obviously some design criterion is necessary and a suitable method of analysis is required.

Synthesis techniques do not appear very suitable because of the presence of the lossy diodes and also because the resistances have to vary between wide limits, if the attenuator is to be variable. One of the few contributions to the subject[1] uses the method of image impedance together with certain approximations as a basis for analysis. While the nature of the problem is well illustrated, the design curves given are very limited and not well substantiated by measurements on an actual attenuator. (The authors point out that this disparity is mainly due to the wide tolerances on the diode parameters.) The image approach, being based on an infinite number of identical cascaded sections becomes progressively more approximate for small numbers of diodes and becomes difficult to apply when the important parasitic reactances of the diode mount are considered.

Bearing in mind the above requirements and difficulties, it was decided that a computer approach was justified provided that any simple but useful expressions, which would result from an analysis, were not overlooked. The aim of this paper is therefore to produce sufficient design data for the most likely practical cases together with expressions which serve to illuminate the problem still further.

The order of presentation in this paper will be as follows: First a computer program which is based upon an equivalent circuit will be briefly described. Then using actual results it will be shown that this equivalent circuit is adequate for most purposes. Next, this program will be used to explore the various methods of optimizing the solution. Finally a solution based on results obtained from the computer will be tried out and examined in practice.

2. The Computer Program

2.1. *Equivalent Circuit of p–i–n Diode*

The usual [1,2,3] equivalent circuit for n p–i–n diodes placed across a transmission line is as in Fig. 1, where R_v is the resistance of the vth diode and l_v is the length of transmission line preceding the vth diode. The diode junction capacitance, capsule capacitance and any stray capacitance are represented by C which is in shunt with the diode resistance. The connection of the diode junction between the inner and outer conductor of the line involves some type of capsule and/or post which is assumed to be predominantly inductive and represented by a series inductance L. This simple equivalent circuit may be inadequate over a wide band for two reasons: Firstly some terms have been ignored, and secondly L, C and R_v may vary over the frequency band if it is wide enough. The validity of this simple equivalent circuit is again discussed in Section 2.3.

2.2. *Details of Computer Program*

A program has been written for the Elliot 803 computer using Autocode, to solve the following problem:— Print out values of v.s.w.r., insertion loss and input impedance for a coaxial attenuator over a given frequency range when it is inserted in a matched coaxial system. The attenuator consists of n p–i–n diodes placed across a lossless coaxial transmission line at given distances from one another. The equivalent circuit of the diode assembly is as described in Section 2.1 and a complete equivalent circuit for the attenuator in the matched line is given in Fig. 1. Any value of L and C (0 and ∞ may be excluded) can be used and the diode resistances, which can have any value (e.g. each diode resistance can be altered independently of the others) can be varied in step with one another to simulate the effect of varying the bias current through the diodes. The distances between the diodes can also be staggered in a given manner. Fuller details of the program are given in Appendix 1.

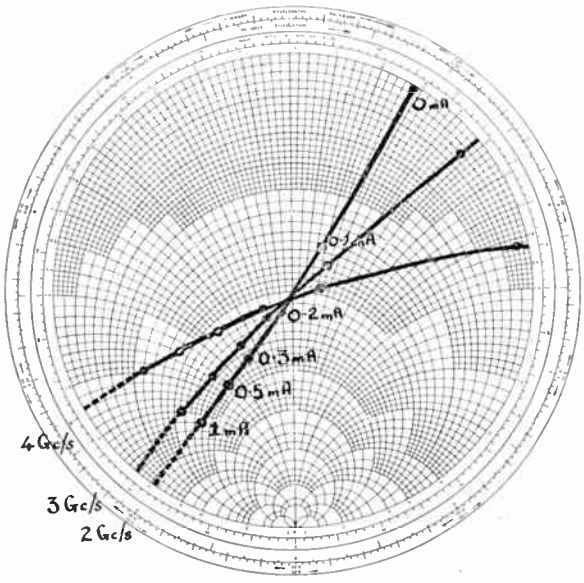

Fig. 2(a). Admittance measurements on MA4571C p–i–n diode.

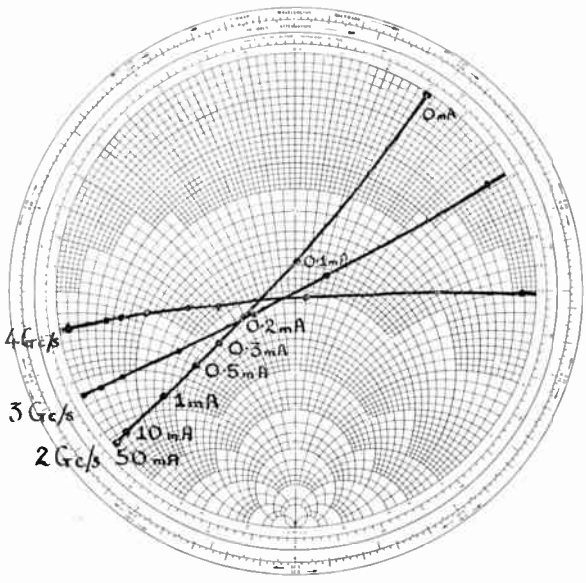

(b). Admittance measurements on MA4571C p–i–n diode with post.

2.3. *Comparison of Computer Solution and Practical Case*

Three MA4571C p–i–n diodes were measured and used in a three-diode coaxial attenuator. An admittance plot of one diode at 2, 3 and 4 Gc/s is shown in Fig. 2(a) and a repeat of the measurement with a series inductance in Fig. 2(b). This inductance is in the form of small rod and is identical in dimensions to the diode post used in the attenuator (Fig. 5). These measurements were carried out using a General Radio slotted line and the jig is shown in Fig. 3, where the short circuit reference plane is taken as the plunger surface held against the inner conductor of the 50-ohm line, in the absence of the diode or diode and post. As the electrical length of this unknown impedance is fairly small compared with a quarter wavelength at the frequency of measurement, this method was considered to be reasonably accurate. These measurements were repeated for the other two diodes and the results are shown in Table 1 and Fig. 4. Any variations in C or L were within the error of measurement and were not observed, but there was clear variation of diode

Table 1

Measured parameters for MA4571C p–i–n diode

Parameter	Measured	Manufacturer's data
Capacitance C	0·44 pF	0·42 pF
Inductance L_c due to capsule	1·2 nH	About 1·0 nH
Inductance L_p of post	0·48 nH	
Total inductance $L = L_p + L_c$	1·68 nH	

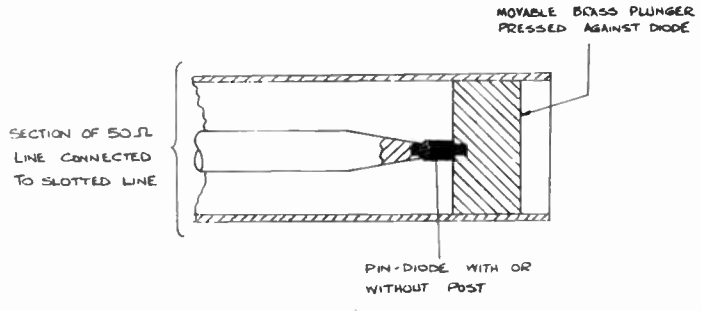

Fig. 3. Measurement jig for p–i–n diode or p–i–n diode with post.

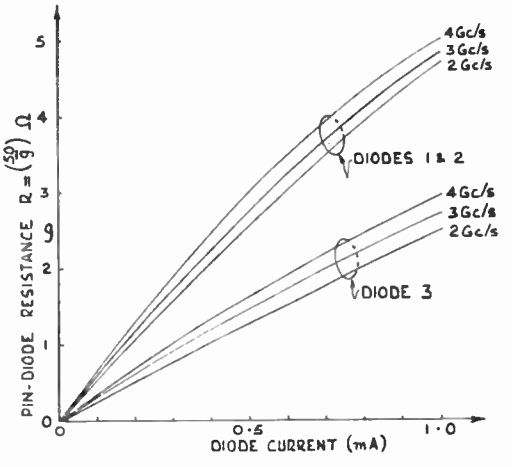

Fig. 4. Measured values of resistance R plotted against frequency and bias current for MA4571C p–i–n diode.

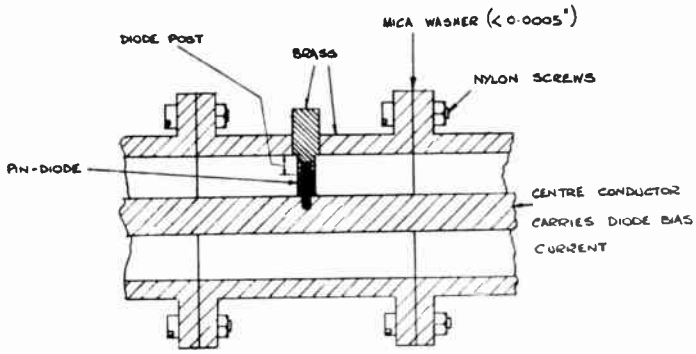

Fig. 5. p–i–n diode and mounting post in 50-ohm coaxial line with mica insulating washer.

resistance R with frequency (Fig. 4). The capacitance C and inductance L_c appear to be dominated by the capsule and as such are fairly constant from diode to diode. The likely tolerance between diode resistances is also seen from Fig. 4 and is considerable.

It is a common practice[1, 2, 3] to bias a p–i–n diode, by passing the bias current through a thinly insulated plunger which passes through a hole in the outer conductor to make contact with the diode. The insulated plunger acts as a low impedance line which can transform a high impedance at the bias end into a very low impedance at the diode end. The diode can therefore be effectively shorted to the outer conductor at high frequency. (The diode post inductance L_p must still be accounted for.) However, this plunger method of biasing needs applying with care over a wide band because of possible resonances in the wires at the bias end of the plunger, and therefore the following method was adopted: The outer conductor of a 50-ohm rigid brass coaxial line was interrupted in four places by mica washers. Each washer produced a capacitance of about 200 pF, and measurements of v.s.w.r. showed that over the band 2 to 4 Gc/s, the outer acted as if continuous. Each of the three diodes could now be mounted in one of the d.c. isolated sections as shown in Fig. 5. The diode return current was taken from the centre conductor via a narrow band tuning stub. In practice a wide-band d.c. return may have to be included in the attenuator. Recent literature[4] suggests that the design of a d.c. return with excellent properties will not present any problem. The spacing between the diodes was a quarter wavelength at 3 Gc/s and for inductance purposes, the diode post (inductance L_p in Table 1) is taken as that length of rod protruding into the air space of the line.

Using the data from Fig. 4, the bias on each diode was set so that each diode resistance was equal and of a desired value. The measurements were now per-

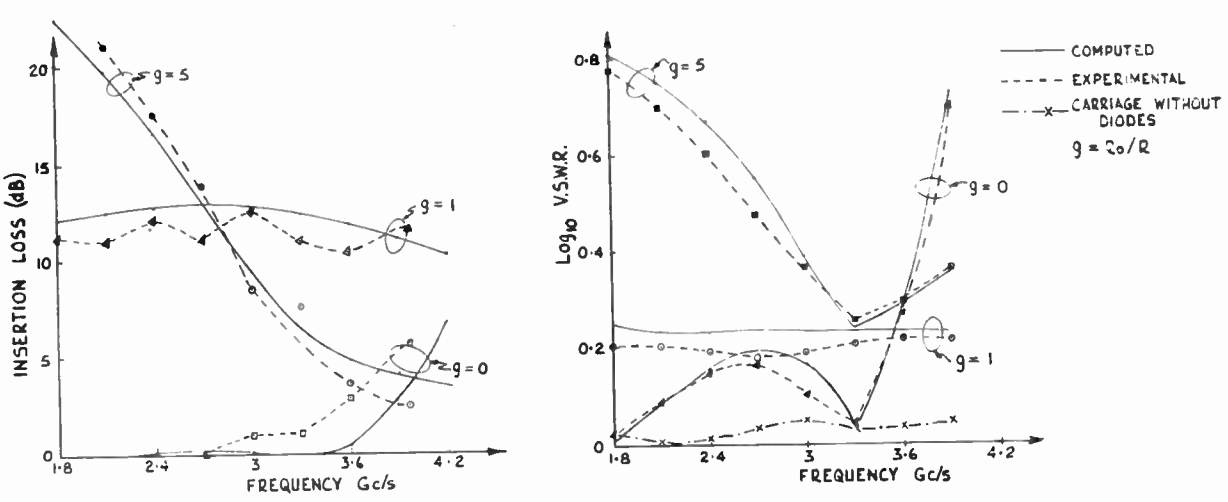

Fig. 6. Computed and measured results for an attenuator with three MA4571C p–i–n diodes.

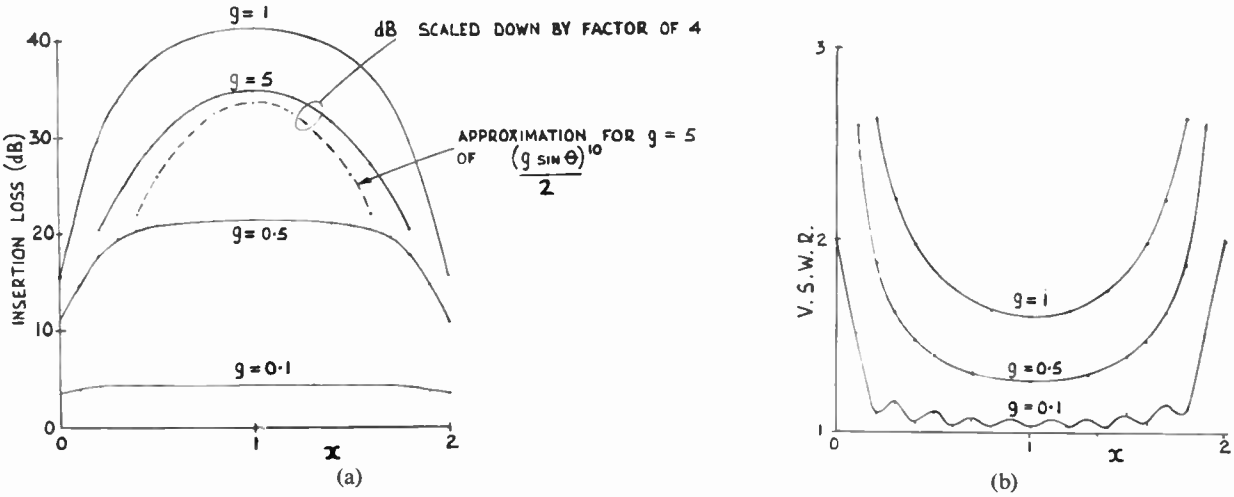

Fig. 7. Computed curves for a ten-diode attenuator with L and C zero.
($g = R_0/R_1$, $x = f/f_0$, $z = 0$, $y = 4$, and all diodes have equal resistance.)

formed and are shown in Figs. 6(a) and 6(b). These results compare very well with those computed assuming the simple equivalent circuit and the value of L, C and R as measured. The sources of error in the measurement are as follows: The v.s.w.r. of the line without diodes ($\sim$1·12) includes the imperfections of the General Radio terminations, a blocking capacitor and the 50-ohms load. The insertion loss was measured at low level (to avoid any non-linearity in diodes) on a Hewlett Packard power meter and was difficult to read. The small variation of p–i–n diode resistance R over the pass band did not make itself apparent, being swamped by the measurement error.

It is concluded that the simple equivalent circuit given in Fig. 1 is adequate in the practical case considered. Since the L and C values used in this case are not unrealistic of many other cases it is thought that this circuit and the program using it can be applied to these other situations with reasonable confidence.

3. Design Data for Wide-band Attenuator

3.1. *Case when both L and C are Zero*

Since the resistance R of a p–i–n diode is not infinite even when biased at zero current, a p–i–n diode attenuator will have a minimum insertion loss. This can be calculated from (9) in Appendix 2.

As the resistance of each diode decreases, the insertion loss increases and the v.s.w.r. deteriorates as shown by Figs. 7(a) and 7(b). The approximation for the insertion loss given in eqn. (8), Appendix 2, is also shown in Fig. 7(a).

Methods of maintaining the flatness of insertion loss and a good v.s.w.r. over a wide band when the diode resistances are all equal and very small, will now be considered. Equations (10) and (11) of Appendix 2 suggest that staggering line lengths or resistance values will not avoid the insertion loss resembling in form the functions

$$\prod_{v=1}^{n} \sin_v \theta \qquad \text{or} \qquad \sin^n \theta$$

A detailed examination using the computer solution has been carried out and is in complete agreement with this approximation. An example of the effect of staggering the line lengths when the diode resistances are equal and small, is given in Figs. 8(a) and 8(b). This illustrates that no improvement in bandwidth is obtained. The approximation of eqn. (10), Appendix 2, is also shown.

The staggering of line lengths or diode resistances is therefore considered to be of little use in improving the v.s.w.r. and insertion loss characteristics of an attenuator when all the diode resistances are very small.

The case of all, or some, of the diodes having a large resistance will now be considered. The effect of staggering line lengths has been investigated and is again considered to be of little advantage. An example when all diode resistances are large and equal is also given in Fig. 8(a).

However, the staggering of diode resistances is advantageous.[1,3] Ripples can be created over the pass-band on the attenuation and v.s.w.r. curves by making the diode resistances dissimilar. This immediately suggested a Chebyshev type response but an examination of the equations in Appendix 3 does not support this expectation since the polynomials involved do not have poles and zeros throughout the pass-band in the usual way. The number of ripples does increase with the number of diodes but no straightforward pattern could be recognized and the search was not

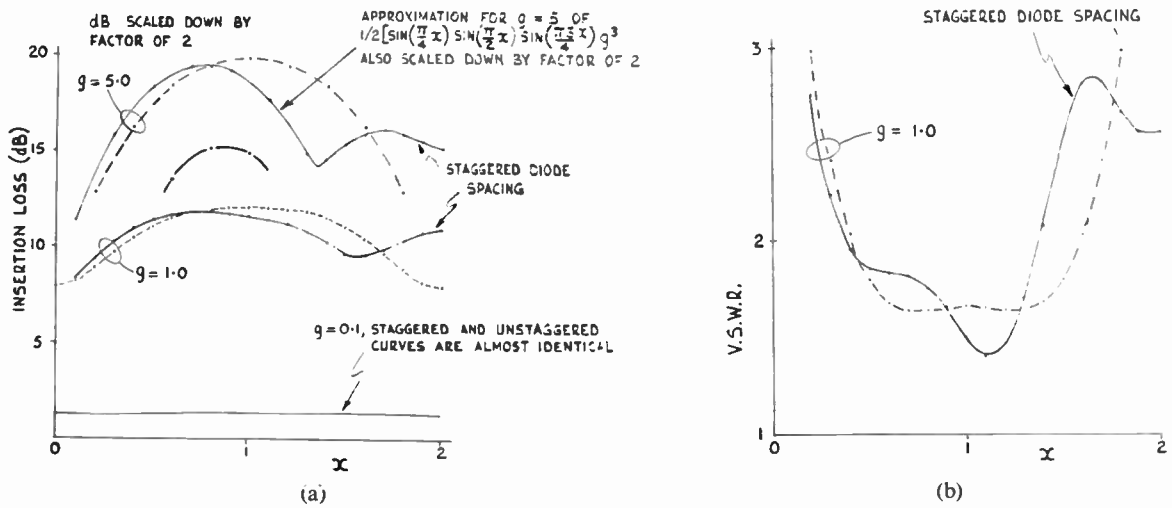

Fig. 8. Performance curves for three-diode attenuator with L and C zero. For no line staggering, $y = 4$, for staggering, $y = 2$, $z = 2$.

continued because the analysis, although already formidable, must in addition embrace the parasitic L and C of the diodes to be of any practical use. These points can be demonstrated by examining the curves for a seven-diode attenuator with and without staggered resistances shown in Fig. 9(a) and (b). The pronounced effect of realistic values of L and C on these curves is also shown. The staggered values used here were arrived at by trial and error but it is possible to calculate the values of R_v so as to obtain a perfect match at centre frequency. There is in fact an infinite variety of solutions (Appendix 4), which may or may not give a good performance throughout the band. No definite rule has been found so far which would lead to a particularly good solution.

Another complication in this problem is that of the power handling capacity of the diodes. If the attenuator is to absorb a considerable amount of power then diodes which carry more bias current will absorb most power and may be overloaded.[5]

With all these likely constraints in mind it seems that a designer may be forced to determine the staggered resistance ratios on a trial and error basis, bearing in mind the obvious requirement that the diode resistances should be large near the ends of the attenuator and progressively smaller towards the middle. No attempt will be made to recommend staggered values because these would be greatly modified by the presence of L and C.

This section is concluded with tables of computed data for 3, 5, 7, 10 and 15 diodes for both L and C zero and no staggering of lines or resistances. Since the values are symmetrical about $x = 1$, only values up to 1 are given in Table 2.

3.2. *Case when L is Zero*

As the diode resistances decrease in value the effect of the shunting capacitance C becomes negligible. But as the resistances increase the response curves are no longer symmetrical about $x = 1$ and the insertion loss and v.s.w.r. becomes more frequency dependent. Computed values for 3, 5, 7, 10 and 15 diodes with four realistic values of capacitance are given in Table 3 for $g = 0$ only. To economize in space, data for other values of g are given elsewhere.[5]

It is seen that for a given capacitance, the usable bandwidth when the diodes have a very high resistance decreases as the number of diodes increase. Staggering diode resistances obviously does not affect this condition because each diode is biased to zero current anyway. Staggering the line lengths has some effect but is of little consequence.

3.3. *Case when C is Zero*

In this case the attenuator characteristics are modified when the diode resistances become small. The necessary modifications to Table 2 are given in Table 4 for four realistic values of inductance and one value of g. For a given value of inductance it is seen that the usable bandwidth is reduced as the number of diodes increases. More complete data are given elsewhere.[5] If the diode resistances are staggered some small improvement in the effect of L is observed.

3.4. *Case when both C and L are Non-zero*

If C and L are small their effect on the attenuator characteristics can be studied separately as in Sections 3.2 and 3.3. If both, or either, of L and C are appreciable, high Q resonances can occur. This property is

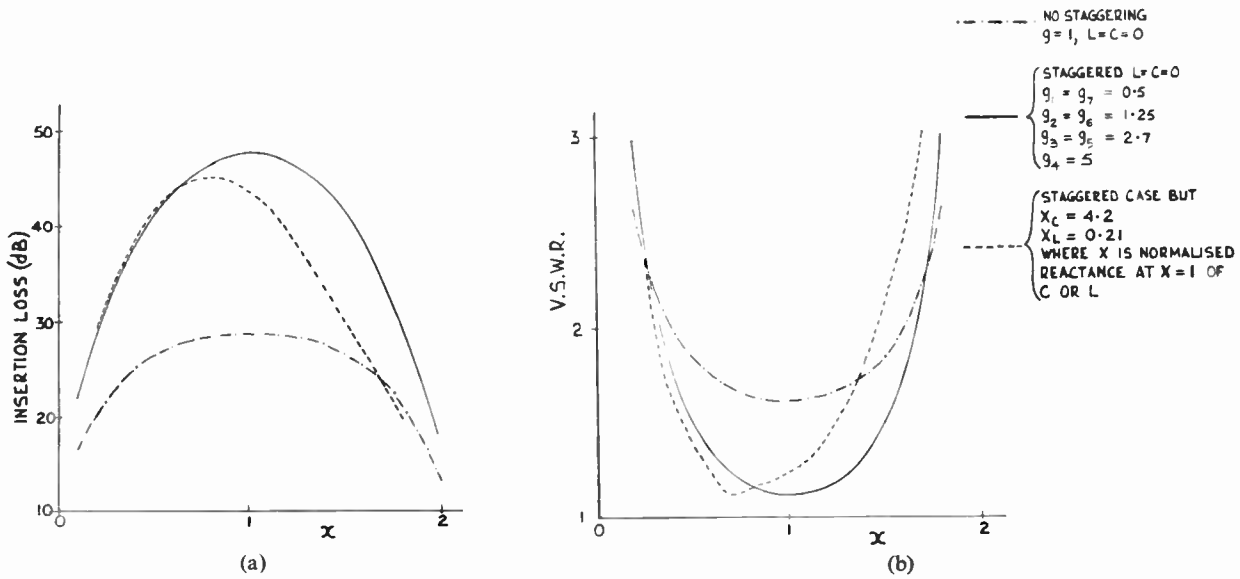

Fig. 9. Curves for seven-diode attenuator showing effects of L and C when diode resistances are staggered.

made use of when a p–i–n diode acts as a narrow band switch in a line, but is considered to be disastrous in a wide band attenuator if resonance occurs when the diode resistance is still large. For any given R_v, L and C, this diode network will resonate at f_R^v where

$$(2\pi f_R^v)^2 = \frac{1}{C}\left[\frac{1}{L} - \frac{1}{CR_v^2}\right]$$

The attenuator dealt with in Section 2.3, whose curves are shown in Fig. 6, exhibits such resonances.

3.5. *Conclusions from Computer Solution*

If the attenuator is free from parasitic L and C it is possible to design a very wide band device. The number of diodes will be dictated by permissible variation in attenuation and standing-wave ratio and by the insertion loss when the attenuator is biased to the off position. Some improvement in performance is possible by staggering the diode resistances. Table 2 contains typical results for unstaggered resistances. (For full information see Ref. 5.)

However, in a practical design it may not be possible to neglect the effects of L and C and the recommended design procedure depends on the minimum values of L and C that can be achieved in the actual case.

Having chosen a type of line and a method of mounting the diodes it is necessary to test for resonance. If resonance is found within the band of interest for any given value of R_v then the chances of producing an attenuator over that band are small.

If no resonance is observed then further steps will depend primarily on the value of C. If C is small then optimum design is likely to result from separating the

Table 2

Insertion loss α (dB) and v.s.w.r. for p-i-n diode attenuator with L and C zero, $y = 4$, $z = 0$, $x = f/f_0$, $g = R_0/R$

No. of Diodes	x	$g = 0.1$ α	V.S.W.R.	$g = 0.5$ α	V.S.W.R.	$g = 1.0$ α	V.S.W.R.	$g = 5.0$ α	V.S.W.R.
3	0	1.22	1.30	4.86	2.50	7.96	4.00	18.6	16.0
	0.1	1.22	1.29	4.95	2.40	8.23	3.66	21.5	9.29
	0.2	1.24	1.26	5.19	2.15	8.90	3.00	25.9	6.84
	0.3	1.25	1.21	5.50	1.86	9.72	2.43	29.6	6.06
	0.4	1.27	1.15	5.81	1.60	10.5	2.04	32.5	5.69
	0.5	1.29	1.09	6.05	1.40	11.1	1.81	34.8	5.48
	0.6	1.30	1.04	6.21	1.27	11.5	1.69	36.6	5.36
	0.7	1.30	1.02	6.28	1.24	11.8	1.64	38.0	5.28
	0.8	1.30	1.06	6.30	1.28	12.0	1.64	38.9	5.23
	0.9	1.30	1.08	6.29	1.34	12.0	1.66	39.5	5.20
	1.0	1.29	1.09	6.29	1.36	12.0	1.67	39.7	5.19
5	0	1.94	1.50	7.04	3.50	10.9	6.00	22.6	26.0
	0.1	1.98	1.44	7.58	2.88	12.3	4.04	32.5	8.76
	0.2	2.06	1.30	8.63	2.05	14.7	2.68	41.6	6.82
	0.3	2.13	1.14	9.51	1.59	16.6	2.19	48.7	6.07
	0.4	2.16	1.03	10.0	1.43	17.9	1.98	54.4	5.70
	0.5	2.16	1.09	10.3	1.42	18.8	1.86	58.9	5.49
	0.6	2.16	1.10	10.4	1.39	19.5	1.76	62.4	5.36
	0.7	2.16	1.07	10.5	1.31	19.9	1.68	65.0	5.28
	0.8	2.17	1.02	10.6	1.27	20.2	1.64	66.8	5.23
	0.9	2.17	1.06	10.6	1.29	20.4	1.63	67.9	5.20
	1.0	2.16	1.08	10.6	1.31	20.4	1.63	68.3	5.19
7	0	2.61	1.70	8.79	4.50	13.1	8.00	25.3	36.0
	0.1	2.74	1.53	10.3	2.86	16.7	3.76	43.6	8.79
	0.2	2.94	1.22	12.3	1.86	20.8	2.62	57.3	6.82
	0.3	3.01	1.06	13.5	1.60	23.5	2.23	67.9	6.07
	0.4	3.01	1.13	14.1	1.51	25.3	2.00	76.3	5.70
	0.5	3.02	1.08	14.4	1.40	26.6	1.84	83.0	5.49
	0.6	3.03	1.04	14.7	1.34	27.5	1.75	88.2	5.36
	0.7	3.03	1.09	14.8	1.33	28.1	1.69	92.1	5.28
	0.8	3.03	1.05	14.9	1.29	28.5	1.65	94.8	5.23
	0.9	3.04	1.04	14.9	1.28	28.7	1.63	96.4	5.20
	1.0	3.03	1.08	14.9	1.29	28.8	1.62	96.9	5.19
10	0	3.52	2.00	10.9	6.00	15.6	11.0	28.3	51.0
	0.1	3.93	1.53	14.7	2.61	23.5	3.62	60.1	8.79
	0.2	4.26	1.11	17.8	1.89	29.7	2.65	80.8	6.82
	0.3	4.29	1.16	19.4	1.63	33.7	2.23	96.7	6.07
	0.4	4.32	1.06	20.2	1.48	36.4	1.99	109	5.70
	0.5	4.32	1.10	20.7	1.41	38.2	1.85	119	5.49
	0.6	4.33	1.04	21.0	1.35	39.5	1.75	127	5.36
	0.7	4.33	1.08	21.2	1.32	40.4	1.69	133	5.28
	0.8	4.34	1.03	21.3	1.29	40.9	1.65	137	5.23
	0.9	4.33	1.07	21.4	1.29	41.2	1.63	139	5.20
	1.0	4.34	1.03	21.4	1.28	41.3	1.62	140	5.19
15	0	4.86	2.50	13.5	8.50	18.6	16.0	31.7	76.0
	0.1	6.06	1.34	22.1	2.56	34.9	3.65	87.7	8.79
	0.2	6.37	1.22	26.9	1.89	44.6	2.65	120	6.82
	0.3	6.46	1.12	29.3	1.63	50.8	2.23	145	6.07
	0.4	6.49	1.07	30.5	1.48	54.8	1.99	164	5.70
	0.5	6.49	1.07	31.2	1.40	57.6	1.85	179	5.49
	0.6	6.50	1.08	31.6	1.35	59.5	1.75	191	5.36
	0.7	6.50	1.06	31.9	1.32	60.8	1.69	200	5.28
	0.8	6.51	1.04	32.0	1.30	61.6	1.65	207	5.23
	0.9	6.51	1.05	32.1	1.28	62.1	1.63	210	5.20
	1.0	6.51	1.06	32.1	1.28	62.2	1.62	211	5.19

Table 3

Insertion loss α (dB) and v.s.w.r. for p-i-n diode attenuator with $L=0$, $y=4$, $z=0$, $x=f/f_0$, $g=R_0/R=0$ and $X_c=1/2\pi f_0 C R_0$

No. of Diodes	x	$X_c=6$ α	V.S.W.R.	$X_c=4$ α	V.S.W.R.	$X_c=2.5$ α	V.S.W.R.	$X_c=1$ α	V.S.W.R.
3	0.1	0.004	1.05	0.008	1.08	0.016	1.12	0.089	1.35
	0.2	0.010	1.09	0.020	1.14	0.046	1.22	0.242	1.61
	0.3	0.014	1.11	0.028	1.17	0.063	1.27	0.278	1.66
	0.4	0.013	1.11	0.024	1.15	0.050	1.24	0.144	1.44
	0.5	0.007	1.07	0.012	1.10	0.018	1.13	0.006	1.07
	0.6	0.002	1.02	0.002	1.02	0.002	1.01	0.108	1.37
	0.7	0.004	1.04	0.008	1.08	0.029	1.17	0.430	1.88
	0.8	0.013	1.11	0.031	1.18	0.091	1.33	0.622	2.15
	0.9	0.025	1.16	0.056	1.25	0.140	1.43	0.378	1.81
	1.0	0.030	1.18	0.061	1.26	0.123	1.40	0.002	1.00
	1.1	0.023	1.15	0.037	1.20	0.043	1.21	1.07	2.75
	1.2	0.007	1.07	0.005	1.06	0.008	1.08	4.12	8.19
	1.3	0.004	1.05	0.024	1.15	0.224	1.57	7.42	20.0
	1.4	0.046	1.22	0.168	1.48	0.845	2.45	10.1	38.6
	1.5	0.158	1.46	0.481	1.95	1.79	3.77	12.0	61.0
	1.6	0.345	1.76	0.926	2.56	2.81	5.44	13.2	80.6
	1.7	0.575	2.08	1.40	3.21	3.65	7.11	13.6	90.0
	1.8	0.793	2.38	1.79	3.76	4.15	8.28	13.4	84.3
	1.9	0.939	2.58	1.98	4.07	4.24	8.50	12.2	64.6
	2.0	0.971	2.62	1.94	4.00	3.88	7.63	10.0	38.0
5	0.1	0.009	1.08	0.016	1.12	0.036	1.20	0.192	1.52
	0.2	0.014	1.11	0.027	1.16	0.059	1.26	0.228	1.58
	0.3	0.007	1.07	0.011	1.09	0.017	1.12	0.007	1.07
	0.4	0.003	1.02	0.004	1.04	0.012	1.10	0.200	1.54
	0.5	0.012	1.10	0.026	1.16	0.068	1.28	0.324	1.73
	0.6	0.017	1.12	0.032	1.18	0.060	1.26	0.018	1.13
	0.7	0.007	1.06	0.007	1.07	0.004	1.03	0.303	1.70
	0.8	0.005	1.05	0.013	1.10	0.059	1.26	0.576	2.09
	0.9	0.023	1.15	0.055	1.25	0.140	1.43	0.015	1.11
	1.0	0.028	1.17	0.048	1.23	0.054	1.24	0.972	2.62
	1.1	0.007	1.06	0.004	1.03	0.031	1.17	1.23	2.97
	1.2	0.015	1.11	0.062	1.26	0.312	1.71	2.06	4.17
	1.3	0.072	1.29	0.177	1.50	0.348	1.76	12.7	71.2
	1.4	0.076	1.30	0.099	1.35	0.006	1.05	19.5	348
	1.5	0.006	1.05	0.041	1.20	1.68	3.60	23.6	889
	1.6	0.168	1.48	0.967	2.61	5.37	11.7	25.8	
	1.7	0.898	2.52	2.84	5.49	8.23	24.5	26.2	
	1.8	1.88	3.90	4.38	8.83	9.52	33.7	24.9	
	1.9	2.46	4.84	4.86	10.1	9.16	30.9	21.3	535
	2.0	2.29	4.56	4.09	8.12	6.99	17.9	14.2	102
7	0.1	0.013	1.10	0.024	1.15	0.054	1.24	0.260	1.63
	0.2	0.010	1.08	0.015	1.11	0.026	1.16	0.032	1.18
	0.3	0.005	1.03	0.008	1.06	0.020	1.13	0.234	1.59
	0.4	0.016	1.11	0.031	1.17	0.066	1.27	0.118	1.39
	0.5	0.007	1.06	0.007	1.06	0.004	1.03	0.193	1.52
	0.6	0.009	1.08	0.022	1.14	0.070	1.28	0.265	1.64
	0.7	0.020	1.13	0.035	1.19	0.050	1.23	0.160	1.46
	0.8	0.004	1.02	0.004	1.01	0.027	1.16	0.510	1.99
	0.9	0.021	1.13	0.053	1.24	0.139	1.43	0.200	1.53
	1.0	0.025	1.15	0.032	1.18	0.008	1.07	0.973	2.62
	1.1	0.005	1.03	0.025	1.15	0.196	1.53	0.985	2.63
	1.2	0.053	1.24	0.123	1.39	0.162	1.47	0.673	2.21
	1.3	0.029	1.17	0.012	1.09	0.166	1.47	17.4	213
	1.4	0.033	1.18	0.203	1.54	0.800	2.38	29.0	
	1.5	0.181	1.50	0.300	1.69	0.235	1.58	35.3	
	1.6	0.021	1.13	0.226	1.57	7.46	20.1	38.5	
	1.7	0.691	2.24	3.90	7.67	13.3	82.0	38.8	
	1.8	3.05	5.88	7.48	20.3	15.4	137	36.4	
	1.9	4.48	9.08	8.30	25.0	14.4	107	30.3	
	2.0	3.73	7.30	6.09	14.2	9.47	33.3	17.0	198
10	0.1	0.016	1.11	0.028	1.16	0.059	1.25	0.221	1.57
	0.2	0.005	1.02	0.006	1.04	0.013	1.09	0.170	1.48
	0.3	0.016	1.11	0.027	1.16	0.048	1.22	0.021	1.13
	0.4	0.006	1.04	0.011	1.08	0.036	1.19	0.310	1.71
	0.5	0.017	1.11	0.025	1.15	0.029	1.16	0.156	1.45
	0.6	0.008	1.06	0.020	1.13	0.073	1.29	0.006	1.27
	0.7	0.017	1.11	0.021	1.13	0.009	1.07	0.506	1.99
	0.8	0.013	1.09	0.036	1.19	0.117	1.38	0.295	1.68
	0.9	0.018	1.12	0.015	1.10	0.011	1.08	0.051	1.23
	1.0	0.022	1.13	0.067	1.27	0.150	1.44	0.974	2.62
	1.1	0.019	1.12	0.008	1.05	0.103	1.35	2.01	4.10
	1.2	0.043	1.20	0.126	1.40	0.120	1.38	3.98	7.85
	1.3	0.019	1.12	0.009	1.06	0.484	1.95	24.2	931
	1.4	0.102	1.35	0.254	1.62	0.016	1.09	43.3	
	1.5	0.015	1.10	0.142	1.43	1.34	3.11	53.0	
	1.6	0.353	1.77	0.505	1.98	9.75	35.3	57.5	
	1.7	0.028	1.14	4.50	9.11	21.0	477	57.8	
	1.8	4.62	9.43	12.5	68.8	24.5		53.7	
	1.9	8.04	23.3	13.9	95.0	22.3	662	43.7	
	2.0	5.77	13.0	8.61	26.9	12.3	65.9	20.0	402
15	0.1	0.011	1.06	0.014	1.09	0.019	1.12	0.010	1.07
	0.2	0.018	1.11	0.028	1.15	0.048	1.22	0.023	1.13
	0.3	0.017	1.01	0.031	1.16	0.067	1.27	0.043	1.20
	0.4	0.010	1.05	0.019	1.11	0.061	1.25	0.070	1.28
	0.5	0.007	1.02	0.007	1.02	0.033	1.17	1.102	1.35
	0.6	0.015	1.09	0.014	1.08	0.009	1.05	0.135	1.41
	0.7	0.024	1.14	0.037	1.18	0.016	1.10	0.161	1.46
	0.8	0.021	1.12	0.052	1.23	0.064	1.26	0.164	1.46
	0.9	0.010	1.05	0.040	1.19	0.132	1.41	0.107	1.35
	1.0	0.010	1.05	0.014	1.08	0.182	1.50	0.009	1.00
	1.1	0.034	1.17	0.013	1.08	0.184	1.50	0.819	2.40
	1.2	0.059	1.24	0.073	1.28	1.136	1.41	3.68	7.15
	1.3	0.052	1.22	0.178	1.48	0.069	1.27	35.4	
	1.4	0.016	1.09	0.259	1.62	0.029	1.14	67.1	
	1.5	0.029	1.15	0.274	1.64	0.127	1.38	82.3	
	1.6	0.227	1.57	0.285	1.65	12.0	58.7	89.2	
	1.7	0.872	2.47	2.74	5.27	34.0		89.4	
	1.8	6.43	15.3	21.2	487	39.8		82.6	
	1.9	14.6	111	23.5	832	35.6		66.2	
	2.0	8.61	26.9	11.8	58.2	15.7	146	23.5	901

Table 4

Insertion loss α (dB) and v.s.w.r. for p-i-n diode attenuator with $C=0$, $y=4$, $z=0$, $x=f/f_0$, $g=R_0/R=1$ and $X_L=2\pi f_0 L/R_0$

No. of Diodes	x	$X_L=0.1$ α	V.S.W.R.	$X_L=0.4$ α	V.S.W.R.	$X_L=0.7$ α	V.S.W.R.	$X_L=1.0$ α	V.S.W.R.
3	0.1	8.24	3.66	8.28	3.67	8.31	3.68	8.33	3.68
	0.2	8.95	3.01	9.05	3.04	9.12	3.07	9.14	3.11
	0.3	9.79	2.45	9.94	2.51	9.98	2.57	9.92	2.62
	0.4	10.6	2.07	10.7	2.14	10.6	2.21	10.4	2.27
	0.5	11.2	1.83	11.2	1.90	11.0	1.96	10.4	2.00
	0.6	11.6	1.70	11.5	1.74	11.0	1.77	10.1	1.76
	0.7	11.9	1.65	11.6	1.65	10.7	1.63	9.38	1.59
	0.8	12.0	1.64	11.4	1.60	10.1	1.54	8.47	1.46
	0.9	12.0	1.65	11.1	1.60	9.37	1.51	7.48	1.42
	1.0	12.0	1.66	10.7	1.61	8.61	1.53	6.56	1.46
	1.1	11.8	1.66	10.2	1.63	7.87	1.56	5.80	1.51
	1.2	11.7	1.64	9.70	1.61	7.19	1.56	5.16	1.50
	1.3	11.4	1.63	9.16	1.56	6.54	1.48	4.57	1.41
	1.4	11.1	1.65	8.53	1.51	5.86	1.37	3.97	1.26
	1.5	10.6	1.73	7.82	1.50	5.18	1.32	3.40	1.20
	1.6	9.89	1.94	7.03	1.65	4.50	1.48	2.95	1.42
	1.7	9.10	2.31	6.30	2.02	4.04	1.88	2.71	1.80
	1.8	8.32	2.89	5.84	2.62	3.90	2.42	2.72	2.23
	1.9	7.82	3.59	5.83	3.30	4.08	2.93	2.90	2.59
	2.0	7.82	3.98	6.23	3.67	4.43	3.20	3.12	2.76
5	0.1	12.4	4.05	12.5	4.08	12.6	4.12	12.6	4.15
	0.2	14.8	2.70	15.1	2.77	15.2	2.84	15.4	2.90
	0.3	16.8	2.21	17.1	2.27	17.3	2.33	17.2	2.39
	0.4	18.1	2.00	18.5	2.04	18.4	2.08	18.1	2.11
	0.5	19.0	1.87	19.3	1.90	18.9	1.92	18.0	1.92
	0.6	19.7	1.77	19.6	1.80	18.7	1.80	17.1	1.78
	0.7	20.1	1.70	19.8	1.71	18.0	1.70	15.8	1.67
	0.8	20.3	1.65	19.3	1.64	17.0	1.61	14.2	1.57
	0.9	20.3	1.65	18.8	1.60	15.8	1.53	12.6	1.46
	1.0	20.3	1.62	18.1	1.58	14.5	1.49	11.0	1.40
	1.1	20.1	1.62	17.2	1.57	13.2	1.49	9.69	1.43
	1.2	19.8	1.63	16.3	1.56	12.0	1.48	8.51	1.42
	1.3	19.3	1.66	15.3	1.54	10.8	1.42	7.45	1.31
	1.4	18.7	1.72	14.2	1.57	9.63	1.42	6.50	1.31
	1.5	17.9	1.81	13.1	1.66	8.59	1.55	5.72	1.50
	1.6	16.8	1.92	11.9	1.74	7.68	1.62	5.09	1.51
	1.7	15.5	2.07	10.6	1.75	6.87	1.49	4.30	1.30
	1.8	13.6	2.48	8.99	1.98	5.53	1.74	3.60	1.68
	1.9	11.4	3.84	7.84	3.45	5.36	3.26	3.91	3.04
	2.0	10.7	5.97	8.96	5.59	6.81	4.94	5.12	4.27
7	0.1	16.8	3.77	16.9	3.83	17.1	3.88	17.2	3.93
	0.2	20.9	2.64	21.3	2.70	21.8	2.76	21.8	2.82
	0.3	23.7	2.25	24.2	2.30	24.5	2.35	24.5	2.39
	0.4	25.6	2.01	26.1	2.06	26.1	2.10	25.7	2.13
	0.5	26.9	1.86	27.2	1.90	26.7	1.93	25.5	1.94
	0.6	27.8	1.76	27.7	1.79	26.4	1.79	24.3	1.78
	0.7	28.3	1.70	27.7	1.71	25.4	1.69	22.3	1.65
	0.8	28.6	1.65	27.2	1.65	24.0	1.61	20.0	1.56
	0.9	28.7	1.63	26.5	1.60	22.2	1.55	17.6	1.49
	1.0	28.6	1.62	25.4	1.57	20.4	1.50	15.5	1.42
	1.1	28.3	1.62	24.2	1.56	18.5	1.48	13.5	1.40
	1.2	27.8	1.63	22.9	1.55	16.8	1.46	11.9	1.39
	1.3	27.2	1.67	21.5	1.56	15.1	1.43	10.4	1.32
	1.4	26.3	1.72	19.9	1.59	13.5	1.47	9.09	1.41
	1.5	25.2	1.79	18.3	1.63	12.0	1.49	7.99	1.38
	1.6	23.7	1.92	16.6	1.68	10.6	1.48	6.89	1.37
	1.7	21.7	2.13	14.7	1.87	9.24	1.73	6.08	1.66
	1.8	19.1	2.45	12.6	2.03	7.86	1.70	5.07	1.44
	1.9	15.3	3.44	9.96	2.74	6.29	2.52	4.36	2.53
	2.0	12.9	7.97	11.1	7.54	6.75	6.77	6.86	5.91
10	0.1	23.6	3.64	23.9	3.69	24.1	3.74	24.3	3.79
	0.2	29.9	2.67	30.5	2.72	31.0	2.78	31.3	2.83
	0.3	34.0	2.24	34.9	2.30	35.3	2.35	35.4	2.40
	0.4	36.8	2.01	37.6	2.06	37.7	2.10	37.2	2.13
	0.5	38.7	1.86	39.2	1.90	38.5	1.92	36.8	1.93
	0.6	39.9	1.76	39.9	1.79	38.0	1.79	34.9	1.78
	0.7	40.6	1.70	39.8	1.71	36.6	1.69	32.0	1.65
	0.8	41.1	1.65	39.1	1.65	34.4	1.61	28.6	1.55
	0.9	41.2	1.63	38.0	1.61	31.9	1.55	25.2	1.48
	1.0	41.0	1.62	36.5	1.58	29.2	1.51	22.1	1.43
	1.1	40.6	1.62	34.7	1.56	26.5	1.47	19.4	1.39
	1.2	39.9	1.63	32.8	1.55	24.0	1.46	16.9	1.37
	1.3	39.0	1.66	30.7	1.56	21.5	1.45	14.8	1.36
	1.4	37.8	1.72	28.5	1.58	19.3	1.46	13.0	1.37
	1.5	36.1	1.80	26.2	1.62	17.1	1.48	11.3	1.37
	1.6	34.0	1.92	23.6	1.70	15.1	1.54	9.83	1.46
	1.7	31.1	2.12	20.9	1.83	13.1	1.61	8.46	1.43
	1.8	27.2	2.49	17.8	2.09	11.0	1.88	7.20	1.62
	1.9	21.4	3.32	13.9	2.58	8.60	2.00	5.52	1.64
	2.0	15.4	11.0	13.5	10.5	11.1	9.61	9.03	8.55
15	0.1	35.0	3.66	35.4	3.71	35.8	3.76	36.2	3.80
	0.2	45.0	2.66	45.9	2.72	46.7	2.78	47.3	2.83
	0.3	51.3	2.24	52.6	2.30	53.4	2.35	53.8	2.40
	0.4	55.5	2.01	56.8	2.06	57.0	2.10	56.7	2.13
	0.5	58.3	1.86	59.2	1.90	58.2	1.92	55.7	1.93
	0.6	60.1	1.76	60.1	1.79	57.4	1.79	52.7	1.78
	0.7	61.3	1.70	59.9	1.71	55.1	1.69	48.1	1.65
	0.8	61.9	1.65	58.9	1.65	51.8	1.61	43.0	1.55
	0.9	62.0	1.63	57.1	1.61	47.9	1.55	37.9	1.48
	1.0	61.7	1.62	54.9	1.58	43.9	1.51	33.2	1.43
	1.1	61.1	1.62	52.2	1.56	39.8	1.47	20.0	1.39
	1.2	60.1	1.63	49.3	1.55	35.9	1.46	25.4	1.37
	1.3	58.7	1.66	46.1	1.56	32.3	1.45	22.2	1.36
	1.4	56.8	1.72	42.8	1.58	28.8	1.46	19.4	1.37
	1.5	54.4	1.80	39.2	1.63	25.6	1.48	16.9	1.38
	1.6	51.1	1.92	35.4	1.70	22.5	1.53	14.7	1.40
	1.7	46.8	2.12	31.3	1.83	19.4	1.63	12.6	1.48
	1.8	40.7	2.48	26.4	2.08	16.2	1.84	10.6	1.68
	1.9	31.6	3.37	20.2	2.73	12.6	2.43	8.48	2.31
	2.0	18.4	16.0	16.5	15.5	14.0	14.5	11.8	13.2

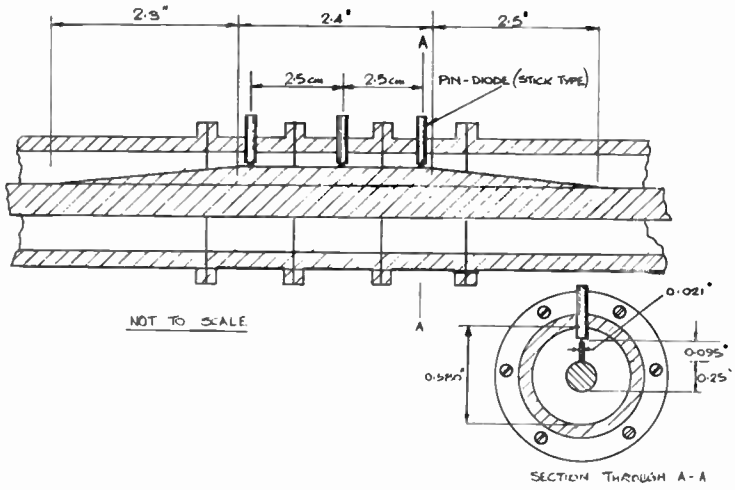

Fig. 10. Three-diode attenuator with ramp.

diodes by $\lambda/4$ at the centre of the band. Table 2 can then be used to select the minimum number of diodes to meet the maximum attenuation and v.s.w.r. variation over the band at elevated attenuation levels. Table 3 will give the corresponding attenuation and v.s.w.r. variations at zero bias for the known value of C. Table 4 can be used to estimate the deterioration in performance for given values of L. On the other hand some improvement can be obtained by staggering the values of R_v.

If no satisfactory answer can be found then this will be most likely because C is too large. In that case, short of taking steps to reduce C it may still be possible to find satisfactory design data by making the $\lambda/4$ separation correspond to a higher frequency, closer to the upper end of the band. For example, if $\lambda/4$ is made to correspond to the upper band edge then, as seen from Table 3, the effect of C can be much reduced but inspection of Tables 2 and 4 shows that performance at higher attenuations may deteriorate. It should however be possible, by careful inspection of the tables, to arrive at a reasonably satisfactory design of at least an octave wide attenuator up to 10 Gc/s, even with currently obtainable diodes which are designed by the manufacturers for switching microwave power.

4. Some Practical Cases based on above Recommendations

4.1. *Methods of Minimizing Parasitic L and C*

The capacitance is mainly determined by the diode construction and is therefore not under the control of the designer. The inductance is brought about because the diode junction is too small to fit between the inner and outer conductor of the line, thus creating the need for a post. If length is unimportant the distance between the conductors can be reduced by altering the impedance and using long-tapered transitions. One of the simplest ways of doing this is to mount the diodes near the middle of a long line where the inner conductor has been pulled to one side by two spacers, causing the line to be eccentric near the middle. Since length is usually important, another method has been tried (Fig. 10), where a thin ramp has been introduced into the line in contact with the inner. This method bears a resemblance to ridge waveguide and will be dealt with again in Section 4.3. A way of removing the effect of inductance has been suggested by Gray,[3] whereby the impedance of the transmission line in the vicinity of the diode is increased, thus creating an inductive effect which compensates for the diode inductance. However, the steps are likely to produce additional capacitances. These additional capacitances would probably only be important at low attenuation levels and therefore are not very troublesome for levellers with which that paper[3] is in fact concerned.

4.2. *Design of Levellers*

A leveller[3] need not have as flat a response as a quality attenuator because any deviations from flatness are absorbed in the control loop. Also its insertion loss at zero bias is less critical. The design of a leveller from Table 2 is quite straightforward if the effects of L and C can be ignored. However, the device must be capable of low frequency square wave modulation with a reasonable v.s.w.r. during the 'off' cycle. If this is not achieved, the source oscillator may initially 'chirp' when switched to the 'on' cycle. The method of arranging this requires an additional diode which is placed at the input to the leveller. By placing a p–i–n diode, with suitable resistance R', in parallel with the input impedance of the leveller, the resulting v.s.w.r. can be greatly improved, as shown in Fig. 11. The optimum value of R' is easily found experimentally using a slotted line. The attenuation

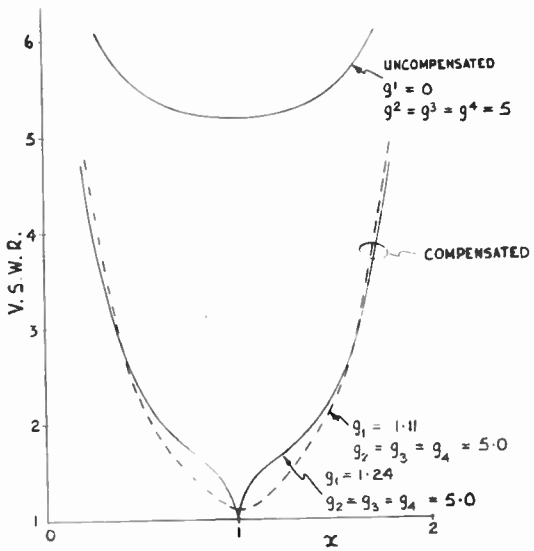

Fig. 11. Three p–i–n diode leveller ($z = 0$, $y = 4$) with and without compensation p–i–n diode at input. Insertion loss > 32 dB for $0{\cdot}4 \leqslant x \leqslant 1{\cdot}6$ see Table 2. Curves to Smith chart accuracy. L and C are zero.

of the leveller under this condition is only slightly modified by R'. When the leveller is biased to the 'on' cycle of the modulation, R' is then biased off. However, to avoid the use of an additional diode, a disk of resistance card across the line could be used for R', but this restricts the low attenuation range of the leveller.

4.3. *Wide-band Attenuator*

Three A.E.I. p–i–n diodes type VX4190 were measured by the methods used in Section 2.3. As these diodes were unencapsulated and mounted on brass rods, some of the redundant brass was turned off the end to reduce the capacitance C down to 0·32 pF. A nominal diode inductance L_c of 0·15 nH, as stated by the manufacturers, was confirmed. The three diodes were mounted in coaxial line ($\lambda/4$ apart at 3 Gc/s), with insulated outer sections as in Fig. 5, but this time a thin brass ramp was fixed to the inner so that the required length of the diode post was about halved. The diode post inductance L_p was now 0·4 nH and the total inductance $L = 0{\cdot}55$ nH. The critical physical dimensions of this attenuator are given in Fig. 10, and measured and computed performance curves in Fig. 12(a) and (b). As in Section 2.3 each diode was set to a known value of resistance and therefore no diode tolerance effects are present. The method of measurement and sources of error are as in Section 2.3.

This attenuator gave a maximum insertion loss of about 12 dB ± 0·75 dB, and v.s.w.r. < 1·8 over the band 2–4 Gc/s. It is seen from the computed tables that it is the value of C rather than L that degrades the performance of this attenuator. Some small improvement results by staggering resistances. This device was used to assess the effects of the ramp. The peaks and troughs of the measured curves are in step with the computed ones and also there is reasonable agreement between their values. It is therefore concluded that the actual values of L and C are as anticipated and the only effect of the ramp is to degrade the v.s.w.r. of the device when the diodes are biased off.

The use of a ramp to reduce the inductance L_p therefore seems advantageous providing the degradation of the v.s.w.r. at zero bias can be tolerated.

4.4. *Use of Stripline*

This paper has so far been devoted to coaxial transmission line but the results can be extended to strip line. To test this, a length of 50-ohm high-Q

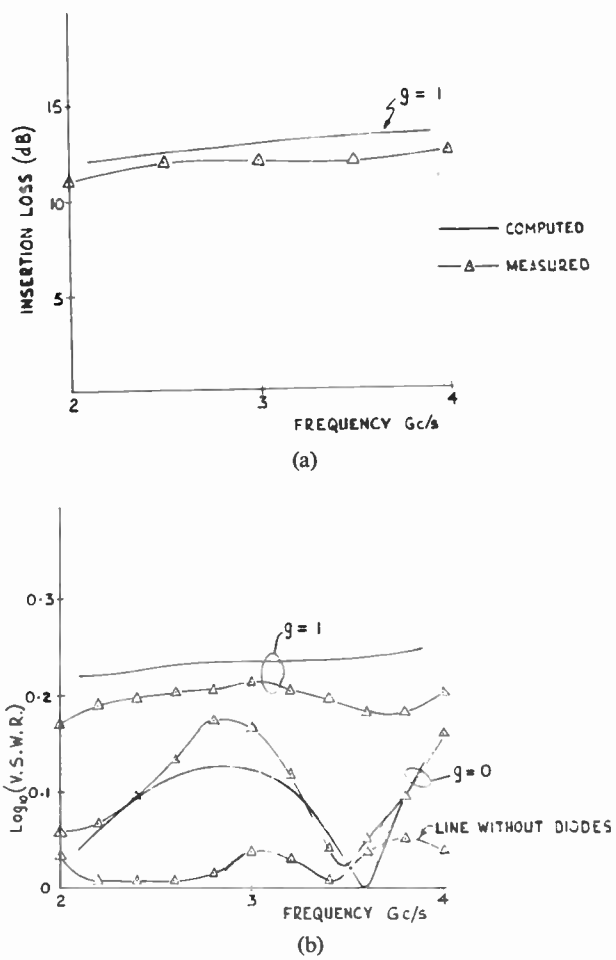

Fig. 12. Curves for three p–i–n diode attenuator with ramp and all diode resistances equal ($z = 0$, $y = 4$, $L = 0{\cdot}55$ nH, $C = 0{\cdot}32$ pF).

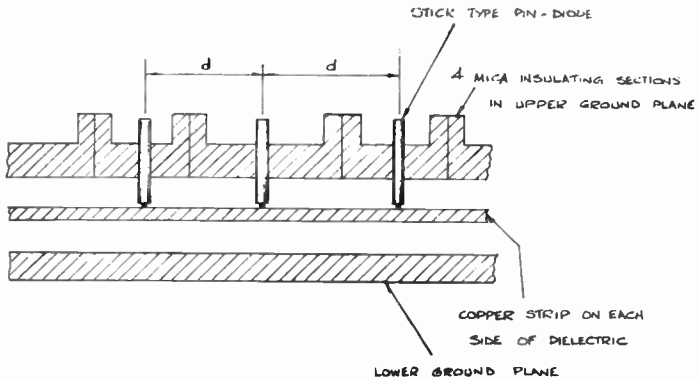

Fig. 13. Modified 50-ohm triplate strip line showing mica discontinuities in upper ground plane and position of stick p–i–n diodes. $d = \lambda/4$ in line at 3Gc/s = 2·184 cm.

triplate strip line was terminated in type *N* connectors and four splits arranged in one of the ground planes, in which mica insulating strips were held (Fig. 13). The diodes used in Section 4.3 could now be placed through holes in this split ground plane $\lambda/4$ apart at 3 Gc/s and biased separately. The wavelength in this strip line was 0·8738 of that in coaxial air-spaced line. The mica discontinuities were found to have no effect on the operation of the strip line. Performance curves for this device are shown in Fig. 14(a) and (b). The method of measurement and sources of error are as in Section 2.3.

By coincidence, the diode post, protruding into the air space of the strip line, was practically the same length as the post used in Section 4.3. Since the diode capacitance is unaltered, the computed curves in Fig. 14 are the same as those in Fig. 12. It is therefore likely that this attenuator will have a similar specification to the coaxial attenuator of Section 4.3.

The general shape of the measured curves of Fig. 14 agrees reasonably well with the computed ones but there are deviations in the v.s.w.r. curves in the form of ripples, particularly at the high end of the band. Since for strip line, the electromagnetic field is more concentrated in the vicinity of the diode post, this could be a field disturbance effect. However, it is the authors' considered opinion that it is mainly due to the significant v.s.w.r. in the absence of diodes, created by the *N* type connector transition.

Apart from these peaky deviations, the strip line attenuator appears to behave in a similar fashion to the coaxial version.

5. Conclusions

(*a*) The design of wide-band transmission line attenuators with shunt diodes has been considered in some detail. The series and shunt-series versions have not been dealt with.

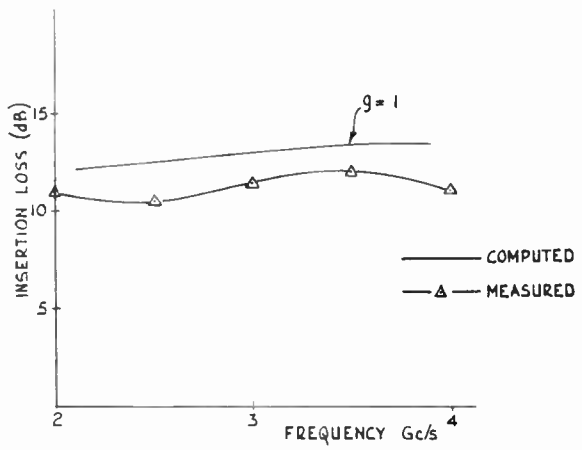

(a)

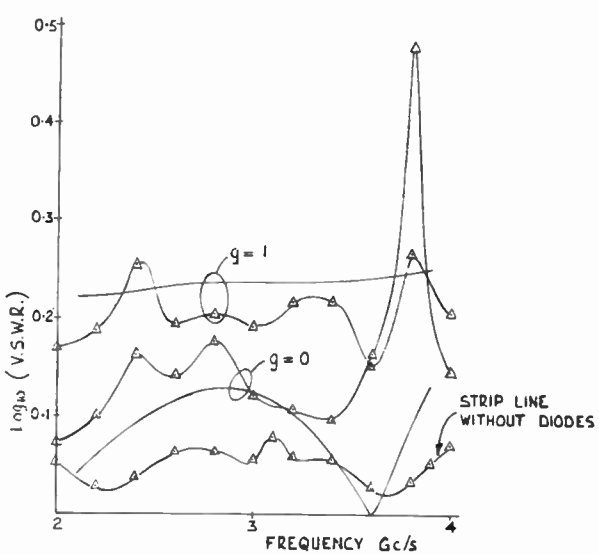

(b)

Fig. 14. Curves for three p–i–n diode attenuator. (High *Q* triplate strip line with all diode resistances equal ($z = 0$, $y = 4$, $L = 0{\cdot}55$ nH, $C = 0{\cdot}32$ pF).)

(*b*) When the parasitic reactances are negligible the attenuator design has been shown to be straightforward and the performance can be further improved by staggering the diode resistance values. When these reactances are not small, computed data[5] have to be referred to, covering most practical requirements.

(*c*) An almost linear relationship, between bias current and diode conductance (at high frequency) (Fig. 4), has been observed on two types of diodes. This suggests that, for production purposes, diodes could be selected by one high frequency measurement.

(*d*) Measurements on a strip line containing p–i–n diodes agreed reasonably well with computed data for coaxial case. Waveguide attenuators using p–i–n diodes have not been considered. The waveguide solution will be more involved, due to the frequency dependence of the guide impedance.

(*e*) A method of reducing the diode post inductance has been described but the reduction of diode capacitance is largely in the hands of the diode manufacturer. The inductance of the stick diode was much less than that of the encapsulated one (due to a thin wire in latter) but their capacitances were similar.

(*f*) The results obtained show that using the computed data it is possible to design an octave-wide attenuator whose attenuation can be varied over a wide range by diode bias, with a performance comparing favourably with that obtained by conventional attenuators.

(*g*) The data can be used to design a power leveller. This can be used also for square on/off modulation of the signal by the addition of another switched p–i–n diode.

(*h*) Measurements have been carried out only up to 50 mW input power and in that range no distortion was observed on account of the p–i–n diode.

6. Acknowledgments

The authors wish to acknowledge the Dean of the Royal Military College of Science, Sir Donald Bailey, O.B.E., for permission to publish this work.

Thanks are due to Mr. G. Triggs who assisted with the measurements and computations and to Cossor Electronics Ltd., Harlow, who designed the triplate strip line to our specification.

7. References

1. J. K. Hunton and A. G. Ryals, 'Microwave variable attenuators and modulators using p–i–n diodes', *Trans. Inst. Radio Engrs on Microwave Theory and Techniques*, **MTT-10**, No. 4, p. 262, July 1962.
2. T. H. B. Baker, 'Semiconductor-diode waveguide switch', *Electronic Technology*, **38**, p. 300, August 1961.
3. D. A. Gray, 'How to design p–i–n diode control devices', *Microwaves*, 4, p. 22, November 1964.
4. M. M. McDermott and R. Levy, 'Very broadband coaxial d.c. returns derived by microwave filter synthesis', *Microwave J.*, **8**, p. 33, February 1965.
5. J. R. James and M. H. N. Potok, 'Computer Results on p–i–n-Diode Attenuators', R.M.C.S. Internal Report No. RT22, 1965.

8. Appendix 1

The A matrix of a section of lossless transmission line impedance R_0, which is terminated in an admittance Y is given in (1):

$$\begin{pmatrix} \cos\theta & \mathrm{j}R_0\sin\theta \\ \dfrac{\mathrm{j}\sin\theta}{R_0} & \cos\theta \end{pmatrix}\begin{pmatrix} 1 & 0 \\ Y & 1 \end{pmatrix} = \begin{pmatrix} \cos\theta+\mathrm{j}R_0Y\sin\theta & \mathrm{j}R_0\sin\theta \\ \dfrac{\mathrm{j}\sin\theta}{R_0}+Y\cos\theta & \cos\theta \end{pmatrix} \quad \ldots\ldots(1)$$

In Fig. 1, each section of line l_v, is terminated in an admittance $[g'_v - jb_v]$ which has been normalized by the line admittance $(1/R_0)$ and is a function of diode and post inductance L, diode capacitance C and resistance R_v. (Note that $g'_v = g_v$ if $L = 0$ or both L and C equal zero.)

Putting R_0 equal to unity, the A matrix (A_v) of each of these terminated sections is of the form (2).

$$\left.\begin{aligned} (A_v) &= \begin{pmatrix} \cos\theta_v+b_v\sin\theta_v+\mathrm{j}g_v\sin\theta_v & \mathrm{j}\sin\theta_v \\ g_v\cos\theta_v+\mathrm{j}(\sin\theta_v-b_v\cos\theta_v) & \cos\theta_v \end{pmatrix} \\ \theta_v &= (\pi/8)x[y+(v-1)z] \end{aligned}\right\} \quad \ldots\ldots(2)$$

where $x = f/f_0$ and is the frequency f of the wave in the line, normalized by f_0. The factors y and z determine the length of the line. If $z = 0$, then all sections are of the same length, but if $z \neq 0$, a linear staggering of the lengths of line is achieved.

Now let the source resistance R_0 be absorbed into (A_1) and load resistance R_0 into (A_n). These two matrices become (3) and (4):

$$(A_1) = \begin{pmatrix} ((1+g'_1)\cos\theta_1+b_1\sin\theta_1) \\ \quad +\mathrm{j}((1+g'_1)\sin\theta_1-b_1\cos\theta_1) & \mathrm{e}^{\mathrm{j}\theta_1} \\ g'_1\cos\theta_1+\mathrm{j}(\sin\theta_1-b_1\cos\theta_1) & \cos\theta_1 \end{pmatrix} \quad \ldots\ldots(3)$$

$$(A_n) = \begin{pmatrix} \cos\theta_n+b_n\sin\theta_n+\mathrm{j}(g'_n+1)\sin\theta_n & \mathrm{j}\sin\theta_n \\ (g'_n+1)\cos\theta_n+\mathrm{j}(\sin\theta_n-b_n\cos\theta_n) & \cos\theta_n \end{pmatrix} \quad \ldots\ldots(4)$$

The A matrix (A) of the entire network in Fig. 1 is now given by (5).

$$(A) = \begin{pmatrix} a_{11} & a_{12} \\ a_{21} & a_{22} \end{pmatrix} = (A_1)(A_2)\ldots(A_v)\ldots(A_n) = \prod_{v=1}^{n}(A_v) \quad \ldots\ldots(5)$$

To facilitate programming, each (A_v) was resolved into the matrix sum of a real and imaginary matrix. (See (12), Appendix 3.)

The insertion loss, v.s.w.r., etc., were then extracted from the elements of the A matrix (A). (See (8) Appendix 2 and also Appendix 3.)

9. Appendix 2

The limits of the approximations in this section are not rigorously justified. They are included in order to show the nature of the problem under the conditions stated.

When L and C are put equal to zero and the diode resistances R_v, $(v = 1, 2, \ldots n)$ are all equal to R, each $b_v = 0$ and $g'_v = g_v = g = R_0/R$ for all v. With no staggering of lengths $(z = 0)$ each $\theta_v = \theta$. It can be deduced by taking $n = 3$, 4, 5, etc., that the a_{11} element of the matrix (A) (Appendix 1 (5)) is of the form:

$$|a_{11}|^2 = [(2+ng)^2 + g^2(\sin^2\theta)F_1(g) + g^2(\sin^4\theta)F_2(g) \ldots + \ldots + g^2(\sin^{2n}\theta)F_n(g)] \quad \ldots\ldots(6)$$

$F_n(g)$ is polynomial in g of degree $2(n-1)$.

If θ is now chosen so that $|\sin\theta| \gg |\cos\theta|$ (i.e. θ is near $\pi/2$) it follows that $|a_{11}|$ is approximately given by (if g is very large)

$$|a_{11}| = g^n \sin^n\theta \quad \ldots\ldots(7)$$

The insertion loss α is then defined as:

$$\alpha = 20\log_{10}\left(\frac{|a_{11}|}{2}\right) = 20\log_{10}\left(g^n\frac{\sin^n\theta}{2}\right) \quad \ldots\ldots(8)$$

If, however, g is very small, then from (6), $|a_{11}|$ and α are given approximately as:

$$\left.\begin{aligned} |a_{11}| &= (2+ng) \\ \alpha &= 20\log_{10}\left(1+\frac{ng}{2}\right) \end{aligned}\right\} \quad \ldots\ldots(9)$$

It also follows from (6) that (9) is true for any g if $\theta = 0, \pi, 2\pi, \ldots$. If g is now taken to be very large again, but in this case $z \neq 0$, each θ_v is different for $v = 1, 2, \ldots, n$. If the staggering between the θ_v values is small and for every v, $|\sin\theta_v| \gg |\cos\theta_v|$ then $|a_{11}|$ is approximately given by:

$$|a_{11}| = g^n \prod_{v=1}^{n} (\sin\theta_v) \quad \ldots\ldots(10)$$

If, however, each g_v is very large but different and $z = 0$ and $|\sin\theta| \gg |\cos\theta|$, then $|a_{11}|$ is given approximately by

$$|a_{11}| = \sin^n\theta \prod_{v=1}^{n} (g_v) \quad \ldots\ldots(11)$$

10. Appendix 3

Consider the A matrix (A_v) of eqn. (2), Appendix 1. When there is no staggering of line lengths $(z = 0)$ and the diodes are pure resistances $(b_v = 0)$ then each (A_v) is of the form (12)

$$\left.\begin{aligned} (A_v) &= \cos\theta(B_v) + \mathrm{j}\sin\theta(C_v) \\ (B_v) &= \begin{pmatrix} 1 & 0 \\ g_v & 1 \end{pmatrix} \\ (C_v) &= \begin{pmatrix} g_v & 1 \\ 1 & 0 \end{pmatrix} \end{aligned}\right\} 2 \leqslant v \leqslant (n-1)$$

$$(B_1) = \begin{pmatrix} [1+g_1] & 1 \\ g_1 & 1 \end{pmatrix} \quad (B_n) = \begin{pmatrix} 1 & 0 \\ [g_n+1] & 1 \end{pmatrix}$$

$$(C_1) = \begin{pmatrix} [1+g_1] & 1 \\ 1 & 0 \end{pmatrix} \quad (C_n) = \begin{pmatrix} [g_n+1] & 1 \\ 1 & 0 \end{pmatrix} \quad \ldots\ldots(12)$$

For $n = 3$, (A) is given by (13) where each matrix (ζ_i), $i = 0, 1, 2$ and 3, is two by two and has elements which are functions of g_1, g_2 and g_3

$$\left.\begin{aligned} (A) &= \prod_{v=1}^{3} [\cos\theta(B_v) + \mathrm{j}\sin\theta(C_v)] \\ &= \sin^3\theta[\cot^3\theta(\zeta_3) + \mathrm{j}\cot^2\theta(\zeta_2) - \\ &\qquad - \cot\theta(\zeta_1) - \mathrm{j}(\zeta_0)] \end{aligned}\right\} \quad \ldots\ldots(13)$$

The insertion loss of this attenuator is governed by the $|a_{11}|$ term of (A) (see eqns. (5) and (8), Appendix 1 and 2), and the input impedance is given by

$$\{[a_{11}/a_{21}]-1\}$$

Let $(\zeta_i)_{11}$ and $(\zeta_i)_{21}$ denote the elements of (ζ_i) in the first row and first column, and second row and first column positions respectively.

Then the insertion loss α is given by eqn. (14)

$$\alpha = 20\log_{10}\left|\frac{\sin^3\theta}{2} \times \times [\cot^3\theta(\zeta_3)_{11} + \mathrm{j}\cot^2\theta(\zeta_2)_{11} - - \cot\theta(\zeta_1)_{11} - \mathrm{j}(\zeta_0)_{11}]\right| \quad \ldots\ldots(14)$$

and the normalized input impedance Z_{in} by (15)

$$Z_{in} = \left[\frac{[\cot^3\theta(\zeta_3)_{11} + \mathrm{j}\cot^2\theta(\zeta_2)_{11} - - \cot\theta(\zeta_1)_{11} - \mathrm{j}(\zeta_0)_{11}]}{[\cot^3\theta(\zeta_3)_{21} + \mathrm{j}\cot^2\theta(\zeta_2)_{21} - - \cot\theta(\zeta_1)_{21} - \mathrm{j}(\zeta_0)_{21}]} - 1\right] \quad \ldots\ldots(15)$$

On expanding the (ζ_i) terms and taking the modulus of (14) it follows that $|a_{11}|^2$ is a polynomial of degree three in $\sin^2\theta$. Thus the curve of α is symmetrical about $\theta = \pi/2$, and with suitable choice of diode resistances, may have three ripples on it. This has in fact been observed, and it seems likely that the curve of α for an n diode attenuator may have n ripples.

If Z_{in} from (15) is used to express the v.s.w.r. then a polynomial of degree three in $\sin^2\theta$ is again involved indicating symmetry about $\theta = \pi/2$ and the possibility of three ripples on v.s.w.r. curve. As before several ripples have been observed but there appears to be no simple expression relating the number of ripples to the diode resistances.

While the polynomials in (14) and (15) appear to be in a suitable form to allow induction methods to be applied, in order to find the general case, the coefficients $(\zeta_i)_{pq}$ are polynomials in g_1, g_2, g_3 and do not follow an obvious pattern.

11. Appendix 4.

The A matrix (A) of the complete attenuator (Appendix 1, eqn. (5)) is very easily expanded when there is no staggering or parasitic L and C, and $\theta = n.\pi/2, n = 0, 1, 2.....$ This gives three values of θ at which the insertion loss and v.s.w.r. can be checked. In fact, at $\theta = 0$ or π all the resistances are in parallel and at $\theta = \pi/2$ they form a ladder network.

The values of individual conductances at $\theta = \pi/2$ can be determined by inspection, which shows that all but one value can be freely chosen. For example one can proceed as follows: Let the conductances of the diodes be numbered from the generator end 1 to n. The normalized first diode conductance, g_1, has also across it the generator normalized conductance (1). At the second diode at a distance $\pi/2$ down the line these will produce conductance $(1/(1+g_1))$ which has to be added to g_2. This again gives at a further distance $\pi/2$ the conductance $[g_2+1/(1+g_1)]^{-1}$ to which we add g_3, etc., until one reaches nth diode at which the total conductance for match with the load must equal 1. The only limitation on choice of values of conductances is that $g_n < 1$ and, of course, also by starting from the other end, g_1 must also be < 1.

For a symmetrical attenuator ($g_1 = g_n$, $g_2 = g_{n-1}$, etc.) the number of variables is somewhat reduced but still only one is dependent. Inspection of computed results indicates, however, that for best results one should aim at $g_1 < g_2 < g_3$ and similarly at the other end $g_n < g_{n-1} < g_{n-2}$, etc.

Manuscript first received by the Institution on 1st April 1965, and in final form on 22nd September 1965. (Paper No. 1029.)

U.D.C. 537.228 : 621.375.9.029.62

Acoustic Amplification in Semiconductors

By

R. W. HARCOURT, B.Sc.,†

J. FROOM, B.Sc., B.Sc.(Eng.), C.Eng.†

AND

C. P. SANDBANK, B.Sc., D.I.C., C.Eng.†

Reprinted from the Proceedings of the Joint I.E.R.E.–I.E.E. Symposium on 'Microwave Applications of Semiconductors' held in London from 30th June to 2nd July 1965.

Summary: If the application of semiconductors is to be extended to microwave frequencies, the limitations due to electrode capacitance and transit time must be overcome. To a certain extent this can be done by reducing junction size and using majority carriers where possible. However a much more sophisticated way of overcoming these difficulties is to try to realize in semiconductors the type of continuous interaction obtained in travelling-wave tubes.

In the paper the present state of the art on acoustic amplification in semiconductors is reviewed. Although net gain at microwave frequencies has not yet been obtained, the experiments at lower frequencies have given some general indications about the feasibility of achieving this. The main problems lie in coupling into the crystal in such a way that the insertion losses are minimized and the shape of the acoustic wavefront within the crystal is not disturbed. The amplifiers described use quartz transducers to couple into and out of a CdS crystal. Recently, deposited CdS transducers have been operated at X-band for this type of application. This suggests that there are reasonable chances of making low loss delay lines and ultimately amplifiers for microwave applications.

The importance of the acoustic amplifier as a diagnostic tool leading to a better understanding of other microwave phenomena in semiconductors is discussed briefly and the current instabilities in CdS which show similarities to the Gunn effect are described.

1. Introduction

In 1961 Hutson, McFee and White[1-5] reported that they had obtained amplification of sound waves in a piezo-electric semiconductor using interaction between drifting carriers and the travelling electric wave associated with the sound wave. By so doing, they demonstrated the possibility of making semiconductor devices employing the velocity modulation principles so familiar to microwave tube engineers. The idea of replacing the electron beam in microwave tubes by the carriers in a semiconductor is tempting because of the high carrier densities possible and because all the problems of evacuation, electron emission and beam focusing are avoided. At first sight it seemed unlikely that the mechanism of velocity modulation could survive the effects of collisions and diffusion. The piezo-electric amplifier shows that in some circumstances this is possible and points the way to a means of overcoming the frequency limitation imposed upon junction semiconductor devices by transit time and electrode capacitance in the same way that the introduction of velocity modulation tubes overcame the limitations of grid controlled tubes.

† Standard Telecommunication Laboratories, Harlow, Essex.

Since the original work by Hutson *et al.*[1] the piezo-electric amplifier has been the subject of much study and the purpose of this paper is to review the progress of this work. In the next section the basic mechanism is discussed, followed in Section 3 by a summary of the main theoretical background. Section 4 describes the experimental results obtained using this type of interaction while the problems associated specifically with transducers are discussed separately in Section 5. Section 6 describes briefly the implications this work has for associated fields of study, including the current instabilities observed in piezo-electric materials. In Section 7 the present position of the piezo-electric amplifier and its application prospects are summarized.

2. Principles of Operation

In the piezo-electric amplifier a sound wave is transmitted through a suitable semiconducting, piezo-electric crystal. The travelling acoustic wave is accompanied by a travelling wave of longitudinal electric field. At the same time, a d.c. electric field is impressed across the crystal so that the carriers drift in the same direction as the wave is travelling (Fig. 1). Interaction takes place between them in a similar way to that in a travelling-wave tube; when the carrier

velocity exceeds that of the wave energy is transferred from the carriers to the wave and the wave is amplified. Conversely, when the carrier velocity is less than the wave velocity the wave is attenuated and the carriers gain in energy. The carriers interact with the longitudinal electric wave which is intimately coupled to the acoustic wave by the piezo-electric nature of the material.

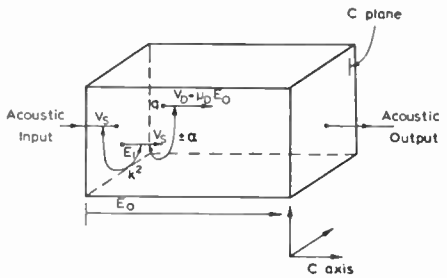

Fig. 1. Sketch showing longitudinal acoustic wave interaction parameters.

E_0 is the drift field, v_D the carrier drift velocity.
v_S is the sound velocity and E_1 the longitudinal electric field accompanying the acoustic wave with velocity v_S.
α is the attenuation constant: + for loss and − for gain.
K^2 is the piezo-electric coupling constant.
μ_D is the drift mobility.

From this description we can see that the piezo-electric properties of the crystal must be such that longitudinal electric fields are produced by the acoustic wave. The materials so far studied have been the II-VI and III-V binary compounds and have either hexagonal or cubic structures. In hexagonal structures longitudinal electric fields are produced when longitudinal waves propagate along the C axis or when transverse waves propagate normal to the C axis with their displacement vectors parallel to the C axis. The transverse mode is the slower of the two and therefore requires a lower drift field and may be preferred on that account. In cubic crystals only shear waves can be used and they must be propagated in the (110) direction with the displacement vector in the (100) direction.

Perhaps the most important property of the crystal is the electro-mechanical coupling constant, which determines the degree of interaction between the acoustic wave and the carriers. Another important parameter is the carrier mobility because this, in conjunction with the velocity of sound in the material, determines the field which must be applied in order to bring the carriers into synchronism with the acoustic wave.

3. Theoretical Analysis

There are two main approaches to the theory of the acoustic amplifier, one by Hutson and White[2] and one by Blotekjaer and Quate.[6]

Hutson and White[2] formulated the theory by using the piezo-electric stress strain relationships

$$T = cS - \mathbf{e}E \qquad \text{.....(1)}$$

$$D = \mathbf{e}S + \varepsilon E \qquad \text{.....(2)}$$

where T is the stress, S the strain, c the elastic constant at constant field E, D the dielectric displacement, ε the permittivity at constant strain and $\mathbf{e}$ the piezo-electric tensor.

Poisson's equation and charge continuity for a one-dimensional model

$$\frac{\partial D}{\partial x} = Q \qquad \text{.....(3)}$$

$$\frac{\partial J}{\partial x} = -\frac{\partial Q}{\partial t} \qquad \text{.....(4)}$$

where J is the current density and Q the charge and finally the current density in an n type semiconductor

$$J = q\mu n_c E + qD_n\left(\frac{\partial n_c}{\partial x}\right) \qquad \text{.....(5)}$$

where q is the electronic charge, μ the mobility, n_c the majority carrier concentration and D_n the diffusion constant for electrons. This assumes that the a.c. quantities above are small compared with the d.c. quantities. Using these equations and assuming propagation of the form $\exp\left|-j(1+\delta)\frac{X}{v}\right|$ and neglecting terms in δ^2 they derived an expression for the complex elastic constant from which the attenuation constant

$$\alpha = \frac{K^2}{2}\frac{\omega_c}{\gamma v_s}\left[1 + \frac{\omega_c^2}{\gamma^2\omega^2}\left(1 + \frac{\omega^2}{\omega_c\omega_D}\right)^2\right]^{-1} \qquad \text{.....(6)}$$

where

$K^2 = \dfrac{e^2}{c\varepsilon}$ is the piezo-electric coupling constant

$\gamma = 1 - \dfrac{v_D}{v_s}$ where v_D is the carrier drift velocity and v_s the sound velocity

$\omega_c = \dfrac{\sigma}{\varepsilon}$ the conductivity frequency

$\omega_D = \dfrac{v^2}{v_T^2\tau}$ the diffusion frequency, where v_T is the average thermal velocity of the carriers and τ is their relaxation time

ω is the acoustic wave frequency.

Blotekjaer and Quate arrived at the same result but their approach used the coupled mode ideas as applied to microwave tubes.[6] They formulated the equations for the forward and backward components of the elastic waves and of the carrier waves independently and then coupled the two using the piezo-electric coupling constant. This gave a forward wave with the same attenuation term as in equation (6) and a backward wave the attenuation of which was positive for all carrier velocities.

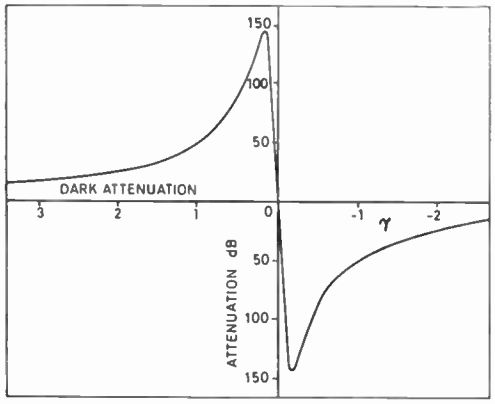

Fig. 2. Typical theoretical curve of a transverse wave amplifier using White's theory at 45 Mc/s $\omega_c = 6 \times 10^7$.

In Fig. 2 the attenuation constant α is plotted against γ for a typical set of parameters. It will be seen that when $\gamma = 0$, i.e. the drift velocity and sound velocity are equal, there will be no net energy exchange between the carriers and the acoustic wave and the latter is therefore unattenuated. The wave is attenuated when the carrier velocity is less than the sound velocity and amplified when it is greater than the sound velocity. At lower frequencies (for example CdS at tens of Mc/s) the term $\omega^2/\omega_c\omega_D$ is much less than 1 in which case α has a maximum value which is

$$\alpha_{\substack{\max \\ \min}} = \pm \frac{K^2}{4} \frac{\omega}{v} \qquad \ldots\ldots(7)$$

when $\omega_c = \gamma\omega$. (This expression assumes that any value of drift velocity is available to us whereas in fact we are limited by drift velocities attainable in practice.) Under these conditions the gain per cm is directly proportional to the frequency and to the electromechanical coupling constant.

In the theory discussed so far no consideration has been given to the possibility of trapping of the carriers. Hutson and White[2] assume that the trapping relaxation time T_τ is much less than $1/\omega$ and that this can be taken into account by taking the drift mobility μ to be less than the Hall mobility by a factor f. Ishiguro, Uchida, Sasaki and Suzuki[7] have pointed out that if τ_t is comparable to $1/\omega$ the trapped electrons may be released in the wrong phase and have modified the theory to take this into account, using an expression for f which is complex and frequency dependent. Their modified theoretical expression for α is in closer agreement with the asymmetrical curves observed experimentally at frequencies around 100 Mc/s and low conductivities. This leads them to conclude that in CdS τ_t may be in the range $10^{-7}-10^{-9}$ seconds. The mobility of their samples appears to be low—about 80 $cm^2/V\,s$ which is at least half the value which we usually find in a good amplifier.

4. Experimental Results

Most of the experimental results obtained so far have been in the frequency range 10–100 Mc/s. In a typical experimental arrangement (Fig. 3) a crystal is cut to cubic shape of, say, 5 mm side so that the C axis (in the case of hexagonal structures) is perpendicular to two opposite faces. These faces (in the case of the longitudinal wave amplifier) are then polished flat and parallel and covered with a metallic layer which serves both to provide ohmic contacts and to bond transducers to the crystal. The transducers are usually of quartz and are resonant at the operating frequency. The ohmic contacts serve both to apply the d.c. drift field across the crystal and the r.f. fields across the transducers.

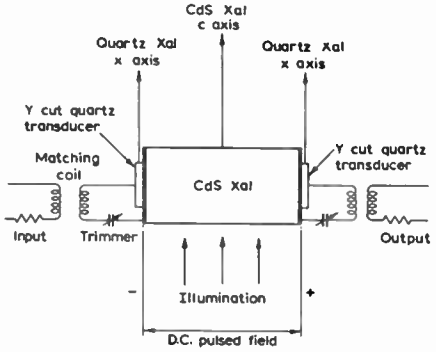

Fig. 3. Transverse wave acoustic amplifier showing supplies and crystal orientation requirements.

Because of the limited dissipation of the crystal it is usual to pulse the drift field. It is difficult to design transducers to present a good match to the acoustic wave and therefore the drift field is only applied for a time sufficient for one carrier transit through the

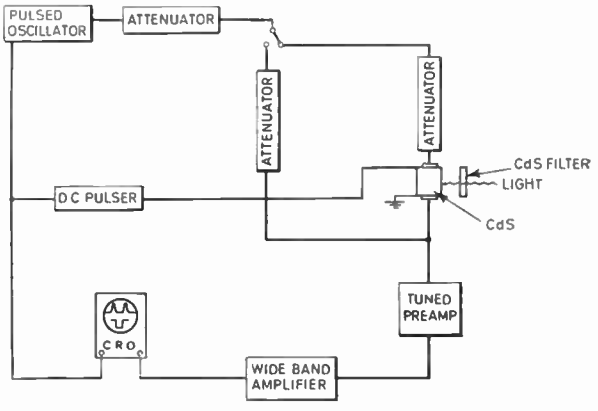

Fig. 4. Acoustic amplifier experimental apparatus.

crystal, thus avoiding the danger of 'round trip' oscillations caused by reflections at the acoustic terminations. The r.f. drive to the transducers is usually also pulsed and the drift field pulses are timed so that they occur during the periods when the acoustic pulses are applied. A block diagram of the equipment is shown in Fig. 4.

4.1 *Results with CdS*

By far the greatest number of results obtained so far have been with CdS. Typical of our results is the curve of attenuation against drift field as shown in Fig. 5.

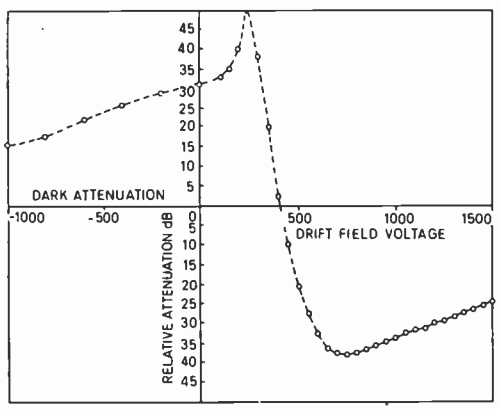

Fig. 5. Typical experimental curve of a transverse wave amplifier. Attenuation vs. drift voltage at 45 Mc/s $\omega_c = 6{\cdot}5 \times 10^7$.

In CdS the carriers have usually been obtained by photo-excitation and the zero attenuation level is taken to be that given by the dark crystal with no drift field applied. The field at which the curve crosses the axis from attenuation to gain is that which produces a carrier drift velocity equal to the known velocity of sound in the crystal and therefore enables the drift mobility of the carriers to be calculated. The gain and attenuation parts of the curves are not symmetric, as is predicted by the simple theory[2] and the maximum gain is usually considerably less than that predicted.[3] These discrepancies are probably in large part attributable to the affects of trapping as discussed in Section 3.

Gains of up to 100 dB/cm have been obtained at 45 Mc/s with transverse waves. Drift mobilities are typically up to 150 $cm^2/V\,s$ and Hall mobilities are around 250 $cm^2/V\,s$. Saturated acoustic powers of 5 W/cm^2 have been reported.[8] Much of the electronic gain is lost in coupling to and from the crystal, but the net gain obtained by us with transverse waves at 60 Mc/s is typically 20 dB. Electronic gains have been reported[5] at frequencies around 1 Gc/s.

4.2 *Selection of CdS Crystals*

To obtain gain at frequencies of about 50 Mc/s in CdS the optimum resistivity is about 10^4 ohm cm. This we have normally obtained by using crystals with a dark resistivity of 10^6 ohm cm and illuminating with an intensity of approximately 200 ft candles to produce the necessary carriers. However, we have found that crystals with the desired dark resistivity show widely different behaviour and many, in fact, do not amplify at all. Of those that have amplified, drift mobilities calculated from the cross-over field have been as low as 50 $cm^2/V\,s$. Different crystals have shown wide variations both in magnitude of photo-conductivity and speed of response.

A strong indication of whether a crystal will give gain may be obtained by performing a *V-I* plot on a small sample of the material. When the field reaches a value at which the velocity of the carriers just exceeds that of sound, if there is interaction with acoustic waves acoustic noise will be amplified, extracting energy from the carriers, reducing their mobility and hence producing a knee in the *V-I* plot. The amount by which the slope changes is a measure of the intensity of the interaction (Fig. 6). A final method of selection we have used is to cut the crystal on two of its *C* planes and press it between two quartz-rods having transducers on their outer ends and using grease to bond to the crystal. The attenuation of longitudinal waves through the crystal can be measured and for a potentially good crystal this will increase by 20 dB when the crystal is illuminated.

To summarize, the crystal should have a dark resistivity of 10^6 ohm cm which can be reduced to 10^4 ohm cm by illumination. It is not known definitely whether good amplifiers can be made with material of 10^4 ohm cm extrinsic resistivity, the preference for optically produced carriers may be associated with the higher density of scattering centres in material of lower resistivity. However, there does appear to be evidence that a high photo-response is important and that the response should be fast, indicating a short trapping relaxation time. The drift mobility should be $> 150\ cm^2/V\,s$, partly because a low mobility material will require high drift fields and increase the dissipation but probably also because it is an indication of trap density. The *V-I* plot should show a marked change in slope as the carriers exceed the sound velocity and finally the acoustic attenuation should rise at least 20 dB when the crystal is illuminated. If these conditions are successfully satisfied then the crystal can be made up into an amplifier with confidence that it will have a good performance. The reasons for the poor interaction found in some crystals may include strain and dislocations but no study of these factors has so far been reported.

4.3 *Other Piezo-electric Materials*

Acoustic gain has also been reported in CdSe,[9] GaAs[10,11] and in ZnO.[5] The properties of these materials are compared with CdS in Table 1.

Table 1

	Crystal structure	Sound velocity m/s L	Sound velocity m/s T	k^2	μ_H	Band gap eV
CdS	Hexagonal	4470 $\parallel C$	1700 $\perp C$	0·04	200–350	2·4
CdSe	Hexagonal	3860 $\parallel C$	1590 $\perp C$	0·02	500	1·7
GaAs	Cubic		3350[110]	0·0024	2000–7000	1·4
ZnO	Hexagonal	6100 $\parallel C$	2730 $\perp C$	0·06	180	3·2

CdSe has the same hexagonal crystal structure as CdS but has a coupling constant only half as large. The mobility is higher (500 $cm^2/V\ s$) while the acoustic velocities are lower, giving gain at lower fields and to some extent counter balancing the effects of the lower coupling constant. An acoustic gain of 10 dB at 45 Mc/s has been observed with longitudinal waves in material having a dark resistivity of 2×10^6 ohm cm and a resistivity of $2{\cdot}5 \times 10^4$ ohm cm when illuminated.[9] As the band gap is 1·7 eV the carriers are released by infra-red radiation. The photo-response time is fast because of smaller trapping effects and for the same reason the drift mobility is close to the Hall mobility. The material is brittle and therefore difficult to prepare, and tracking occurs readily across the surface at fields in the neighbourhood of those required for amplification.

GaAs has a cubic structure and therefore interaction is only possible with transverse waves. The coupling constant is more than an order of magnitude lower than that of CdS and at present it is difficult to obtain suitable material of 10^4 ohm cm resistivity which is optimum for operation at about 50 Mc/s. It therefore may turn out to be a more attractive material at higher frequencies when higher gains per unit length will be available. The material has a very high mobility, which reduces the power dissipation, and it also has the attraction that it can be readily doped n or p type, making integral transducers more readily realizable. (See Section 5.)

ZnO has the highest coupling constant of the materials discussed, although the sound velocities are

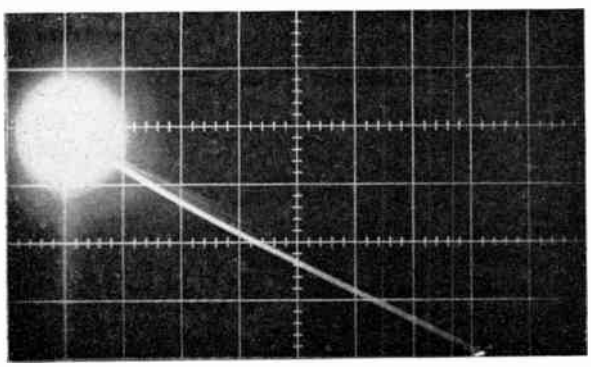

(a)
812 2-S (1) $E \parallel C$ 500 V/cm

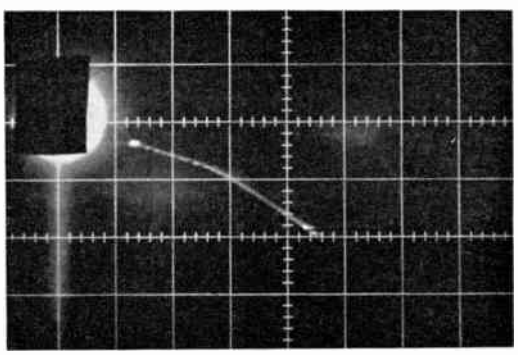

(b)
B.T.1 $E \perp C$ 500 V/cm

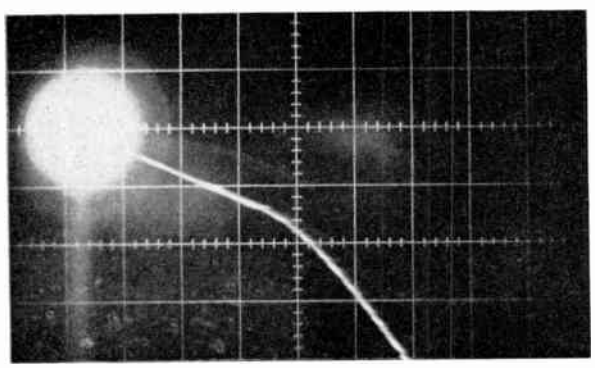

(c)
A.L.7 $E \parallel C$ 200 V/cm

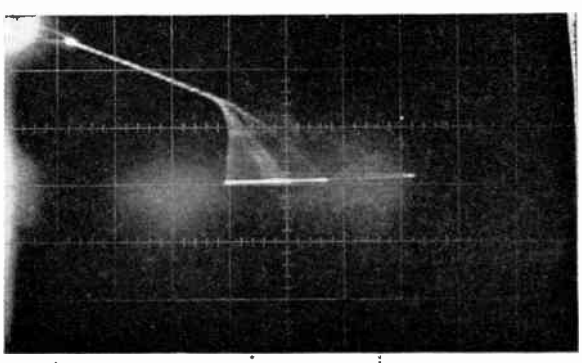

(d)
007-7-P $E \perp C$ 500 V/cm

Fig. 6. Voltage-current plots for different samples. Voltage on vertical axis.

half as high again as those of CdS and the mobility is slightly lower. At the moment the material is not readily available in large single crystals or at resistivities of 10^3 ohm cm. However, it is believed that considerable efforts are being made to produce suitable material and it will presumably become available before long.

CdS and ZnO are the most promising of the piezo-electric semiconductors whose properties have been studied in detail. However, there are other piezo-electric materials such as tellurium in which interaction with drifting carriers may be obtained.

4.4 *Microwave Operation*

There is an upper limit to the frequency at which the acoustic amplifier will work, given by the maximum energy interchange which can occur in an electron-phonon collision. This is about 100 Gc/s. There are, however, considerable problems to be overcome before this limit is approached. In the first place, different transducer techniques have to be developed as will be discussed in greater detail in Section 5. Secondly, the acoustic loss, which is generally so low at v.h.f. compared to the available gain that it may be ignored, will become the dominant factor.

Acoustic loss arises from the scattering of the ordered phonons of the acoustic wave either by the random thermal phonons or by inhomogeneities of the material. Both will increase as the frequency increases. The first may be reduced by cooling the crystal but the device then becomes less useful. If the losses due to crystal inhomogeneities are to be minimized the material must be grown in such a way that dislocations, impurities and non-stoichiometry are reduced to a minimum. No figures of acoustic loss for amplifier materials at microwave frequencies have been published and measurements are complicated by the acousto-electric interaction on which the amplifier is based. In theory, the losses increase with the square of the frequency, making extrapolation into the microwave range hazardous.

At microwave frequencies acoustic wavelengths are comparable with free space electromagnetic wavelengths in the optical region so that the opposite faces of the crystals must have a flatness and parallelism of high optical quality. CdS is a rather soft material and difficult to polish. Flatness can be achieved by careful techniques but parallelism is more difficult. It may be that these problems will determine the highest frequencies attainable, but they will be eased if much harder materials become available. The problem is, of course, eased to some extent by the fact that as the frequency increases, so does the gain per unit length. It is therefore possible to use a shorter crystal and also possible to preserve a plane wavefront in a crystal with a smaller cross-sectional area.

4.5 *Deformation Potential Amplifier*

It is possible to obtain acoustic amplification in semi-conductors which are not piezo-electric, such as silicon and germanium.[12,13] When a crystal is strained the conduction band is disturbed. An acoustic wave will be accompanied by an a.c. variation in the level of the conduction band which, through relaxation mechanisms will tend to redistribute the carriers. Unlike the piezo-electric effect, this interaction is small at low frequencies but it increases with frequency until at 10–100 Mc/s it is comparable with piezo-electric coupling. However, to study phonons at 10 Gc/s it is necessary to cool to low temperatures as the attenuation due to phonon-phonon scattering is very high. At 10°K the mobility of CdS, say, is about 5 $cm^2/V\,s$ while that of Ge is about 10^4 $cm^2/V\,s$ and hence much less power is needed to get the same amplification. These figures are quoted for cold electrons. It has been shown[11] that much lower values can be expected in reality, as the applied field will heat the electrons. This must, of course, apply to both deformation potential and piezo-electric amplifiers so that the former will still have advantages in microwave devices.

5. Electro-Acoustic Transducers

Because of the very low dispersion of acoustic waves at v.h.f. and microwave frequencies the gain mechanism is intrinsically very broad band. Octave instantaneous bandwidths are possible for gains in the region of 50 dB.[6] However, when used as an amplifier of electrical signals, the bandwidth is severely limited by the transducers which have, in general, very narrow band and high insertion loss. This problem is, in part, a fundamental one, deriving from the fact that acoustic wavelengths are about five orders of magnitude smaller than the corresponding electrical wavelengths.

5.1 *Quartz Crystal Transducers*

For the frequencies in the region of 10–500 Mc/s the most readily available transducer is the resonant quartz plate which can be cut to give either longitudinal or transverse waves. Although transducers are available with fundamental frequencies up to 60 Mc/s, they are very thin and fragile at the higher frequencies and a fundamental of about 10 Mc/s is usually chosen, overtones being used to obtain frequencies up to 500 Mc/s. Typically, such transducers have a loss of 16 dB with a bandwidth of 5%.

It is necessary to bond such transducers to the amplifying crystal in such a way that as much as possible of the energy generated is transmitted into the crystal. With longitudinal waves it is sufficient to wring the transducer onto the crystal with a film of grease or oil and to keep it together by pressure but for transverse waves a bond which is stiff in shear is required.

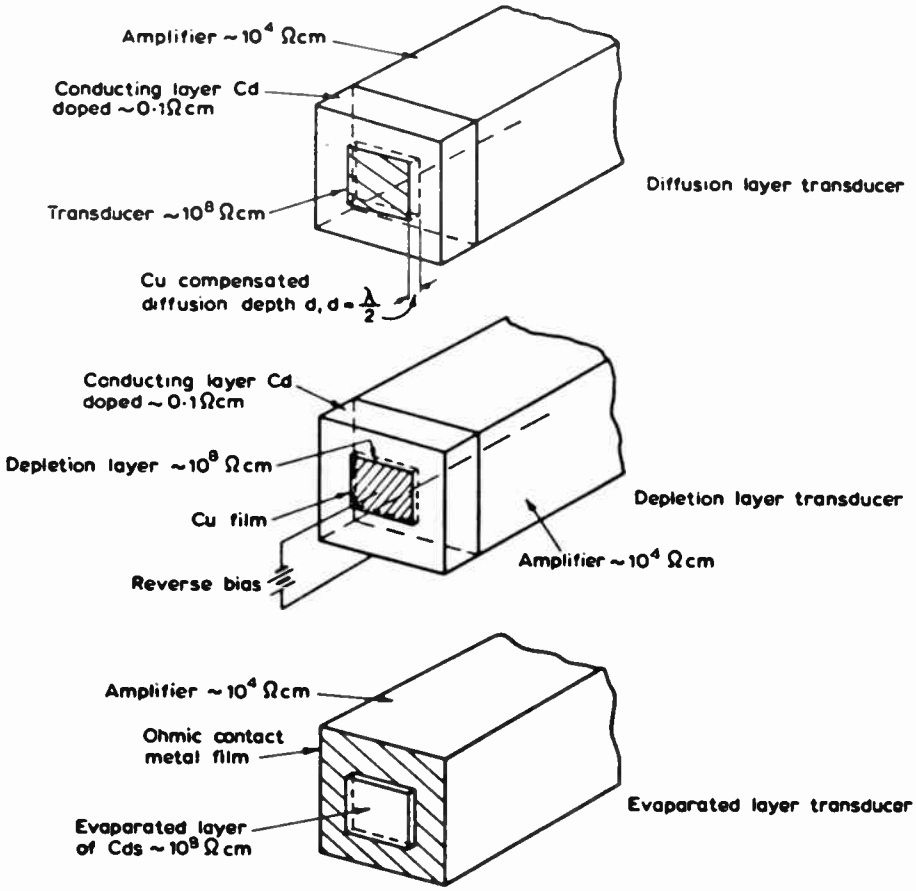

Fig. 7. Diagram of three integral transducers for use on an acoustic amplifier.

A suitable bonding material for acoustic amplifiers is indium. This has a characteristic impedance for shear waves of 10×10^6 kg/m^2 s which is not very different from the geometric mean of quartz (10·2) and CdS (8·2) and therefore will act as a matching transformer between these two materials if it is made a quarter of an acoustic wavelength thick. It can be evaporated onto both materials with good adhesion and thermocompression bonds can be made at low enough temperatures (160°C) not to change the properties of the CdS. If the CdS surface is first mechanically polished and then slightly etched the indium acts as a good ohmic contact.

At frequencies of 1 Gc/s and above the tuned quartz transducer becomes impracticable. In their experiments on the attenuation of quartz, Bommel and Dransfeld[14] have launched acoustic waves by inserting the end of a quartz rod into the high E field region of a microwave cavity. Because of the low coupling the insertion loss of such a transducer is high. The quartz element is not resonant and therefore the bandwidth of the transducer is determined by the cavity.

5.2 *Integral Layer Transducers*

In making high frequency transducers, two problems arise. In order to obtain reasonable coupling with the materials available, which usually have low electromechanical coupling coefficients, the transducers must be resonant and at high frequencies they become extremely fragile. To obtain acoustic amplification it is necessary to launch and propagate an acoustic wave which has a wave front which is plane to a fraction of a wavelength. As the frequency rises it becomes more and more difficult to make acoustic bonds which are sufficiently thin to have acceptable loss.

An alternative approach to this problem is to make the transducer integral with the amplifying crystal either by modifying a thin surface layer of the crystal or by evaporating onto it a thin layer of modified material. In this way, only the surface of the crystal has to be polished to the necessary degree of flatness; techniques exist for the diffusion or deposition of thin layers of material with very great accuracy and the

need for a bonding material is eliminated. Three types of integral layer transducers have so far been proposed; the depletion layer, the diffused layer and the evaporated layer (See Fig. 7).

The material of which piezo-electric amplifiers are made must, of necessity, be semiconducting and if a surface layer of this material is to be used as a transducer it must in some way be made insulating. White[15] first suggested that this might be done by forming a depletion layer at the surface of the material. In one arrangement, a metal film is deposited on the surface to form a rectifying contact and is then reverse biased. The object is to form a depletion layer half an acoustic wavelength in depth which would act in the same way as a tuned quartz plate. It should be possible to tune the transducer by changing the bias field. However, no satisfactory use of this type of transducer has since been reported.

It was next suggested by Foster[16,17] that an insulating layer might be produced by diffusing in impurity atoms. He diffused copper into CdS to make transducers which operated in the range 100 Mc/s to 1 Gc/s for longitudinal waves and up to 300 Mc/s for shear waves. Conversion losses from 7 to 28 dB with 15% bandwidth were obtained over this frequency range. The construction of a CdS amplifier using this principle has been described by Wada.[18] A rectilinear crystal of 10^3 ohm cm was doped on all surfaces by diffusing in Cd, covering the crystal with a thin layer of conducting material. This layer was then etched away from four sides but left on two opposite faces onto which copper was then evaporated. The copper was then diffused in to form an insulating layer, backed by a high conductivity Cd doped layer which acted as one electrode for the transducer and as a contact for the d.c. bias field for the semiconducting crystal.

Finally, it has been shown that when CdS is evaporated onto a flat substrate under controlled conditions of heat and vacuum hard adherent polycrystalline layers are formed with a preferred orientation of the *C* axis perpendicular to the substrate surface.[16,19,20] Such a layer is usually highly conductive but the conductivity may be reduced by further heat treatment. It has also been shown that if the substrate is inclined at an angle to the direction of deposition the layer will have its *C* axis inclined to the substrate and, under some conditions, it can be parallel to the substrate and be used for launching shear waves. Using these techniques Foster[16] has constructed longitudinal transducers resonant at frequencies up to 2 Gc/s with 17 dB conversion loss and 20% bandwidth. De Klerk and Kelly[21] report making transducers with fundamental resonances up to 3 Gc/s and operating them at 9 Gc/s. As the structure of the evaporated layer is independent of the substrate it should be possible to first evaporate a thin metallic layer to provide an ohmic contact to the amplifier crystal but the use of such a geometry has not yet been reported.

5.3 *Nickel Film Transducers*

Transverse waves have been launched along a quartz rod by means of a thin nickel film deposited on the end of the rod.[22] If a d.c. magnetic field is applied along the axis of the rod and the film is subjected to an a.c. magnetic field in the plane of the film, at ferromagnetic resonance the surface will undergo a rotational shear motion round the d.c. field and emit circularly polarized acoustic waves into the quartz. Using a film 18,000 Å thick, Bommel and Dransfeld launched acoustic waves at 1 Gc/s for which a magnetic field of 7 kilogauss was required.

5.4 *Yttrium Iron Garnet Transducers*

Spin waves may be launched down a rod of yttrium iron garnet (YIG)[23,24] by an r.f. magnetic field in the presence of a d.c. magnetic field and if the latter is non-uniform, when the spin waves reach a point in the

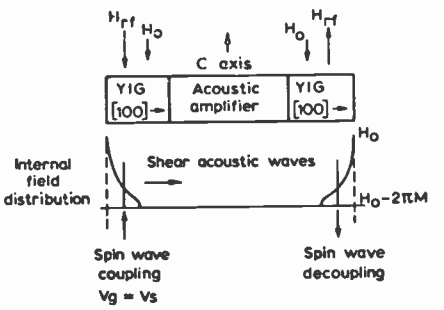

Fig. 8. Yttrium iron garnet transducers on acoustic amplifier.

rod corresponding to a critical (lower) value of field they can couple to acoustic waves with a total transfer of energy. Conversely, an acoustic wave launched in a region of low field will couple to spin waves when the field has risen to the critical value. Such non-uniform field distributions may be conveniently produced inside a YIG rod of uniform cross-section when it is placed in a uniform external magnetic field. If two such pieces of YIG are used as the transducers for an acoustic amplifier (Fig. 8), the delay in the transducers, and hence the delay in the amplifier as a whole, may be varied by changing the magnitude of the d.c. magnetic field and hence altering the point in the transducers at which conversion from spin waves to acoustic waves takes place. A notable advantage of YIG is its low acoustic loss at high frequencies.

5.5 *Optical-acoustic Transducers*

We have already commented that the basic difficulty in transducing from an electro-magnetic signal to an acoustic signal is the great difference in wave-

length of the two types of propagation. However, when we get to optical frequencies this discrepancy disappears and this fact makes it possible to transduce from an electromagnetic signal at optical frequencies to an acoustic signal at v.h.f. without encountering this problem. If the incoming optical signal and a locally generated optical signal of different frequency are allowed to impinge on a photo-conductor from slightly different angles an interference pattern of illumination is set up which travels across the surface of the photo-conductor with a phase velocity which depends on the difference frequency and the angle between the beams (Fig. 9). Carriers will be created by this illumination and, if a suitable drift field is imposed, they will travel along in phase with the generating illumination. In this way an alternating current is created in the photo-conductor which can be made to travel at the acoustic velocity in that medium. If an acoustic amplifier crystal is used as the photo-conductor the alternating current will generate an acoustic

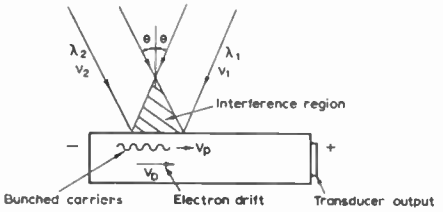

$$v_p = \frac{v\lambda}{2\sin\theta}$$

$$\lambda = \frac{\lambda_1 + \lambda_2}{2}$$

$$v = v_1 - v_2$$

Fig. 9. Optical input travelling-wave mixer and acoustic amplifier.

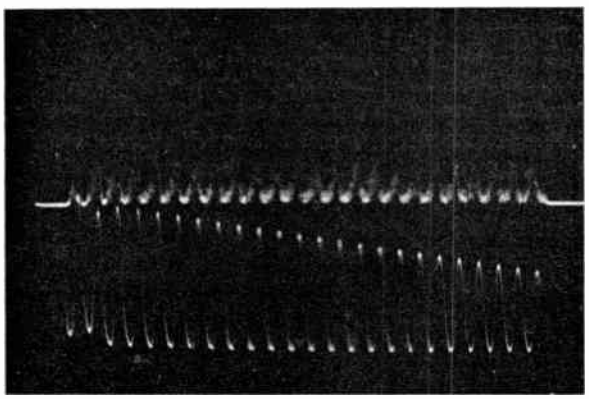

(a)
Current 50 mA/div
Time 10 μs/div

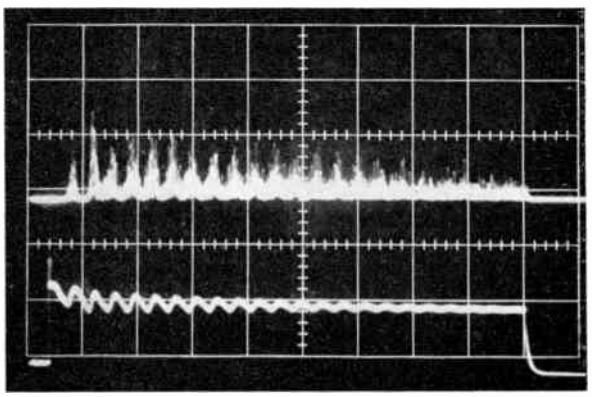

(b)
Decay of acoustic noise with current oscillations.

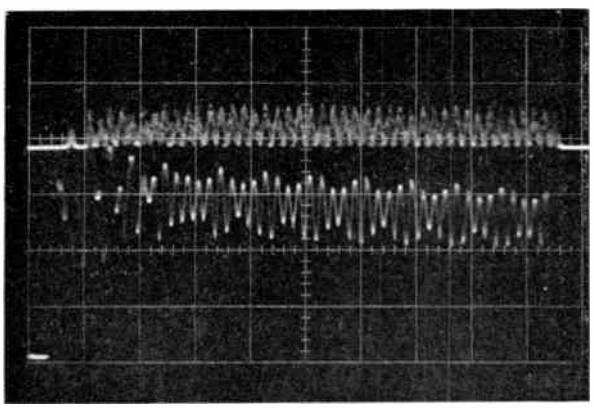

(c)
Current 100 mA/div
Time 10 μs/div
Oscillations immediately after crystal taken above gain voltage.

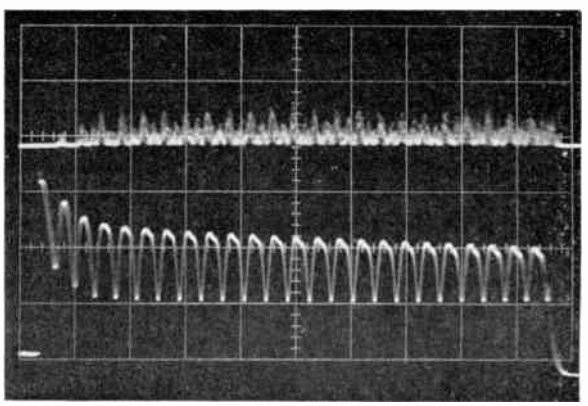

(d)
Current 100 mA/div
Time 10 μs/div
Same as (c) 15 seconds later.

Fig. 10. Current oscillations in CdS.

wave at the difference frequency which will then be amplified in the normal way and may be extracted by means of a conventional transducer. The principle of travelling wave mixing has already been demonstrated,[25] but the device has not yet been tried as an input transducer for an acoustic amplifier.

6. Use of Electron-Phonon Interactions as a Diagnostic Tool to Study Related Phenomena

The studies of the interactions between electrons and phonons in piezo-electric semiconductors give good agreement between the theoretical and experimental results. The confidence in the theoretical background of the acoustic amplifier makes this type of experimental arrangement an important analogue for studying related phenomena. An example of this is the relation between the high field instabilities in GaAs and CdS.

In a companion paper,[26] the concept of 'virtual cathode' is introduced to explain the transit time obtained from the period of the oscillation when this differs from the calculated time taken for the charge carriers to travel from one electrode to the other. In crystals of CdS which exhibit strong interaction, it is possible to obtain oscillations[27,28] very similar to the Gunn effect in GaAs[29] but with the carriers travelling at around $1{\cdot}75 \times 10^5$ cm/s in CdS as opposed to 10^7 cm/s in GaAs.

Figure 6(d) is a photograph of the V/I characteristics for a crystal exhibiting very strong interaction. Figure 10(a) shows the oscillations obtained when d.c. bias is applied for periods of around 100 microseconds. The current minima are associated with pulses of acoustic noise (upper trace). These oscillations are compared with the Gunn effect because in both cases the period of the oscillations corresponds to a single transit of the carriers from cathode to anode. If the amplifier were oscillating, the period would correspond to the 'round trip' time and the acoustic output would be continuous.

When the CdS crystal is uniformly illuminated the period corresponds to the transit time at acoustic velocity from one end of the crystal to the other. If an inhomogeneity is deliberately introduced part of the way along the crystal, this acts as an enhancing nucleation source from which instabilities are launched.

Figure 11 shows the results of an experiment where a narrow slit of light was used to launch the instabilities at some distance from the negative electrode. The graph gives the variation in the period of oscillation as the slit is moved towards the anode.

These experiments demonstrate the validity of the virtual cathode concept and may lead to a better understanding of the domain formation phenomena associated with high field instabilities.

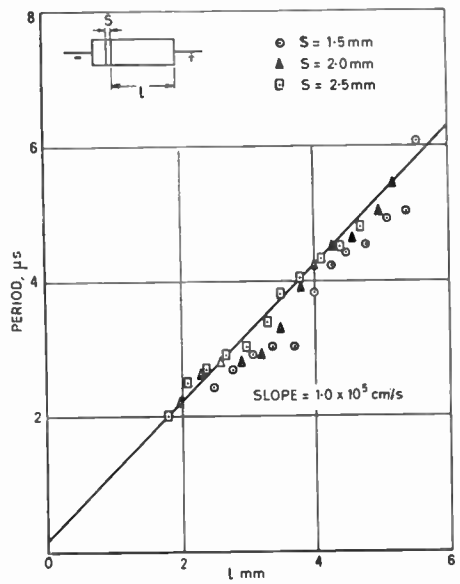

Fig. 11. Period of current oscillation vs. distance of light slit from anode.

The fact that useful interaction can be obtained between travelling electric fields in the semiconductor and drifting carriers gives hope that analogues of microwave tubes may be possible using the carriers in a semiconductor in place of the electrons in an electron beam. Solymar and Ash[30] have developed a general theory of interaction which includes electron beam tubes as a special case and have obtained an expression for Pierce's parameter C for a solid-state travelling-wave amplifier. By showing how it is related to the electro-mechanical coupling constant of the piezo-electric amplifier, the conditions under which such a device might give gain are derived.

7. Conclusions

The progress of work, both theoretical and experimental, on the acoustic amplifier has been surveyed. As an amplifier of acoustic waves the device is capable of very high gains at v.h.f. Thus it has immediate applications in conjunction with acoustic delay lines at these frequencies and may shortly be available as a component of low-loss delay lines at microwave frequencies. As an electrical amplifier it is not at present very competitive but there is good hope that, with the development of new transducers and improved materials a useful, compact microwave amplifier will emerge.

Of equal, if not greater, importance is the basic information which the study of acoustic amplification is providing for the development of bulk solid state microwave devices which rely on the interactions between drifting carriers, electromagnetic waves and the lattice.

8. References

1. A. R. Hutson, J. H. McFee and D. L. White, 'Ultrasonic amplification in CdS', *Physical Review Letters*, **7**, p. 237, 1961.
2. A. R. Hutson and D. L. White, 'Elastic wave propagation in piezoelectric semiconductors', *J. Appl. Phys.*, **33**, pp. 40–7, January 1962.
3. D. L. White, 'Amplification of ultrasonic waves in piezoelectric semiconductors', *J. Appl. Phys.*, **33**, p. 2547, 1962.
4. A. R. Hutson, 'Acousto-electrical explanation of non-ohmic behaviour in piezoelectric semiconductors and bismuth', *Physical Review Letters*, **9**, p. 296, October 1962.
5. J. H. McFee, 'Ultrasonic amplification and non-ohmic behaviour in CdS and ZnO', *J. Appl. Phys*, **34**, pp. 1548–53, May 1963.
6. K. Blotakjaer and C. F. Quate, 'The coupled modes of acoustic waves and drifting carriers in piezoelectric crystals', *Proc. Inst. Elect. Electronics Engrs*, **52**, pp. 360–77, April 1964.
7. I. Uchida, T. Ishiguro, Y. Sasaki and T. Suzuki, 'Effect of trapping of free carriers in CdS ultrasonic amplifiers', *J. Phys. Soc. Japan*, **19**, pp. 674–80, May 1964.
8. T. Ishiguro, I. Uchida and T. Suzuki, 'Ultrasonic amplification characteristics and non-linearity in CdS', *I.E.E.E. Convention Record*, **12**, Pt. 2, pp. 91–101, March 1964.
9. T. A. Midford, 'Ultrasonic amplification in cadmium selenide', *J. Appl. Phys.*, **35**, pp. 3423–4, November 1964.
10. J. R. A. Beal and M. Pomerantz, 'Acousto-electric effect of microwave phonons in GaAs', *Physical Review Letters*, **13**, pp. 198–200, August 1964.
11. E. M. Conwell, 'Amplification of acoustic waves at microwave frequencies', *Proc. I.E.E.E.*, **52**, pp. 964–5, August 1964.
12. J. Mertsching, 'Comparison of ultrasonic effects in piezoelectric and simple deformation potential semiconductors', *Phys. Status Solidi*, **4**, p. 453, 1964.
13. G. Weinreich, T. M. Sanders and H. G. White, 'Acousto-electric effect in n-type germanium', *Physical Review*, **114**, No. 1, pp. 33–44, April 1959.
14. H. Bommel and K. Dransfeld, 'Excitation and detection of hypersonic waves in quartz', *Physical Review*, **117**, p. 1245, March 1960; see also by the same authors: *Physical Review Letters*, **1**, p. 234, 1958, and *Physical Review Letters*, **2**, p. 83, July 1959.
15. D. L. White, 'The depletion layer transducer', *Trans. I.R.E. on Ultrasonic Engineering*, **UE-9**, pp. 21–27, July 1962.
16. N. F. Foster, 'Ultra-high frequency cadmium sulphide transducers', *Trans. I.E.E.E. on Sonics and Ultrasonics*, **UE-11**, pp. 63–8, November 1964.
17. N. F. Foster, 'The performance of dilatational mode cadmium sulphide diffusion layer transducers', *Trans. I.E.E.E. on Sonics and Ultrasonic*, **UE-10**, pp. 39–44, July 1963.
18. N. Chubachi, M. Wada and Y. Kikuchi, 'A new ultrasonic amplifier device of CdS crystal with integrated diffusion layer transducers', *Japanese J. Appl. Phys.*, **3**, pp. December 1964.
19. J. Dresner and F. V. Shallcross, 'Crystallinity and electronic properties of evaporated CdS films', *J. Appl. Phys.*, **34**, pp. 2390–5, August 1963.
20. R. R. Addiss Jr., 'Crystallisation of cadmium sulphide films', 1963 *Transactions of the 10th National Vacuum Symposium of the American Vacuum Society* (New York MacMillan 1963), pp. 354–63.
21. J. De Klerk and E. F. Kelly, 'Coherent phonon generation in the gigacycle range via insulating cadmium sulphide films', *Applied Physics Letters*, **5**, No. 1, pp. 2–3, July 1964.
22. H. Bommel and K. Dransfeld, 'Excitation of hypersonic waves by ferromagnetic resonance', *Physical Review Letters*, **3**, p. 83, July 1959.
23. W. Strauss, 'A new approach to high frequency delay lines', *Trans. I.E.E.E. on Sonics and Ultrasonics*, **UE-11**, pp. 85–9, November 1964.
24. J. H. Collins and G. G. Neilson, 'Garnet delay lines at microwave frequencies', *British Communications and Electronics*, **11**, pp. 186–91, March 1964.
25. R. J. Strain and C. C. Tooke, 'The travelling wave photoconductive mixer', to be published.
26. J. S. Heeks, A. D. Woode and C. P. Sandbank, 'The mechanism and application of high field instabilities in GaAs', Proceedings of the Symposium on Microwave Applications of Semiconductors, London 1965. Reprinted in *The Radio and Electronic Engineer*, **30**, No. 6, pp. 377–87, December 1965.
27. J. Okada and H. Matino, 'Continuous oscillations of acousto-electric current in CdS', *Japanese J. Appl. Phys.*, **3**, pp. 698–704, November 1964.
28. H. Kroger, E. W. Prohofsky and H. R. Carleton, 'Current oscillations and collective waves in CdS', *Physical Review Letters*, **12**, p. 555, May 1964.
29. J. B. Gunn, 'Instabilities of current in III–V semi-conductors', *IBM J. Res. and Develop.*, **8**, p. 141, April 1964. See also by the same author 'Instabilities of Current and Potential Distribution in GaAs and InP', IBM Research Paper R.C. 1216, June 1964.
30. L. Solymar and E. A. Ash, 'Some travelling wave interactions in semiconductors. Theory and design considerations', to be published.

Manuscript first received by the Institution on 15th April 1965, and in final form on 18th May 1965. (Paper No. 1030/EA26.)

# of current interest . . .

PAL Colour Television System for B.B.C. 2

On Thursday, 3rd March, the Postmaster-General, Mr. Anthony Wedgwood Benn, announced in Parliament the British Government's decision to start colour television transmission towards the end of 1967, using the PAL system with 625-lines on B.B.C. 2. The decision is subject to one reservation: next June there is to be a C.C.I.R. conference in Oslo to consider the choice of system which offers the best prospect for common use in Europe. Unless the Oslo conference were to show that another system found general acceptance, the decision to adopt the PAL system would stand.

The B.B.C. aims to begin with about four hours' colour television a week (in addition to transmission of programmes already in colour on tape or film); this would rise to about ten hours a week within a year and it is estimated that the cost to the Corporation of colour transmission would be from £1 million to £2 million a year, against which it has made provision. Estimates of the cost of receivers suggest that they would start at about £250 each and the Postmaster-General said that the industry was confident that sufficient qualified engineers would be available for the necessary work through transferring from other aspects of television engineering.

Precise Engineering Measurements Using Laser Light

A new optical method, known as 'holography', is being applied at the National Physical Laboratory for precise measurements in engineering.

Holography is a type of photography without lenses originally proposed in 1947 by Dr. D. Gabor, now Professor of Applied Electron Physics at the Imperial College of Science and Technology. At that time it was not possible to develop the technique into a practical tool because of the lack of a light source of sufficient coherence and intensity. Because the laser generates a continuous train of light waves instead of incoherent 'bursts' of waves, it overcomes this problem.

In holography, the laser, the object to be studied, and a photographic plate are so arranged that part of the laser beam falls on the object and is reflected back to the plate, while another part of the beam passes directly to the plate. Where the beams meet interference patterns are formed and these are recorded on the plate. The image is reconstructed when the developed plate is illuminated by a coherent light source.

The National Physical Laboratory's work has shown that holography can be used to carry out interferometric measurements on rough surfaces of ordinary 'engineering' shapes. Hitherto these measurements, which record small changes caused by mechanical strain or thermal expansion, have only been possible where the surface is highly polished and of a simple shape, such as flat or spherical.

Other promising uses for this technique are in the measurement of vibration patterns of surfaces, the examination of the insides of tubes, and in observations through imperfect windows. It may also be used in the inspection of a series of nominally identical products if of a sufficiently good surface finish.

First Educational Television O.B. Unit

The University of Glasgow has recently taken delivery of the first television outside broadcast unit designed for an educational establishment in the United Kingdom. The four-camera unit, supplied by the Marconi Company, contains all the facilities normally found in an educational studio control room. The unit will be used to record lectures on video tape for subsequent use by the University of Glasgow and associated educational establishments and will also be used to link lecture theatres within the University.

Three light-weight vidicon television studio cameras fitted with electronic viewfinders are provided. Two have four-lens turrets and the other is fitted with a zoom lens. The cameras are simple to use and can be operated at distances of up to 500 ft from the vehicle using the cables provided. The camera complement is completed with a caption camera. This is normally housed in the vehicle, but can be used externally.

Full vision mixing facilities are provided for the four cameras and sound mixing for up to 8 microphones and 4 high-level sources. In addition to the normal communication facilities between the producer and the camera and sound crews, facilities are provided for students in the linked lecture theatres to communicate with the lecturer.

A keynote of the new unit is the simplicity of operation. None of the controls, which are situated on a control desk beneath five $8\frac{1}{2}$ in monitors, have to be operated by engineers during transmission.

The caption camera is placed to one side of the control panel and can accept ordinary artwork or transparent material such as that used to illustrate lectures. Size of material is not important as the caption camera is fitted with a zoom lens.

Distribution amplifiers contained in the vehicle each provide five output signals. These can be used to feed lecture theatres or video tape recorders. A table is provided in the vehicle's control room for a helical scan video recorder.

U.D.C. 621.317.373:621.396.6:534.76

Measurement of Phase Errors in the Pilot-Tone System for Stereophonic Broadcasting

By

G. J. PHILLIPS, Ph.D., M.A., B.Sc., C.Eng.†

Summary: In the pilot-tone system for stereophonic broadcasting, any small phase error of the pilot signal may be deduced from a waveform display of the multiplex signal, when using an appropriate modulating signal. An expression is derived for the error in terms of characteristics of the display, and a simple approximation is also given.

1. Introduction

The pilot-tone system for stereophonic broadcasting has been described in a past issue of the *Journal*.[1] The principle of the system is that the sum of the left and right stereophonic signals, $A+B$, is transmitted normally by the f.m. transmitter while the difference, $A-B$, is transmitted by suppressed-subcarrier modulation, the subcarrier sidebands being fed together with the $A+B$ signal to the f.m. modulator. In addition, a 19 kc/s reference signal of controlled phase is transmitted. This pilot signal has a frequency of one half of the subcarrier frequency (38 kc/s) and enables receivers to regenerate the subcarrier component. The present contribution discusses a simple method of obtaining a quantitative measure of small phase errors of the pilot signal.

2. The Pilot-Tone System

The complete modulating signal, or multiplex signal, can be written as follows:

$$\tfrac{1}{2}(A+B) + \tfrac{1}{2}(A-B)\sin\omega t + 0{\cdot}1\sin\tfrac{1}{2}\omega t$$

where $\omega/2\pi = 38$ kc/s and the stereophonic signals A and B lie within the limits ± 1. In this expression the second term (subcarrier signal) and the third term (pilot signal) also define the required phase relation. If the phase is incorrect, the receiver will detect the difference signal inefficiently—or will even reverse the left- and right-hand channels if the pilot phase is subject to a large error.

It has been pointed out[2,3,4] that, assuming phase errors are known not to exceed 45 deg, a convenient method of checking the accuracy of phasing can be based on examination of the multiplex waveform with suitably applied modulation. The reason for the provision regarding the maximum error is that the display to be described is identical in appearance for the correct phase and for a phase error of ± 90 deg. The latter condition is equivalent to a 180 deg phase-shift of the subcarrier so that A and B become effectively interchanged. The display also repeats for a shift of 180 deg, but this is again the correct phase since it is equivalent to 360 deg phase shift at the subcarrier frequency.

† British Broadcasting Corporation, Research Department, Kingswood Warren, Surrey.

3. Method of Checking Pilot Signal Phase

The method requires a difference-channel modulation of about 10% of the maximum permitted level with zero modulation in the sum channel, i.e. $A+B=0$ and $A-B=0{\cdot}2\sin pt$ where $p/2\pi$ corresponds to a convenient modulating frequency such as 400 c/s. The type of waveform obtained when the phase is correct is shown in Fig. 1(a). If the phase of the pilot component is changed by 15 deg the waveform becomes that shown in Fig. 1(b). It will be seen that the symmetrical cusps are displaced about the horizontal line of symmetry and that the phase can be easily adjusted to reduce this displacement, the final error being much smaller than 15 deg, i.e. one or two degrees at the most.

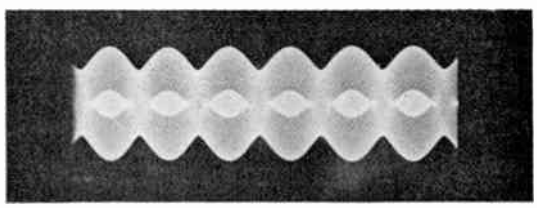

(a) Correct phase.

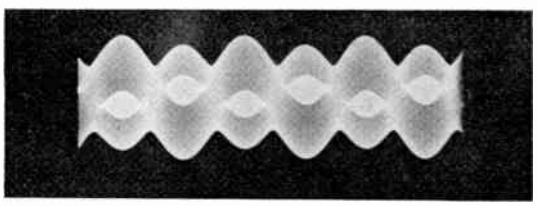

(b) Phase error of 15 deg.

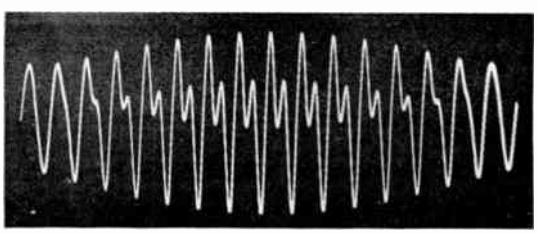

(c) Detail of waveform.

Fig. 1. Waveform display for measuring pilot phase.

The purpose of this contribution is, however, to derive a quantitative relationship between the displacement of the cusps and the phase error. It will, in fact, be shown that the displacement varies very closely in proportion to sin ϕ where ϕ is the phase error of the pilot at 19 kc/s.

Figure 1(c) shows the detailed structure of the waveform; it was obtained by using the 1/32nd subharmonic of 19 kc/s as a modulating frequency. At the pointed ends of the cusps the condition is such that the waveform F(t) passes through a point of inflection with a horizontal tangent, as illustrated in Fig. 2, at a certain time t_0. This means that the first and second differentials are simultaneously zero. Now the waveform has a fixed component at 19 kc/s and a component at 38 kc/s whose amplitude varies through the modulation cycle. Assuming the former component to have an amplitude of unity, the second component may be taken to have an amplitude a, for which the necessary conditions are fulfilled. We then have, assuming a phase lag of ϕ in the pilot signal,

$$F(t) = a \sin \omega t + \sin (\tfrac{1}{2}\omega t - \phi)$$

$$\frac{dF(t)}{dt} = a\omega \cos \omega t + \tfrac{1}{2}\omega \cos (\tfrac{1}{2}\omega t - \phi)$$

$$= 0, \text{ at } t = t_0$$

$$\frac{d^2F(t)}{dt^2} = -a\omega^2 \sin \omega t - \tfrac{1}{4}\omega^2 \sin (\tfrac{1}{2}\omega t - \phi)$$

$$= 0, \text{ at } t = t_0$$

Hence
$$\cos (\tfrac{1}{2}\omega t_0 - \phi) = -2a \cos \omega t_0 \quad \text{.....(1)}$$

$$\sin (\tfrac{1}{2}\omega t_0 - \phi) = -4a \sin \omega t_0 \quad \text{.....(2)}$$

Equations (1) and (2) may be solved in terms of t_0 and a for a given value of ϕ. But, ultimately, we wish to know only the displacement from the zero line given by the value

$$F(t_0) = \sin (\tfrac{1}{2}\omega t_0 - \phi) + a \sin \omega t_0,$$

or, from eqn. (2)

$$F(t_0) = 0{\cdot}75 \sin (\tfrac{1}{2}\omega t_0 - \phi) \quad \text{.....(3)}$$

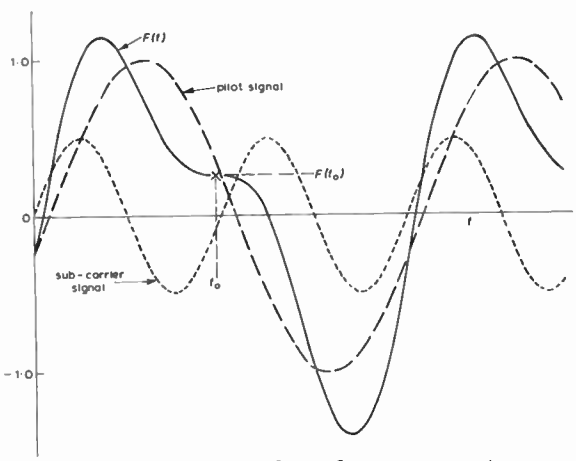

Fig. 2. Summation of waveform components.

A solution of the equations for t_0 only is therefore sufficient. Eliminating a from eqns. (1) and (2) we have†

$$\tan (\tfrac{1}{2}\omega t_0 - \phi) = 2 \tan \omega t_0 \quad \text{.....(4)}$$

By selecting a suitable range of values of ωt_0 we can derive ϕ from eqn. (4) and the corresponding value of F(t_0) from eqn. (3), and thus construct a table or curve relating ϕ and F(t_0).

It is also possible to obtain an explicit function of this relationship. Making the following substitutions in eqn. (4)

$$x = \tan \tfrac{1}{2}\omega t_0, \quad k = -\tan \phi$$

gives
$$\frac{x+k}{1-kx} = \frac{4x}{1-x^2}$$

or
$$x^3 - 3kx^2 + 3x - k = 0 \quad \text{.....(5)}$$

The real solution of this cubic equation is

$$x = k + [(1-k^2)(1-k)]^{\frac{1}{3}} - [(1-k^2)(1+k)]^{\frac{1}{3}}$$

and we select the solution† $\tfrac{1}{2}\omega t_0 = \pi + \tan^{-1} x$

Hence the final expression for the displacement is

$$F(t_0) = \tfrac{3}{4} \sin [\phi + \tan^{-1} (\tan \phi + A^{\frac{1}{3}} - B^{\frac{1}{3}})] \quad \text{.....(6)}$$

where
$$A = (1 - \tan^2 \phi)(1 - \tan \phi)$$

$$B = (1 - \tan^2 \phi)(1 + \tan \phi)$$

Note that F(t_0) is in terms of a unit corresponding to the pilot-tone amplitude; the displacement should therefore be expressed as a fraction of half the total vertical width of the waveform at its narrowest part between the cusps, where the 38 kc/s component is zero. In practice, the vertical separation of the points of adjacent cusps is more easily measured, and is then divided by the total minimum vertical width.

Table 1

Pilot phase lag and displacement of cusps

ϕ	F(t_0)	$\sin^{-1}$F(t_0)
5°	0·087	5·0°
10°	0·174	10·0°
20°	0·343	20·05°
30°	0·504	30·25°
40°	0·657	41·05°
42°	0·688	43·5°
44°	0·722	46·2°
45°	0·750	48·6°

Table 1 gives values of F(t_0) for various values of ϕ, and also the ϕ that would be deduced by assuming the

† If ωt_1 is one solution for ωt_0 in eqn. (4), then $\omega t_1 + 2\pi$ is also a solution, but only one of these two solutions will simultaneously satisfy eqn. (2). Failure to select the correct solution will lead to an error of sign in F(t_0), but this is not important if just the magnitude is required.

simple relation $F(t_0) = \sin \phi$. It is seen that the simple relation is accurate to a quarter of a degree for pilot signal phase errors up to 30 deg.

4. Acknowledgment

The author is indebted to the Director of Engineering of the British Broadcasting Corporation for permission to publish the paper.

5. References

1. J. G. Spencer and G. J. Phillips. 'Stereophonic broadcasting and reception', *The Radio and Electronic Engineer*, **27**, pp. 399–416, June 1964. (See note below.)
2. A. Csicsatka and R. M. Linz. 'The new stereo f.m. broadcasting system—how to understand the FCC specifications and generate the composite signal', *J. Audio Engng Soc.*, **10**, pp. 2–7, January 1962.
3. G. J. Phillips and J. G. Spencer. 'The Zenith-G.E. stereophonic broadcasting system', *Wireless World*, **89**, pp. 39–44, January 1963.
4. L. M. Jones. 'Planning a new f.m. stereo station', *J. Audio Engng Soc.*, **11**, p. 155, 1963.

Manuscript received by the Institution on 23rd August 1965. (Contribution No. 87/EA29).

Note:

Since the publication of the paper cited as Ref. 1 in the preceding contribution, attention has been drawn to the following typographical errors:

Page 414, Section 9, Appendix 1, Column 1, Line 29,
The expression '$\omega_a/2\pi$' should be preceded by '$f_a =$'

Column 1, last line,
In the formula for a_2, the denominator should be $\sqrt{3}$ and not 3.

Satellite Communications Ground Station on Ascension Island

A British satellite communications earth terminal station, to be operated by Cable and Wireless Limited for the American *Apollo* 'man-on-the-moon' programme, is to be designed, built and installed on Ascension Island in the South Atlantic by The Marconi Company. The contracts have been awarded to Cable and Wireless by the National Aeronautics and Space Administration in Washington and COMSAT Corporation for the provision of communications systems, on Ascension Island and in Bermuda, for the *Apollo* project.

The communications system which is being set up for the *Apollo* project comprises two synchronous orbit satellites at an altitude of 22 300 miles at 6°W for Atlantic cover and between 130 and 170°E to cover the Pacific. The Atlantic satellite will connect Andover, in the U.S.A. with any two of the three tracking and communications stations situated on Ascension, on Grand Canary and a ship station. The Pacific satellite will connect Hawaii, or a station on the West coast of the U.S.A., with two ships and Carnarvon in Western Australia.

The satellites will be modified versions of *Early Bird*; they will be larger, have higher power output and be more reliable. Each will have a capacity of 200–300 channels to C.C.I.R. standards when using stations with 85 ft diameter antennas; the effective radiated power will be 25 watts and to meet reliability there will be three output tubes in parallel and selection can be made between two receiver sections.

The Ascension Island Earth Station

The earth terminal station on Ascension Island will be linked to the Andover Earth Station via a synchronous satellite in orbit over West Africa. Stations in the Canary Islands, and on an *Apollo* ship in mid-Atlantic will also use this satellite. The equipment will be fully air transportable, as a number of major sub-units, to facilitate rapid installation.

The system uses a 42 ft diameter, steerable, parabolic dish aerial with a focal length of 12 ft and with a centre area accuracy of $\pm$ 0·030 in and an accuracy at the edge which is within $\pm$ 0·075 in of the ideal paraboloid. The

dish surface will be made up of 2-inch thick aluminium honeycomb sandwich panels, mounted on an aluminium backing framework. This very rigid structure is attached to an elevation mounting, which is in turn mounted on a platform which can turn through 370 degrees in azimuth. The majority of the transmitter and receiver equipment will be mounted on this platform, and both the received and the transmitted signals will pass to the ground installation through coaxial cables at the intermediate frequency of 70 Mc/s. The aerial attitude control system will be of the auto-follow type.

The transmitter will operate in the 6000 Mc/s frequency band, with a final output power in the region of 15 kW. The output klystron, mounted on the back of the dish structure, will feed power through a waveguide system to a horn mounted in the surface of the dish. A Cassegrain system will be used, with a small hyperbolic sub-reflector at the focus of the main dish.

The receiver, operating in the 400 Mc/s frequency band, will use the same Cassegrain feed system and circular waveguide horn. It will also be mounted directly on the back of the dish aerial. A cryogenic parametric amplifier, operating at −253°C in a helium system, will be used to reduce the noise temperature of the receiving system. Extremely high amplification is necessary and the small amount of noise produced by receivers at normal temperatures would swamp the tiny signals received from the satellite.

The accuracy of the aerial system, with its very low sidelobe response and low temperature receiver, ensure a low ratio of noise to the required signals, even at amplifications in the region of 200 000. This amplification is essential to ensure the reliability of communications under the worst conditions.

Power supplies and all major elements of both the transmitting and receiving systems are fully duplicated, to ensure maximum reliability. The standby equipment is maintained in a fully prepared condition, and switching to standby for any unit can be effected within a fifth of a second.

The Bermuda Communications Station

The high frequency communications station at Bermuda is designed to carry two high speed data transmission circuits, each with a maximum capacity of 2400 bits, a speech channel and three teleprinter channels to the Goddard Space Flight Center, from Bermuda and from the N.A.S.A. *Apollo* ship, which is normally located some 1000 miles south east of Bermuda.

Five self-tuning 30 kW independent sideband transmitters will be installed at the Cable and Wireless transmitting station at St. George's, to operate with five Collins rotatable log periodic, wideband aerials. Each of two of the transmitters will carry the two data channels, using separate frequencies, to ensure that the effects of noise and fading are minimized. A further two transmitters will each transmit the speech channel and the three frequency modulated, voice frequency teleprinter channels, again providing frequency diversity. The fifth transmitter will act as a standby to cover frequency changes and possible faults.

At the Devonshire receiving station, three dual-path independent sideband, solid-state, electronically tuned receivers will be provided, with two more rotatable log periodic aerials. The third receiver will again act as an emergency standby and an additional aerial will cover emergencies at either the transmitting or receiving stations. Telephone terminal units, will be provided together with twelve channel, frequency modulated, voice frequency equipments which will provide three teleprinter channels and an order wire facility over the telephone cable from Bermuda to New York.

A comprehensive, high stability drive and frequency control system will be provided for both transmitting and receiving stations, based on a Marconi frequency standard 1 Mc/s oscillator, with a short-term stability better than ± 3 parts in 10^{10}.

Ascension Island

Ascension Island (latitude 7°56S and longitude 12°22W) is situated in mid-South Atlantic, 760 miles north of St. Helena and 900 miles from Cape Palmas, West Africa. It has an area of about 38 square miles and is of volcanic origin, having about 35 extinct volcano craters.

The island remained uninhabited until 1815, when it was occupied by British sailors and marines, and used as a base to prevent French attempts to rescue Napoleon from exile on St. Helena. It is now an important communications centre. In 1899 it became a cable station when cables were laid from St. Helena to Ascension and northwards to St. Vincent and other cables now link Ascension with Freetown, Rio de Janeiro and Buenos Aires. In 1939 Cable and Wireless began operating a wireless relay station on the island and the U.S.A. Air Force now has a guided missile tracking station there.

U.D.C. 537.228.1:621.383.8

An Ultrasonic to Electronic Image Converter Tube for Operation at 1·20 Mc/s

By

R. W. G. HASLETT, Ph.D.†

Summary: From 1949 to 1954 a programme of work was undertaken into the design of a cathode-ray image converter tube for transforming a plane section through a continuous-wave ultrasonic field to a television picture.

Eleven different types of high-vacuum sealed-off experimental tubes were investigated. The final tube had a resonant quartz front-plate 5·7 cm diameter and operated at 1·20 Mc/s with a threshold acoustic sensitivity of 7×10^{-7} watts/cm². The overall acuity was 1 mm on the front-plate and the resulting picture appeared on a monitor cathode-ray tube at 16⅔ frames per second with 110 lines per frame.

This tube is compared with those reported by other workers since 1954.

1. Introduction

Over the period 1949 to 1954, an independent programme of research was undertaken into the design of an ultrasonic to electronic converter tube so that a plane 'image' represented by variations in ultrasonic intensity under water, could be transformed into a television picture.

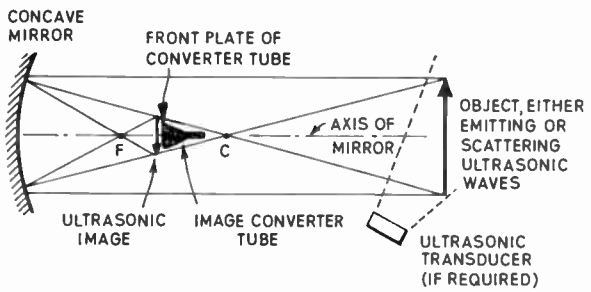

Fig. 1. The production of an ultrasonic image of an object by means of a concave spherical mirror. (C is centre of curvature and F is the focus of the mirror.)

This work formed a part of a much larger project, namely, the Underwater Acoustic Camera[1,2] which had been proposed in order to locate objects in muddy water. (This may be likened to a closed-circuit television system.) An ultrasonic image of an object would be produced either by an acoustic lens or by a concave spherical mirror as in Fig. 1. The object would have either to emit or scatter ultrasonic waves. (If it were not itself a source, it would need to be irradiated by a transducer, which corresponds to the studio lights in the analogy.) The use of a mirror is preferred since this avoids inter-reflections and uneven attenuation within the lens. The converter tube would be placed with its front plate in the image plane of the system and a television picture corresponding to the image would appear on the monitor screen.

In such a system using a mirror of a given size, the resolution improves when the frequency is raised. However, acoustic attenuation in the water increases rapidly with frequency so that the range of detection of the object is greatly reduced. Thus a compromise must be reached between resolution and range and an operating frequency between 1·0 and 1·5 Mc/s was chosen. (The corresponding wavelengths in water are 1·5 and 1·0 mm respectively.)

In 1949 the only prior work published in this field, concerned the ultrasonic microscope devised by Sokolov.[3,4] In this, an object was irradiated with ultrasonic waves at a frequency of 3000 Mc/s under water and its acoustic image was focused by an ultrasonic lens on to the quartz front-plate of a cathode-ray image converter. The wavelength in water was 5×10^{-5} cm.

The basic concept of the converter tube to be described in the present paper is seen in Fig. 2. The

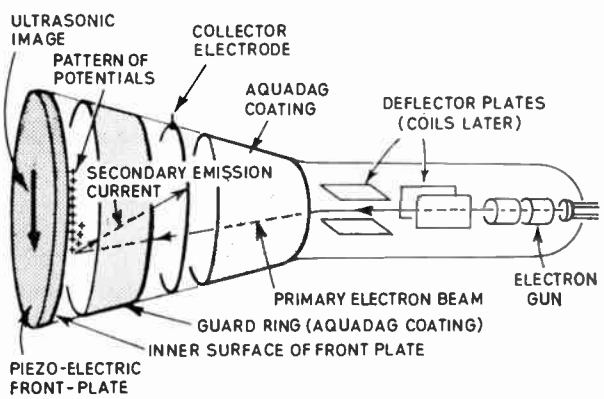

Fig. 2. Details of the construction of the image converter tube used in Fig. 1.

† Kelvin Hughes, a Division of Smiths Industries Ltd., Ilford, Essex.

ultrasonic image impinges on the piezo-electric front-plate and excites a corresponding pattern of potentials (on the rear surface inside the tube) which alternate at the ultrasonic frequency. As in some early types of television camera tube, this potential image is scanned by the primary electron beam in both line and frame. The potential of the picture element under the primary beam at any instant modulates the secondary emission beam which is collected and forms the video signal.

The proposed frequency of operation was greatly different from that of Sokolov, whose tube had no guard ring between collector electrode and front plate.

2. Secondary Emission Tubes which were made

The process of conversion may be divided into two phases:

(*a*) the achievement of best possible definition of the pattern of potentials on the piezo-electric front-plate and

(*b*) the collection of the secondary electrons with minimum loss and the smallest h.f. pick-up through the capacitance between the element and the collector electrode.

To elucidate the various effects and develop a practical converter tube, a series of eleven different types of experimental tubes were made. These employed secondary emission from a target surface stabilized near the final anode potential by a high-velocity beam. In some cases, several tubes were made of each type.

At the time of planning this series of experimental tubes, the success of a tube employing a quartz front-plate was problematical. To provide an entirely separate approach to acoustic image conversion, a secondary emission switching tube was also made, which would have been used for rapid scanning of a line array of small acoustic transducers. (In this case, the frame scan would have taken the form of a mechanical movement.)

Figure 3 indicates the variation in the secondary emission ratio (δ_e) of an insulated target bombarded by electrons for different target potentials (P).[5] δ_e is the ratio

$$\frac{\text{number of secondary electrons emitted by target}}{\text{number of primary electrons incident on target}}.$$

If the collector electrode is held at a potential P_c, the theoretical collected secondary emission ratio δ_c is expressed as

$$\frac{\text{number of secondary electrons collected by collector electrode}}{\text{number of primary electrons incident on target}}.$$

δ_c is similar to δ_e for target potentials less than P_c but falls below δ_e when P exceeds P_c (dashed curve) as a result of the decelerating field from target to collector.

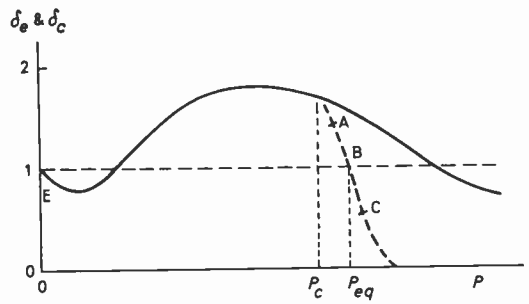

Fig. 3. Typical variation of the secondary emission ratio δ_e versus target potential P (with respect to the tube cathode). When the collector electrode is held at a potential P_c, the theoretical collected secondary emission ratio δ_c (dashed) falls below δ_e. P_{eq} is the equilibrium potential of the target.

At a point A, more electrons leave the target than arrive, so its potential rises, whilst at C more arrive than leave and thus its potential falls. (Some of the incident electrons are secondary electrons which have just been emitted from the target and return to it.) These changes in potential occur very rapidly (e.g. in 10 nanoseconds).

At the point B where $\delta_c = 1$ and the target surface is at a positive potential with respect to the collector, there is a point of equilibrium (P_{eq}). If the potential of the target is changed, the collected current is modulated in sympathy.

On comparing the ultrasonic converter tube with an early iconoscope[6] in which a mosaic of photo-electric globules was scanned by an electron beam, a major difference in the latter is that storage of the charge on the picture element occurs between successive scans of the beam, since photo-emission goes on continuously. This results in a greatly enhanced sensitivity which is not present in the converter tube since it operates instantaneously and the output waveform follows the cycles of ultrasonic pressure.

In the iconoscope, the scanning beam impedance was about 1 MΩ at 1 μA beam current. About 25% of the secondary beam reached the collector, the remainder being re-distributed over the mosaic to give irregular shading of the picture. The limiting noise level is the shot noise of the secondary emission beam.

3. Tubes Nos. 1, 2 and 3

Initially it had been hoped to stick a mosaic of pieces of quartz on the outside of the glass front-plate on the converter tube so that the effect on secondary emission was produced through the capacitance between each piece and the scanning spot. This would have simplified construction and enabled a very large mosaic to be used, corresponding to a wide field of view.

The first experimental tubes were made by modifying a standard type of cathode-ray tube (VCR97) to include a collector ring and later a guard ring. When a conducting plate was stuck to the outside face of these tubes and a high-frequency alternating signal (at 1·5 Mc/s) applied to it, direct capacitive pick-up between the plate and the collector electrode was evident. This was minimized by increasing the distance between front plate and collector to 13 cm, by introducing a guard ring between the two and by making the collector ring as thin as possible (wire of diameter 0·5 mm). The distribution of signal on the inside of the screen was examined by collecting the secondary electrons resulting from a line scan. Considerable spreading beyond the confines of the plate was found and it was clear that the piezo-electric material would have to be mounted inside the tube to obtain good electronic definition.

4. Tube No. 4

This was based on a normal $3\frac{1}{2}$ inch diameter cathode-ray tube (Fig. 4) and was designed to measure the electronic definition. A silver arrow (g) was sputtered on the inside of the screen prior to the deposition of the green fluorescent material (willemite, an insulator) and a connection was brought out from the arrow. The final anode was earthed and all potentials were measured with respect to earth.

The collector was attached to a cathode follower, with anode feedback (amplified and inverted) on to a concentric screen surrounding the lead and extensively screened by mu-metal. Since the impedance of the secondary beam is very high, the cathode follower must have the highest possible input impedance and the unavoidable stray capacitances must be kept to a minimum. The best result which could be obtained was a gain of 0·40 and an input impedance of 40 kΩ at 1·5 Mc/s (equivalent to a capacitance of 3 pF).

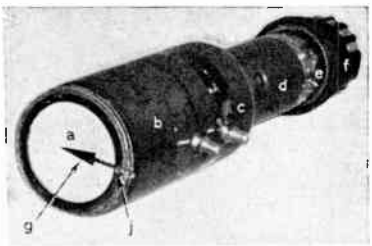

Fig. 4. Experimental tube No. 4 using electrostatic deflection and focus.

a. fluorescent screen (green phosphor)

b. guard ring (Aquadag coating)

c. collector electrode ring in a gap 25 mm wide

d. Aquadag coating (connected to final anode)

e. electron gun

f. contact base

g. conducting electrode of Cerroseal 35 (inside glass) brought out to a cap (j)

j. connecting cap

Useful information was obtained on the scanning of the screen, the collection of the video signal and the noise levels involved. The major source of noise was the shot effect in the secondary beam, in which the noise power is proportional to beam current. It was most important to keep the bandwidth of the system at the minimum required for the definition available. Theoretical predictions of the noise levels were in good agreement with the measured values.[7,8] More recently, other workers have also considered the theoretical operation of the tube.[9–12]

A constant h.f. voltage at 1·5 Mc/s was applied to the arrow and the output signal at the collector was measured on an oscilloscope. Some of the results are seen in Fig. 5. As expected theoretically,[8] the output signal varied with beam current in a non-linear fashion (iii). The operating conditions giving the best compromise between maximum sensitivity and minimum distortion of the waveform are seen in Table 1.

Table 1

Typical operating conditions for tube No. 4

E.H.T.	1·5 kV
Collector potential (V_c)	+ 300 V
Guard-ring potential (V_g)	− 50 V
Frequency	1·5 Mc/s
Cathode current	50 μA
Signal on arrow for 2/1 signal/noise ratio	20 mV
Signal output from collector electrode at this level	175 μV
Loss between arrow and collector electrode	115/1 (amplitude)
Direct capacitive pick-up	5/1 (amplitude) down on signal

A comparison between the sensitivities of tubes Nos. 3 and 4 showed that 70% more signal was required at the element on the outside of tube No. 3 as compared with the arrow inside tube No. 4 in order to give the same output signal at the collector under similar conditions.

To determine the degree of modulation of the collected current, the beam current of tube No. 4 was interrupted by applying a 100 kc/s square wave (having a 50/50 mark/space ratio) to its grid. The degree of modulation† was found to be 3% per volt r.m.s. at 1·5 Mc/s on the arrow for a cathode current of 15 μA. (Jacobs *et al.*[13] quote a value of 6%.)

† Defined as $\frac{\text{peak value of alternating current}}{\text{d.c. component of current}}$.

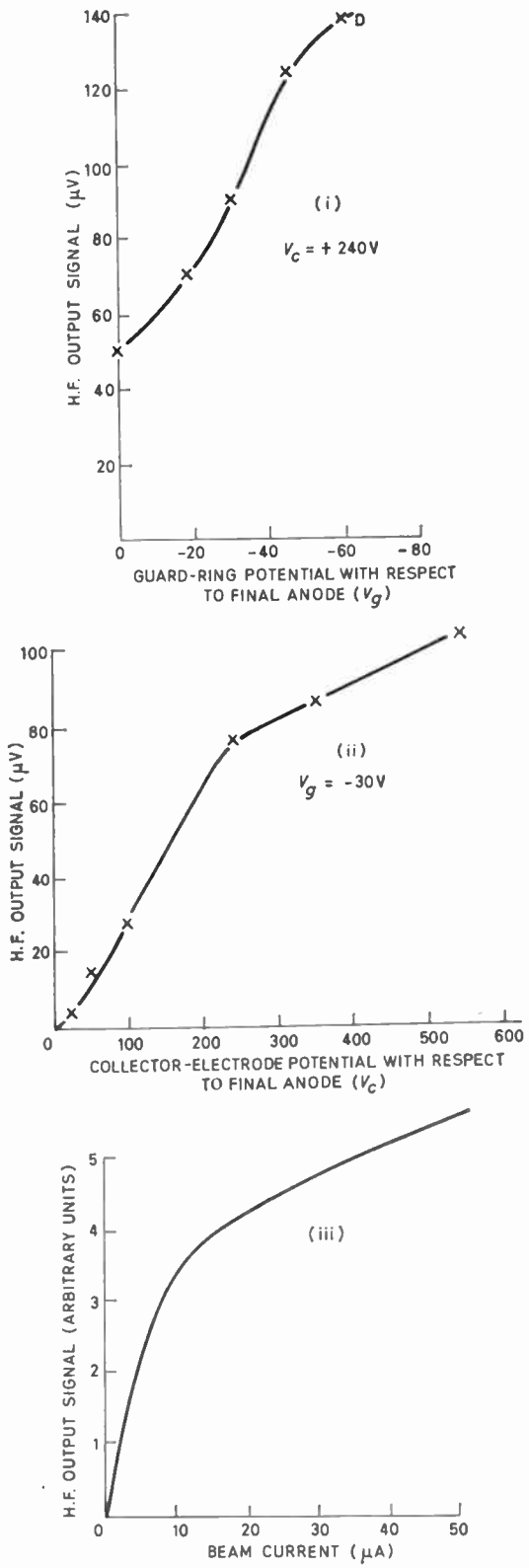

Fig. 5. Tube No. 4—Effects on output signal of variation of (i) guard ring potential (V_g), (ii) collector potential (V_c) and (iii) beam current. (Beyond the point D, distortion sets in.)

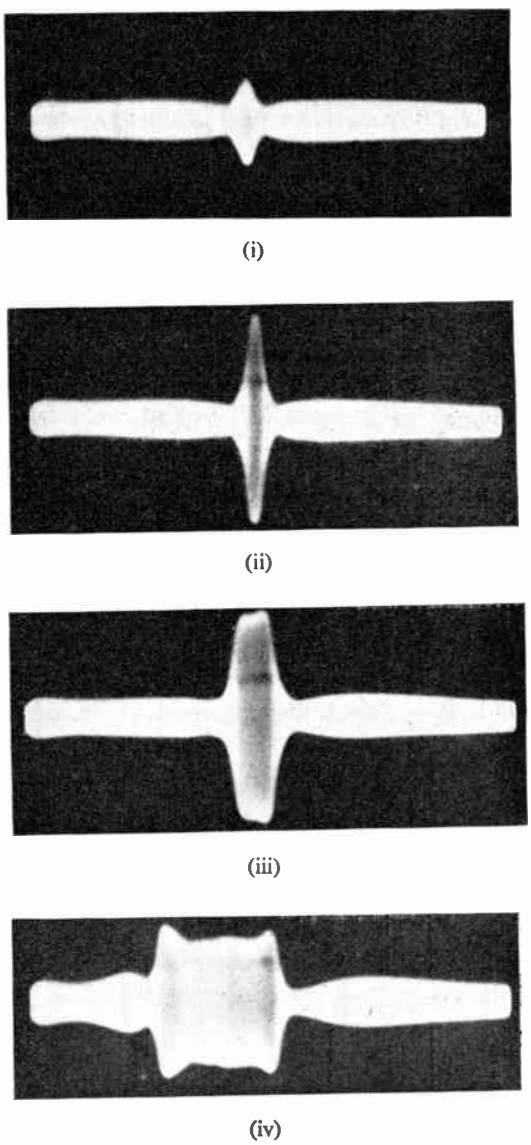

Fig. 6. Output signals (at 1·5 Mc/s) from tube No. 4 using a line scan crossing the arrow electrode at various widths. (The size of the spot was 1·2 mm diameter and the beam current was 15 μA.)

Widths of arrow: (i) 1·5 mm, (ii) 1·8 mm, (iii) 2·3 mm and (iv) 9·2 mm.

At this stage with tube No. 4, Fig. 6 indicates the definition available, which was clearly limited by the spot size.

To obtain a picture of the arrow, the usual closed-circuit picture-monitoring facilities were provided, using intensity modulation with line and frame shading corrections and top and bottom limiters, also hum balancers at the mains frequency and at its second harmonic. The adjustable limiters were included since full tonal rendering of the image might not be

necessary for recognition. They proved of considerable benefit when the signal/noise ratio was low. Figure 7 is a photograph of the monitor screen showing the arrow electrode in tube No. 4. The blemishes are attributed to small changes in the secondary emission characteristics of the phosphor covering the arrow.

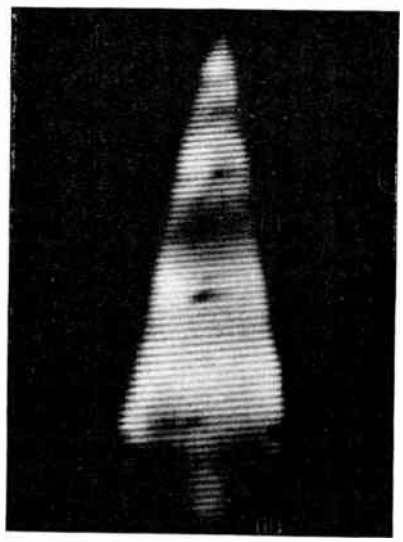

Fig. 7. Representation of the arrow electrode in tube No. 4 as seen on the monitor screen. Voltage on arrow: 1 V r.m.s. at 1·5 Mc/s; beam current 50 μA.

5. Fundamental Acoustic Work

In parallel with the work on the tubes, an apparatus was devised to investigate the spreading of the alternating potential on the reverse side of a resonant quartz crystal irradiated with sound at 1·5 Mc/s. The crystal (2 × 2 cm) was mounted in a metal box, open at the upper end. The outer side was in contact with the water and the inner surface in the dry so that it could be explored by a small metal probe. The latter had a vernier mechanical adjustment and was screened almost up to the crystal. The resulting h.f. signal was applied to a cathode follower.

When a thin cork mask having a straight edge was fixed over part of the face of the crystal in the water and the probe was moved towards the edge (on the opposite side of the crystal), the voltage began to decline at 3·4 mm from the edge and fell to approximately half amplitude when it was reached. This spreading of the charge was mainly attributed to the electrostatic edge effect and not to the acoustic coupling within the crystal. Suckling and Maclean[14] found a decline to half voltage in 1·0 mm at 3 Mc/s.

In an effort to improve the voltage resolution on the crystal, the experiment was repeated with a slotted quartz plate (Fig. 8) also of resonant thickness and 2 × 2 cm. The slots (0·2 mm wide) were made by a thin blade attached through a solid horn to a high-power ultrasonic generator at 10 kc/s. Carborundum powder in the form of a slurry was applied to the blade as an abrasive. The plate was divided into 400 elements, approximately 1 mm square. The slots extended half-way through the plate and were filled with electrically conducting material which could be earthed. In this case, the h.f. voltage fell to half amplitude when the probe was moved a distance of 1·1 mm.

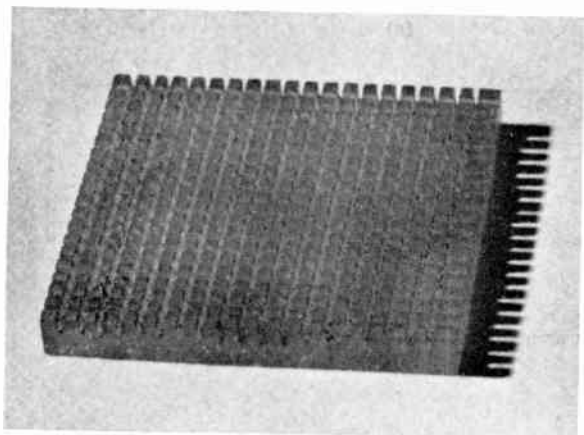

Fig. 8. A slotted quartz crystal 2 × 2 cm, X-cut for resonance at 1·5 Mc/s.

A further experiment was performed with a plain crystal covered by a cork mask in which there were two holes of diameter 1 mm. Several masks were used, the distance between the holes being varied. The minimum separation between the edges of the holes which could be resolved was 2 mm. A limitation must have been imposed by the capacitive coupling in the apparatus, for under actual working conditions in tube No. 6, a better acuity was found (see Section 7).

6. Tube No. 5

This tube was designed to explore the acoustical and crystal aspects of conversion. Two quartz crystals each 2 cm square, X-cut to resonate at 1·5 Mc/s in thickness mode (1·97 mm thick), were stuck inside the glass front-plate on metal electrodes brought out to caps. To facilitate the propagation of sound through the front plate to the quartz, the glass must be an integral multiple of $\lambda/2$ thick (where λ is the wave-length in the glass at 1·5 Mc/s). A thickness of 3·602 mm $\pm 2\frac{1}{2}\%$ was chosen, equivalent to λ (since $\lambda/2$ might have been too thin to withstand the atmospheric pressure). At the same time, the change was made to magnetic deflection and focusing for this and all future tubes, using an electron gun giving a

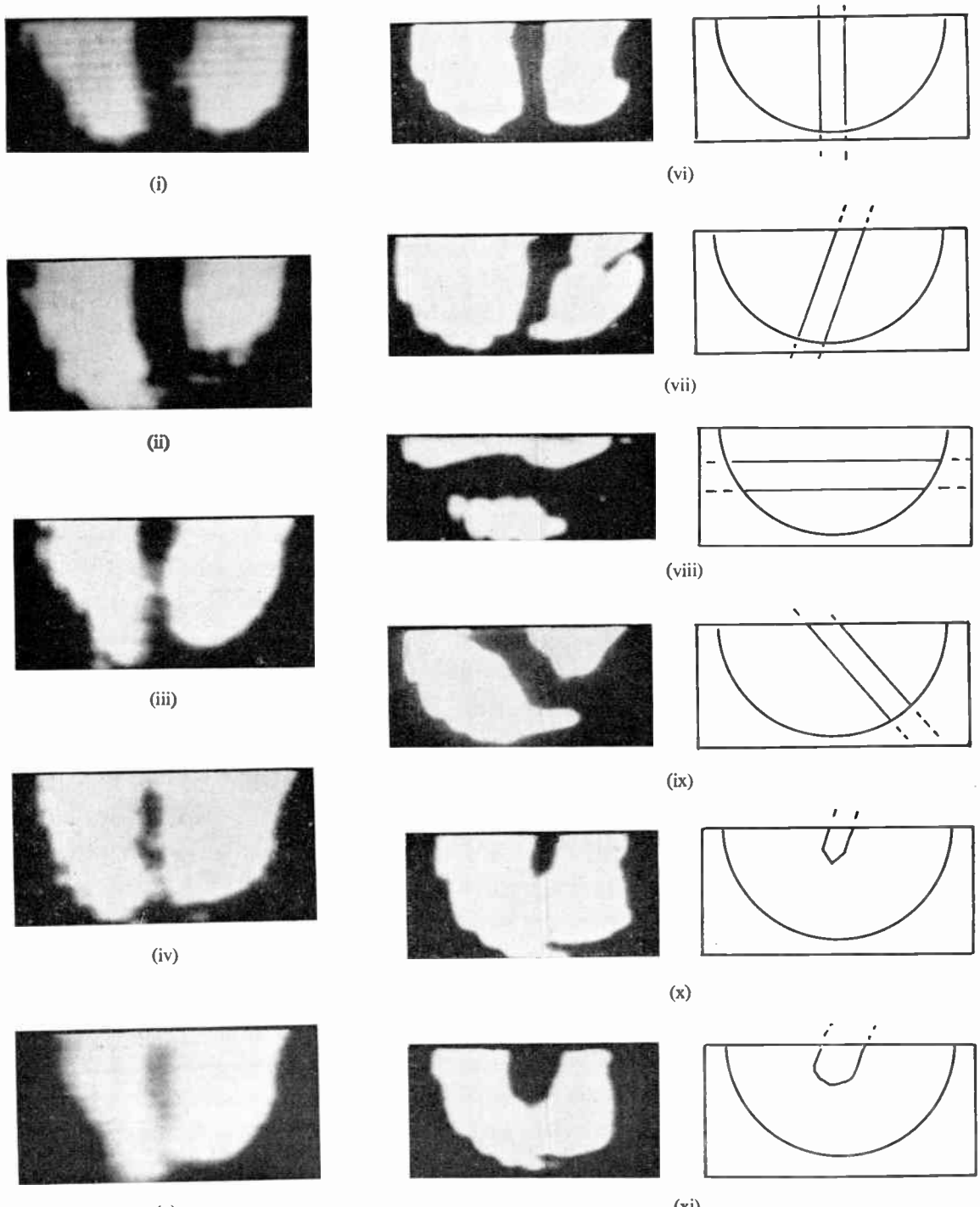

Cylindrical obstacles of various diameters: (i) 4 mm, (ii) 3 mm, (iii) 2 mm, (iv) 1·5 mm and (v) 1·0 mm.

Multimeter test prod at various inclinations as shown in the adjacent sketches: (vi), (vii), (viii), (ix), (x) point and (xi) head.

Fig. 10. The acoustic shadows produced by placing obstacles in front of the unmetallized half of the quartz crystal on tube No. 6.

smaller size of spot at higher beam currents than in tube No. 4. A continuously-heated zirconium getter was also included. The front face was immersed in a small water tank so that acoustic energy at 1·5 Mc/s could be applied from an ultrasonic transducer.

Experiments with this tube showed a promising electronic definition but poor acoustic resolution due to the spreading of the sound energy through the intervening glass and it was clear that the outside surface of the crystal would need to be in direct contact with the water.

7. Tube No. 6 (Fig. 9)

This was similar to tube No. 5, except that a hole (o) of diameter 1·6 cm was drilled in the glass front-plate (k) and a resonant quartz crystal (h) 2 cm square was stuck over this hole on the outside of the tube. Half the crystal (n) was metallized on the inside surface.

Although the sensitivity of the metallized portion to ultrasonic waves was somewhat higher than for the bare quartz, metallizing was not considered worthwhile in view of the added difficulty of manufacture of a mosaic of metallized dots.

On the bare semi-circular portion, acoustic shadows of obstacles placed close to the quartz could be observed, although the field of view was quite small (8 mm high and 16 mm wide). Figure 10 shows the 'shadows' produced by cylindrical obstacles of various diameters. In (v), the presence of the obstacle (1 mm diameter) can just be discerned whilst those of smaller diameter could not be detected. Thus the resolution is about 1 mm at 1·5 Mc/s when the wavelength in water is 1 mm. (It is interesting to note that the radiation impedance of an area of quartz crystal one millimetre square is as high as 100 MΩ.)

This tube gave good electronic definition and high acoustic resolution.

Later tubes in the series incorporated slotted quartz crystals (as in Fig. 8) in an effort to improve the acoustic resolution but a significant improvement in this respect as compared with tube No. 6 was not found.

Three factors militated against the use of slotted quartz crystals as compared with unslotted ones:

(*a*) Slotting greatly impaired sensitivity.

(*b*) Slotting reduced the mechanical strength.

(*c*) A much larger mosaic than 2 × 2 cm was required, which would not withstand the atmospheric pressure if slotted.

In view of these considerations, the final converter tube (No. 11) was made with an unslotted quartz plate.

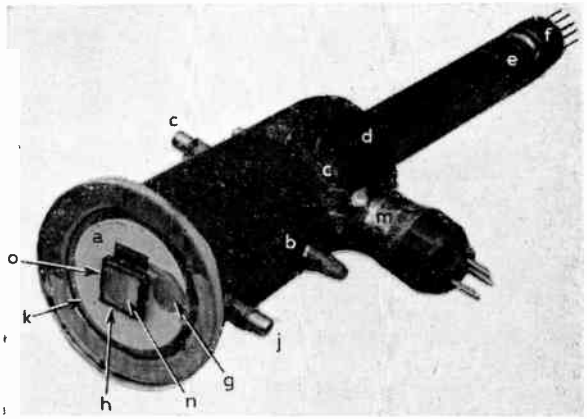

Fig. 9. Experimental tube No. 6 using magnetic deflection and focus. The metallized part (n) of the quartz crystal (h) (mounted over a hole (o) in the front-plate) was joined to an electrode (g) and brought out to a cap (j).

a. fluorescent screen (green phosphor)
b. guard ring (Aquadag coating)
c. collector electrode ring in a gap 25 mm wide
d. Aquadag coating (connected to final anode)
e. electron gun
f. contact base
g. conducting electrode of Cerroseal 35 (inside glass) brought out to a cap (j)
h. quartz crystal
j. connecting cap
k. glass front-plate (stuck on with Cerroseal)
m. zirconium getter
n. metallized half of quartz crystal
o. hole 1·6 cm diameter in glass front-plate (k)

8. The Final Converter Tube (No. 11) (Fig. 11)

An operating frequency of 1·20 Mc/s was chosen since it gave the best compromise between resolution and range (as mentioned in Section 1). This also had the effect of increasing the strength of the plane front-plate which consisted of an X-cut resonant quartz crystal (p) 5·7 cm diameter, the largest that could be readily found in Nature. A pressure test showed that this plate fractured at 70 lb/in^2. (A resonant barium titanate plate of the same diameter would break at 21 lb/in^2 and was not considered safe.) The quartz crystal was examined to ensure that optical and acoustic twinning were absent. The inner surface was highly polished to assist the adhesion of Cerroseal 35† around the periphery and was subsequently given a thin coating of willemite so that the raster could be

† Cerroseal 35 is a solder having a low melting-point so that the piezo-electric properties of the quartz were not impaired in the manufacture of the tube.

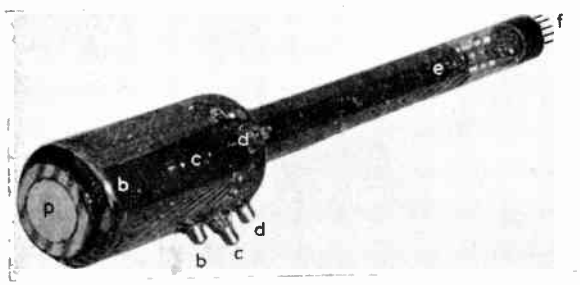

Fig. 11. Final converter tube No. 11 using magnetic deflection and focus. (Note: The Aquadag and Cerroseal coatings have reflected the corrugated cardboard on which the tube was laid while being photographed.)

b. guard ring (Aquadag coating)
c. collector electrode ring in a gap 25 mm wide
d. Aquadag coating (connected to final anode)
e. electron gun
f. contact base
p. quartz disk 5·7 cm diameter

seen for setting-up purposes. There were also two small silver arrows at top and bottom inside the screen, connected to the Cerroseal and earthed. These could be observed on the monitor screen when the acoustic transmitter was switched off and thereby showed that the converter tube was working at the correct sensitivity. The diameter of the body of the tube was 7·5 cm and the overall length 54 cm. A special gun assembly reduced the diameter of the spot to 0·5 mm at 100 μA beam current. The design of the tube was as in Fig. 2 (except that the left-hand side of the tube was cylindrical).

Acoustic results are seen in Fig. 12. For test purposes, a 'gun-sight' obstacle was used. This was made from copper approximately 0·7 mm thick (i) and gave a clear 'shadow' (ii) when irradiated with an ultrasonic transducer under water at 1·20 Mc/s. The area irradiated before the insertion of the obstacle is shown at (iii). The resolution was approximately 1 mm at 1·20 Mc/s.

The transducer was calibrated by the 'self-reciprocity' method so that the minimum detectable intensity could be determined.

Typical operating conditions are given in Table 2.

Table 2

Typical operating conditions for tube No. 11

E.H.T.	1·5 kV
Focus current	10 mA
Collector potential (V_c)	+ 300 V
Guard-ring potential (V_g)	− 100 V
Frequency	1·20 Mc/s
Cathode current	50 μA
Noise level at collector	4 μV
Minimum detectable acoustic intensity at front-plate	10^3 dynes/cm², i.e. 7×10^{-7} W/cm²
Number of picture elements per line	50 approx.
Scanning standards	110 lines per frame 1800 lines per second 16⅔ frames per second Positive modulation
H.F. bandwidth	150 kc/s

9. Comparison with other Image Converter Tubes

Since 1954, a number of papers have been published on different types of cathode-ray converter tubes with piezo-electric front-plates on which the ultrasonic images are focused. These tubes may be divided into two types:

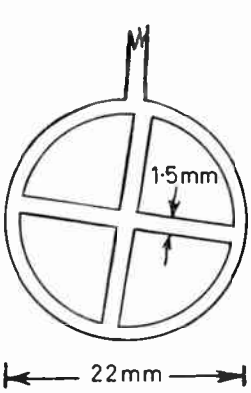

(i) Gun-sight obstacle.

(ii) Picture with obstacle.

(iii) Picture without obstacle.

Fig. 12. Acoustic results with tube No. 11.

First, those employing the secondary emission resulting from high-velocity primary electrons, in which the inner surface of the front plate is stabilized near final anode potential[9–13, 15, 16] and the ultrasonic image is applied continuously, as in the present tube. In one case,[13] an electron multiplier has been built into the tube to increase the sensitivity.

Secondly, a tube in which the inner surface is stabilized at cathode potential and is scanned by a low-velocity beam of electrons[17, 18] (near the point E in Fig. 3). In this case, there is an alternating sequence of charge and erase. In the 'charge' period, the ultrasonic image is energized and the electron beam lays down a pattern of negative charges on the inner surface (during the positive half-cycles of the piezo-electric potential). In this period, a varying current is received from the signal electrode (attached to the outer surface of the front plate) in sympathy with the element of the image under the beam. In the 'erase' period, the ultrasonic energy is switched off and the beam current is increased to form more ions which bring the target back to cathode potential. To allow the formation of ions, a very low level of gas pressure is left in the tube.

The sensitivity of the final converter tube at 1·20 Mc/s (7×10^{-7} W/cm^2) is as high as that obtained by Jacobs *et al.*[13] when using a quartz front-plate at frequencies between 5 and 8 Mc/s, although the latter had an electron multiplier incorporated. It seems that the multiplier becomes necessary at higher frequencies to avoid straight-through capacitive pick-up. A change to barium titanate[9, 12, 15] would increase the sensitivity to about 10^{-9} W/cm^2 but the resonant quartz front-plate is mechanically stronger than one made of barium titanate of equal diameter resonating at the same frequency by a factor 3·4 in terms of breaking pressure. (The strength of the front-plate is of some importance since the tube is for use under water.)

All the tubes used by other workers operated at higher frequencies, for example, 2 Mc/s (Semennikov[12]), 2·4 Mc/s and 4 Mc/s (Koch[19]), 4 Mc/s (Freitag[11] and Smyth *et al.*[18]), 4–10 Mc/s (Prokhorov[9]), 5–8 Mc/s (Jacobs *et al.*[13]) and 7 Mc/s (Lawrie and Feith[16]). This would restrict their use to very short ranges. In two cases[18, 16], the resolution obtained was 0·5 mm both at 4 Mc/s and 7 Mc/s (as compared with 1 mm in tube No. 11 at 1·20 Mc/s). When the frequency is raised, the definition might be expected to improve in proportion since the front-plate is thinner and the wavelength is shorter. The tube made by Freitag[11] appears to have been continuously pumped.

In contrast with most of the above tubes which have a hard vacuum and are continuous in operation, Smyth *et al.*[18] described a tube having a residual gas pressure which works in an alternating on/off sequence.

A different type of converter tube, based on the reflection of electrons from a quartz plate, has been made by Koch.[19]

In a future paper, it is hoped to describe the use of the converter tube in conjunction with a spherical concave mirror.[20]

10. Acknowledgments

The Underwater Acoustic Camera was suggested by Dr. T. Gold (now Professor, Department of Astronomy, Cornell University) who acted as Consultant to the project. The author is grateful for many helpful discussions with Mr. G. S. Freeman (Rank Electronic Tubes Ltd.), Mr. S. A. Byard (late of the Admiralty Research Laboratory) and Dr. D. G. Tucker (now Professor of Electronic and Electrical Engineering, University of Birmingham) and with a number of colleagues, particularly Mr. W. Halliday and Mr. G. Pearce. (The latter undertook the work described in Sections 3 and 5.)

A major contribution to the success of the work was the manufacture of the experimental tubes by Rank Electronic Tubes Ltd.

This paper is published with the permission of the Ministry of Defence (Navy Department) and the Directors of Kelvin Hughes, a Division of Smiths Industries Ltd.

11. References

1. W. Halliday, R. W. G. Haslett, G. Pearce, A. Welsh and K. Hussey, 'Underwater Acoustic Camera; Progress 1.1.51 to 3.4.53', Kelvin Hughes Report, 8th April 1953.
2. W. Halliday, R. W. G. Haslett, G. Pearce, A. Welsh and K. Hussey, 'Underwater Acoustic Camera; Acoustic Results', Kelvin Hughes Report, 18th October 1954.
3. S. Ya. Sokolov, British Patent No. 477,139, 13th May 1937.
4. S. I. Goorevich, 'The ultrasonic microscope', *Priroda*, No. 9, pp. 45–7, 1949.
5. M. Knoll and B. Kazan, 'Storage Tubes and their Basic Principles', p. 11. (John Wiley, New York, 1952.)
6. V. K. Zworykin, G. A. Morton and L. E. Flory, 'Theory and performance of the iconoscope', *Proc. Inst. Radio Engrs*, 25, No. 8, pp. 1071–93, 1937.
7. R. W. G. Haslett, 'Underwater Acoustic Camera; Theoretical factors affecting the performance of the image converter tube', Kelvin Hughes Report, 8th May 1951.
8. R. W. G. Haslett, 'Underwater Acoustic Camera; Experiments with tube No. 4 and theoretical discussions', Kelvin Hughes Report, 17th August 1951 and 7th January 1952.
9. V. G. Prokhorov, 'On the problem of converting an ultrasonic image into a visible image', *Soviet Physics–Acoustics*, 3, No. 3, pp. 272–80, 1957.
10. Yu. B. Semennikov, 'A study of acoustic image converters', *Soviet Physics–Acoustics*, 4, No. 1, pp. 72–83, 1958.
11. W. Freitag, 'Untersuchungen an einem electronischen Ultraschall-Bildwandler', Jenaer Jahrbuch, Vol. 1, pp. 228–74 (Gustav Fischer, Jena, 1958.)

12. Yu. B. Semennikov, 'Certain aspects of the operation of an electron-acoustic image converter', *Soviet Physics–Acoustics*, **7**, No. 1, pp. 56–9, 1961.
13. J. E. Jacobs, H. Berger and W. J. Collis, 'An investigation of the limitations to the maximum attainable sensitivity in acoustical image converters', *Trans. Inst. Elect. Electronics Engrs on Ultrasonic Engineering*, **UE-10**, No. 2, pp. 83–8, September 1963.
14. E. E. Suckling and W. R. Maclean, 'Acoustic optical bench for ultra-sound lens measurement', *Rev. Sci. Instrum.*, **26**, p. 1209, 1955.
15. P. K. Oshchepkov, L. D. Rozenberg and Yu. B. Semennikov, 'Electron-acoustic converter for the visualization of acoustic images', *Soviet Physics–Acoustics*, **1**, No. 4, pp. 362–91, January 1955.
16. W. E. Lawrie and K. E. Feith, 'Electronic imaging of ultrasonic fields', *J. Acoust. Soc. Amer.*, **34**, No. 5, p. 719, 1962.
17. C. N. Smyth and J. F. Sayers, 'Ultrasonic image camera', *The Engineer*, **207**, No. 5379, pp. 348–50, February 1959.
18. C. N. Smyth, F. Y. Poynton and J. F. Sayers, 'The ultrasound image camera', *Proc. Instn Elect. Engrs*, **110**, No. 1, pp. 16–28, 1963.
19. G. Koch, 'Ultraschallbildwandlung mit dem elektronenspiegel', *Acustica*, **10**, No. 3, pp. 167–70, 1960.
20. R. W. G. Haslett, G. Pearce, A. W. Welsh and K. Hussey, 'The Underwater Acoustic Camera', *Acustica*. (In the Press)

Manuscript first received by the Institution on 10th May 1965 and in final form on 19th August 1965. (Paper No. 1031/EA27.)

I.E.C. PUBLICATIONS

The following publications have been issued by the International Electrotechnical Commission in recent months. Copies are obtainable from the Sales Department of the British Standards Institution, 2 Park Street, London, W.1.

I.E.C. Publication: 177 1965. 'Pure tone audiometers for general diagnostic purposes'.

The first edition of this I.E.C. publication has been issued. It applies to audiometers using pure tones, designed for general diagnostic work and for determining the hearing threshold levels of individuals by monaural air conduction earphone listening, and by bone conduction. The recommendation deals primarily with audiometers giving discrete frequencies, but also applies to audiometers giving continuous frequency variation, as far as the provisions are relevant.

The aim of the recommendation is to ensure that tests of the threshold of hearing of an individual, on different audiometers complying with the recommendation, will give substantially the same results under comparable conditions.

I.E.C. Publication 177 deals in separate sections with explanation of terms; requirements for air conduction; requirements for bone conduction; masking device; general characteristics and measurements.

I.E.C. Publication 166: 1965. 'Fixed metallized paper dielectric capacitors, for direct current'.

The first edition of this publication relates to fixed capacitors with self-healing properties, for direct current, with a rated voltage not exceeding 6300 V, containing a dielectric of impregnated paper and thin deposited metal electrodes, intended for use in equipment for telecommunications and in electronic devices employing similar techniques. These capacitors are divided into two categories: Type 1, which may be protected by self-healing properties; and Type 2, for which the self-healing of the metallized dielectric at voltages both below and above the rated voltage is relied upon to provide protection for a capacitor in normal use.

Publication 166 establishes uniform requirements for judging the electrical, mechanical and climatic properties of capacitors; and describes test methods—visual examination and check of dimensions, electrical tests, robustness of terminations, soldering, rapid change of temperature, vibration, container sealing, climatic sequence, damp heat, and endurance.

U.D.C. 550.341

Seismic Data Acquisition and Processing Equipment for Edinburgh Royal Observatory

By

R. PARKS†

Presented at a Symposium on 'Modern Techniques for Recording and Processing Seismic Signals' held in London on 13th May 1964.

Summary: The paper deals with two main subjects: a set of portable recorders for field work, and a data-processing centre for collecting and analysing seismic recordings.

The portable field recorders use frequency modulated recording on magnetic tape to handle the wide range of frequencies and amplitudes involved in seismic signals. Advantages and problems of mobile array stations are outlined, and the system design considerations for the recording equipment are discussed in detail, with a brief description of the units and their performance.

The equipment and operation of the data laboratory are discussed, covering the following functions:

(i) Playback of analogue tapes.

(ii) Building of a library of events.

(iii) Preparation of data for computer input.

(iv) Playback of computer output.

(v) Simplified processing of data.

Proposals are put forward for a special-purpose digital processor, using the existing core-store memory system in conjunction with additional addressing and read-out facilities to perform processing with lags.

1. Introduction

At the beginning of 1962 a new seismological research group was set up at Edinburgh, with the objective of applying modern instrumentation and computer techniques. The natural question for a visiting seismologist to ask is: 'What is to be the equipment for the base station?'

In the case of Edinburgh, this question must be considered in the light of recent developments at Eskdalemuir, some fifty miles to the south, where two new recording stations have been established. The station, operated by the United Kingdom Atomic Energy Authority (U.K.A.E.A.), produces continuous recordings on magnetic tape from a spaced array of short-period vertical seismometers and in a form suitable for subsequent processing by advanced techniques. The second station, operated by the Meteorological Office, produces conventional chart records from a set of seismometers covering three components of long period and three components of short period. The value of this station lies in the fact that a network of some 125 similar stations has been set up around the world, using instruments with accurately matched characteristics so that comparisons can be drawn between records from different regions. In the specially constructed vault for the Meteorological Office station additional space has been provided for other research workers to install their own instruments.

It is evident that a further station producing conventional chart records from the somewhat more noisy site at the Royal Observatory would not make a useful contribution to the world network. To be of value, a new station should at least provide for magnetic recording and the use of arrays of seismometers; the feature which was considered to be an especially worthwhile addition is complete portability of the recording equipment. A set of field recorders has been developed to produce tapes in a format broadly similar to that of existing fixed-array stations, and a data-processing centre has been established to build up a library of tapes and to carry out detailed analysis.

2. Wide Band Recording

The form of recording which has been in use for many years represents the ground motion by the excursion of a line from its mean position, usually on paper or photographic film. The nature of the

† Royal Observatory, Edinburgh.

record produced is governed by the sensitivity and frequency response of the system, the speed of the paper or film, and the orientation of the seismometer. These characteristics have to be chosen in advance, and seldom provide the optimum conditions for more than one phase of an earthquake. The range of frequencies and amplitudes involved in a typical selection of events is greater than could be handled by a conventional record, and for this reason it has been customary to operate a number of different types of seismometer simultaneously, each covering only a relatively narrow band of frequencies.

The desired performance can, however, be achieved more readily by making the initial recording on magnetic tape using frequency modulation. In this case the ground motion is represented by deviations in the frequency of a 'carrier' signal, which is recorded on the tape as reversals of magnetization of the oxide coating. A number of tracks can be employed side by side (as many as 24 tracks on a 1-in tape) allowing simultaneous recording of timing information and the outputs from several seismometers. On playback, suitable sensitivity and frequency ranges can be selected, producing a chart record which is a considerable improvement over the conventional one. Individual phase arrivals may be made to stand out much more clearly by careful choice of filter settings (although due allowance must be made for the substantial phase shifts liable to be associated with such filtering).

A further advantage concerns the chart speed and storage of records. Chart recorders for continuous operation have to be restricted to a rather low chart speed, to keep the bulk of the accumulating records within reasonable bounds. When the initial recording is made on tape, only a small proportion of the record need be reproduced on paper, and bulk is no longer a problem; a sufficiently high chart speed may be employed to resolve the high-frequency components and permit more accurate time measurements.

However, it should be recognized that the study of seismograms has advanced a long way beyond the point where the production of chart records from single instruments is a sufficient goal in itself. With the more elaborate techniques now available for processing the data it is an important advantage to be able to reproduce it directly in the form of electrical signals, rather than taking a tedious series of measurements by hand from a chart record, and also to be able to handle simultaneously the data from a number of seismometers.

3. Fixed-Array Stations

The recording system employed by U.K.A.E.A. has been described in detail elsewhere[4] but the salient features are summarized below for convenience.

A basic array comprises twenty-one seismometers laid out in the form of a cross, with a spacing of around one or two kilometres between adjacent seismometers. The electrical outputs from these seismometers are amplified and fed to a single recording centre by cable, using either direct transmission or amplitude-modulated tones, and recorded in f.m. form on 24-track 1-in magnetic tape. An interleaved pair of 12-track recording heads is used, and the remaining three tracks are occupied by flutter compensation (a separate track for each head) and time code. The time code gives narrow pulses at 1-second intervals, with a wide pulse for each minute mark and a medium-width pulse for each 10-second mark. After each minute mark, groups of pulses are coded to identify the hour, the minute, and the day. At a tape speed of 0·3 in/s, a 7200 ft reel of tape carries over three days of recording.

4. Mobile Array Stations (Fig. 1)

4.1. *Advantages*

One of the principal parameters determining the characteristics of a spaced array is the distance between elements, and the freedom to vary this according to the type of wave motion to be studied is a valuable one.

However, as coverage of the globe from existing array stations is by no means complete, there is a need for a self-contained installation which can be set up in any required location at short notice. Furthermore, as sensitivity and background noise conditions vary widely from site to site, it is an advantage to be able to move the seismometers around readily for evaluation of sites.

4.2. *Problems of Intercommunication*

For an array of short-period instruments, the requirements for relative timing accuracy are fairly stringent. For example, to deal with signals up to 10 c/s the timing error between any two channels should not exceed 8 ms (corresponding to a phase difference of 30 deg). It would obviously be desirable from this point of view to record all channels simultaneously on a single tape-deck, but even with a permanent installation the problems of linking all seismometers to one recording centre are formidable, and if emphasis is placed on mobility a single-recorder system becomes impracticable. Cable links are unsuitable for long distances or work in populated areas, and radio links (at the frequencies available for such work in Great Britain) are limited by line-of-sight propagation. Radio links have been in use for ship-borne seismic surveys for many years,[2] but there are substantial difficulties in their use for land-based surveys. The equipment may be required to operate in rugged terrain where access is limited to

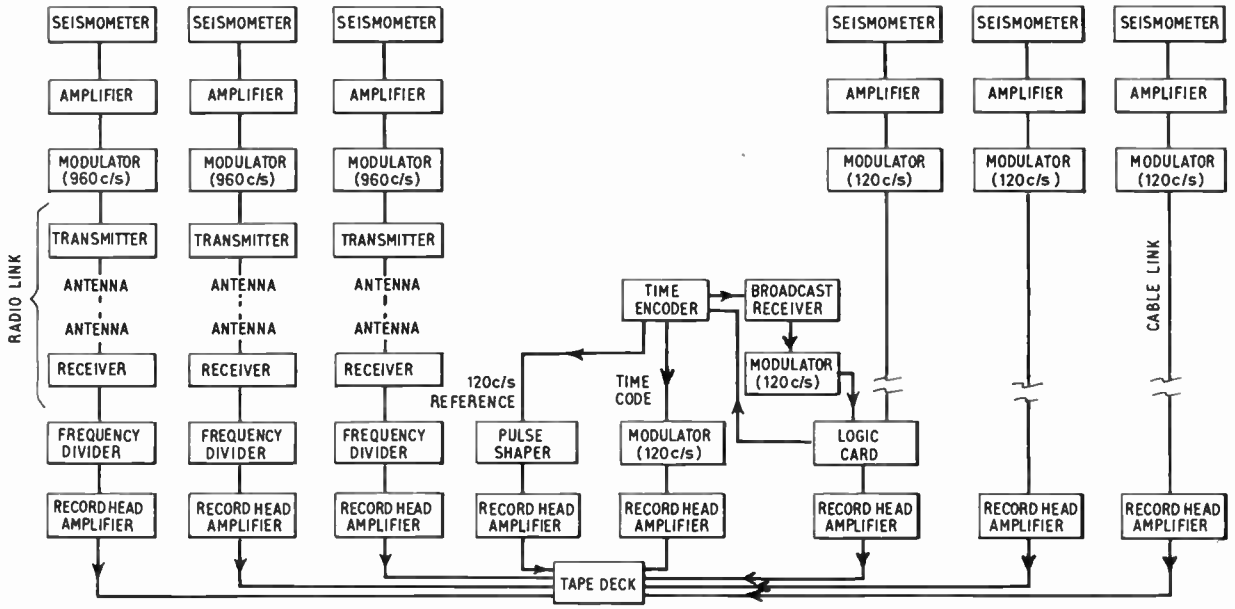

Fig. 1. Block diagram of field recording set.

roads following the line of a valley, or to lakes where a small plane fitted with floats could land; under these conditions it might be virtually impossible to arrange line-of-sight communication to one central recording point.

4.3. *Problems of Spacing*

In the case of fixed arrays it is normally possible to choose a site where the seismometers can be spaced along straight lines at uniform intervals, which simplifies the analysis. However, with the mobile arrays it will often be impossible to achieve an ideal layout, especially for the larger spacing and for populated areas. With non-uniform spacing it is still an easy matter to specify the appropriate time lags for any desired velocity and azimuth, and to obtain resolving power substantially improved over that of a single seismometer; but the problem of defining the precise degree of improvement in this case is a formidable one.

4.4. *Recorder Format*

On first approaching the idea of tape-recorders for field use, it is natural to consider the possibility of using a domestic audio $\frac{1}{4}$-in tape-deck as a basis, because the initial cost of such a deck is much lower than that of an instrumentation deck. However, on closer investigation a number of disadvantages emerge which outweigh the solitary advantage for a large-scale project.

A system employing digital recording on such an audio tape-deck has been successfully developed by Lebel and Gouyet,[3] but it has the drawback of rather high tape consumption; it is more suitable for projects involving short recording times (e.g. explosion seismology) than for continuous operation.

A minimum of three seismometer channels per recording set is considered to be necessary for a wide variety of studies. Coded time signals occupy a fourth channel, and since a high dynamic range is called for in the seismometer channels flutter compensation is required. It is arguable that both the time code and flutter reference information could be combined on a single channel, but it would be extremely difficult to separate them on playback to a sufficiently high degree, bearing in mind that the frequency of the time pulses (1 per second) falls within the most important part of the signal frequency band. This leads to a requirement for five separate channels, but the greatest number of tracks available with a single head-stack on $\frac{1}{4}$-in tape is only four. The use of two interleaved head-stacks could give six tracks, but would demand high precision and rigidity of the head mounting and accurate matching of the head spacing on record and playback decks. Frequency-division or time-division multiplex techniques would, of course, permit all the signal channels to be accommodated on a single track, but only at the expense of a higher tape speed and consequently shorter intervals between tape changes.

Whatever type of deck had been chosen as a basis, considerable modification would have been necessary to give low tape speed, low power consumption, and

operation from d.c. batteries. Because of this and the need for it to withstand continuous use and rough handling while in transit, the deck has to be of rather solid construction, and domestic decks in general fall short of the ideal.

Once the decision has been taken to use decks of instrumentation type rather than domestic, the question of tape width arises, with a strong case for 1-in tape. Half-inch tape has no special attraction since it tends to fall in the same cost bracket as 1-in while giving a lower information capacity.

A minimum of three seismometer channels per set has already been mentioned, but facilities for six seismometer channels would be more widely useful. The original plan of the system provided for three channels per set with a total of six sets, but a substantial part of the cost of each set is due to the timing system and the tape-deck, and it is therefore more economical to provide for up to six channels per set with a total of four sets.

In the choice of track configuration, two standards using interleaved head-stacks were already in existence; the U.K.A.E.A. system mentioned earlier (Sect. 3) employs 24 tracks, and the Inter-Range Instrumentation Group (I.R.I.G.), which is responsible for co-ordination of military equipment in the U.S.A., employs 14 tracks. However, for field use with low tape speed it is considered desirable to have a single in-line head to avoid the problems of accurate head spacing, and also to have a wider track pitch than that for the 24-track system to ease the tolerances on positioning of head and tape guides. A standard which was originated by the Society of British Aircraft Constructors (S.B.A.C.) some years ago meets these needs admirably, using an in-line head with 16 tracks. For the present application eight tracks at a time are used, serving six seismometers and time and flutter compensation channels. Each reel of tape can then be turned over and used for a second pass. A significant additional reason for favouring 1-in 16-track tape is its suitability for future development of digital recording from a direct-digitizing seismometer. Both the U.K.A.E.A. and I.R.I.G. standards use a carrier packing density of 900 cycles/in, and this has been adopted in preference to the original S.B.A.C. figure of 1000. The I.R.I.G. figure for percentage deviation is 40, but since the U.K.A.E.A. and S.B.A.C. both use $33\frac{1}{3}$, the latter has been adopted.

4.5. *Tape Transport*

The highest signal frequency of interest in the field studies is 10 c/s, calling for an f.m. carrier of at least 50 c/s, and preferably in the region of 100 to 120 c/s to leave some margin of safety. The main consideration in choosing the precise value of carrier frequency is the desirability of driving the flutter reference track with a crystal-controlled frequency, which is readily available from the timing system. The crystal and dividing chain can be arranged to provide any required frequency and since 60 c/s is widely in use for such purposes as synchronous-motor drives, the logical choice is 120 c/s. Using the I.R.I.G. carrier packing density of 900 cycles/in, this gives a tape speed of 0·133 in/s.

The tape transports used are commercial units specially modified for the purpose. In the earlier versions the capstan was driven by a d.c. governed motor running at 3000 rev/min, but this proved to be unsatisfactory in service because of rather short motor life and severe electrical interference from the commutator and governor, while most of the power consumption was due to drag in the bearings of a flywheel on the high-speed shaft. For the final version a 60 c/s synchronous motor running at 300 rev/min is used, with an amplifier supplied from the crystal-controlled reference frequency mentioned above.

Because of the need to minimize battery drain, the reel drives have also been altered, with a simple friction brake for the supply reel and a d.c. geared motor for the take-up reel controlled by a micro-switch on a tape-tensioning arm. Rather surprisingly, the latter system gives no trouble with either flutter or electrical interference.

The standard length of tape for the 8-in reels used would be 1800 ft, with a running time of 45 hours, but it is convenient to use 2000 ft lengths to give more than two complete days per reel change.

4.6. *Radio Links*

Provision is made for the alternative use of radio or cable links between seismometers and recording set. On a basis of cost, radio compares favourably with cable for distances greater than 2 miles, but on a basis of convenience radio is preferable even for much shorter distances. The equipment may be distributed as independent stations or a local network for crustal studies, or combined as a single array of any desired configuration for teleseismic work.

With simple whip aerials, radio communication is obtainable up to a range of 3 miles, and by the use of more elaborate aerials this could be extended to 50 miles.

4.7. *Access*

In laying out the equipment it is intended that the recording sets will always be sited where they can be reached by a vehicle of the *Land-Rover* type for servicing, but the individual seismometers may be taken to points which can be reached only on foot. There are obvious attractions in a scheme where the seismometers only require service visits at intervals

of one or two months, and this could be achieved by using direct transmission by cable links with only a battery pre-amplifier of very low power drain located near the seismometer. A prototype system on these lines has been tested, but in the final system the advantages of including radio links have outweighed the disadvantage of higher battery drain at the seismometer end.

4.8. *Signal Channels*

A unit containing the amplifier and f.m. modulator is located adjacent to each seismometer. To provide the correct damping load for the seismometer, the input impedance of the amplifier is adjustable by means of current feedback. The carrier frequency can be switched to either 120 c/s for cable links or 960 c/s for radio links. The carrier amplitude (5 V peak to peak) is adequate for transmission by single-core screened cable without special precautions, and at the recorder it is fed direct to a simple record head amplifier. The 960 c/s carrier is transmitted over the speech channel of a 'walkie-talkie' radio pair, and at the recorder it is divided down to 120 c/s to drive the record head amplifier. Twelve channels in the 150 Mc/s band have been allocated by the G.P.O. for limited use in this country.

4.9. *Timing*

Each set is provided with a crystal controlled time encoder, using an oven-maintained crystal to give a stability of around 1 part in 3×10^6. The coding of the time marks is similar to that used by U.K.A.E.A. To permit the relative timing between recorders to be established accurately, a radio receiver in each set is automatically switched on for 20 seconds every hour, and its output (after being shaped by filtering and rectification) is superimposed on one signal channel. Reliable reception conditions cannot be guaranteed at all times of the day for those stations which provide standard time services (e.g. MSF Rugby), so use is made of the normal local medium-wave stations for time signals. The interval between these signals may be 9 hours in the worst case, but this provides a sufficient check on the absolute timing. For the relative timing it is not necessary to have actual time pips; any burst of speech or music will give a recognizable envelope which should be the same on each recorder. For analysis where accuracy of relative timing is required, the time-check records from each tape will be matched by the computer with a correlation technique.

4.10. *Servicing Facilities*

A high-roof 15-cwt van serves primarily for bulk transport and miscellaneous duties. It could easily be fitted out as a workshop or operations centre for use when no other accommodation is available (as, for example, in regions which are either uninhabited or suffering from earthquake damage).

A long-wheelbase *Land-Rover* has been fitted out as a mobile laboratory, to fill a three-fold role: servicing of the recording sets and seismometers in action, engineering checks on the operation of the equipment, and preliminary seismological assessment of recordings. Routine servicing consists chiefly of changing tapes and batteries, and correcting any drifts which may be observed in amplifiers, modulators, and time encoders. Engineering checks are obviously essential in setting up the equipment initially, but should also form part of the procedure for day-to-day running. Desirable checks include transmission of various test signals, calibration of the entire signal chain, and evaluation of the recorded tapes for (i) carrier amplitude, (ii) carrier mid-frequency, (iii) dynamic range (flutter and instrument noise), (iv) similarity of performance between channels. The amount of seismological assessment depends on the nature of the project in hand, but will include such questions as: (i) how well specific events (e.g. explosions) have been recorded, (ii) how many events of a given character have been observed, (iii) how uniformly the different seismometers have been functioning, and whether any require to be moved to a better site. For the latter point it is important to have proved by engineering checks that the signal channels are above suspicion and that any observed differences can therefore be ascribed to the siting of the seismometers.

A high degree of mobility has been considered essential for the complete field system and the servicing equipment has therefore been limited to that which can be accommodated in a single *Land-Rover*. Electrical power (240 V, 50 c/s) is supplied by a built-in 3 kW alternator driven from the engine in conjunction with a servo speed control. The facilities include a tape-deck with five channels of f.m. playback, a jet-pen recorder, and an audio monitor. Certain items such as a digital frequency meter and an oscilloscope can be operated directly from batteries, for checking the seismometer amplifiers and modulators *in situ*, where they may not be accessible by vehicle. For working in unfavourable weather conditions a sliding roof can be extended from the back of the vehicle to cover the recording set, and a canvas windshield erected around it.

Power for each recording set is supplied by two car-type lead-acid batteries (12 V, 90 Ah), and these are changed at two-day intervals, as are also the tapes. The service vehicle is fitted with a 60-A battery charger, so that when no mains facilities are available at the base-station the recorder batteries can be re-charged in the course of the service visit. Each seismometer unit is powered by three motorcycle-type

batteries (6 V, 12 Ah) requiring changes at intervals of four days for cable links or two days for radio links.

4.11. *Performance*

The frequency response of the seismometer amplifiers is level from 0·025 to 20 c/s (see Fig. 2), and amplifier noise in the seismic signal band is approximately 6 μV peak-to-peak, referred to the input. The noise due to the f.m. modulators and demodulators is substantially below that of the amplifier. The seismometers used at present are of the short-period

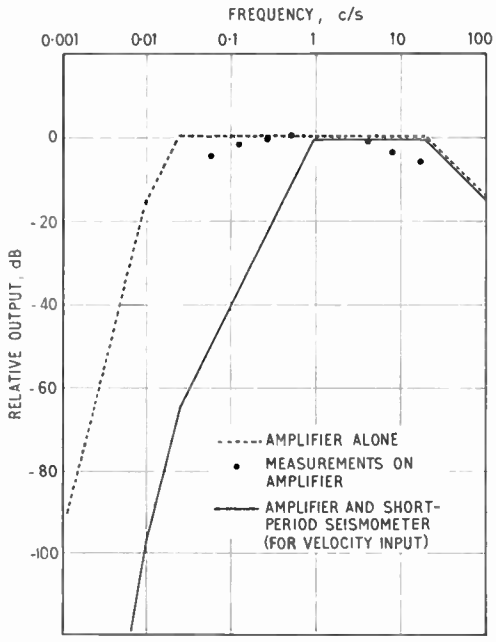

Fig. 2. Frequency response of field recording set.

Willmore pattern (having the period adjustable between 0·6 and 3 seconds) but further development is planned for a system using such seismometers with photocell amplifiers and feedback to give a level response to ground velocity over the range 0·01 to 10 c/s.[7]

The operating temperatures encountered in field work can vary over a wide range, even in the course of a single day, but in general the rate of change is slow in comparison to seismic frequencies, and thermal drifts do not therefore contribute greatly to the noise level. The limitation which does arise is that the total drift must not be sufficient to shift the operating range of the amplifiers and modulators beyond the linear part of their characteristics. The equipment is designed to operate in ambient temperatures between −10 and +45°C.

Figures for the dynamic range of the f.m. tape system are of little value unless the conditions of measurement are specified in great detail. The chief factor which degrades the dynamic range is flutter on the low-speed recording deck, and the form of subtractive flutter compensation which is in general use is effective only around zero deviation; in the region of maximum deviation the flutter is not fully compensated but only reduced by approximately two-thirds. If an interlaced pair of heads were used, a separate flutter-compensation track should be used for each head, although I.R.I.G. practice normally ignores this point. Crosstalk between adjacent channels also presents problems, and the use of interlaced heads or of only alternate tracks on an in-line head appears to offer lower crosstalk than the use of adjacent tracks on an in-line head. Under favourable conditions, a dynamic range of the order of 60 dB can be achieved, but a figure of 50 dB is more realistic for typical operating conditions.

5. Data Laboratory

The basic processing technique for a spaced array is the operation of 'velocity filtering'.[6] This involves summation of the signals in two groups, with appropriate weightings and time-lags corresponding to the time taken for a chosen wave-front to pass across the array, followed by cross-correlation of the outputs of the two groups. By this means the sensitivity of the array is enhanced for signals of a particular azimuth and apparent velocity (i.e. allowing for the angle of emergence) and diminished for other signals.

Originally the project had been planned in terms of the development of special-purpose analogue equipment. For example, a tape-deck with a set of staggered heads could be used for introducing the inter-element time-lags. However, the use of a large general-purpose digital computer is now preferred, because of the freedom to change the techniques of analysis merely by writing a fresh program. It also simplifies the problem of combining data from several recording stations to form a single array. Unfortunately, sharing a large computer with other users is liable to involve delays, and there is therefore a great attraction in having laboratory facilities for processing array data, even in a limited way.

The data laboratory combines the following functions:

(i) Playback of original analogue tapes for preliminary assessment.

(ii) Building of a library of events.

(iii) Preparation of data for computer input.

(iv) Playback of computer output.

(v) Simplified processing of data.

5.1. *Analogue Playback*

The main playback deck is provided with 24 channels of f.m. demodulators, and for normal operation the tape speed is $7\frac{1}{2}$ in/s. Some channels are also provided for operation at $\frac{15}{16}$ or 30 in/s as required. The deck carries an interleaved pair of 12-track heads for fixed-array tapes, and a 16-track head for mobile-array tapes. The system is compatible with I.R.I.G. standards except in the matter of track spacing, and any future studies which may require the use of tapes of I.R.I.G. format (14 tracks on 1 in width) can be accommodated by the addition of the appropriate head stacks.

Any four selected outputs may be displayed on a jet pen recorder handling frequencies up to 1000 c/s, with three channels of variable band-pass filtering. For monitoring purposes an audio amplifier and loudspeaker have proved to be extremely valuable; using speed-up ratios in the region of 30 to 100, much of the seismic information falls within the audible range, and an experienced operator can readily assess the characteristics of events from various distance ranges, and of background noise. Experience to date indicates that the detection capability by ear is superior to that by eye for the conventional chart record, especially for arrivals which are partially obscured by noise, although a longer time is required for scanning.

5.2. *Library*

A comprehensive library of tape recordings is to be built up, both from fixed array stations and from the field recorders. Ideally, the data should be collected on a very general basis, with the objective of providing suitable material for a wide range of studies in due course. However, the tape cost for such a library would be excessive, and in practice the events will have to be carefully selected. Obviously all the larger events should be included, but it would also be desirable to have a series of events which fall just below the limit of detection on a conventional record. In the initial stages the selection process will have to rely heavily on the judgement of an experienced seismologist, but later it should be possible for it to be performed automatically; a computer search of epicentral data from such organizations as the U.S. Coast and Geodetic Survey or the International Seismological Research Centre could provide a list of all the times when suitable events should have been recorded at a given station, and a simple correlation technique applied to the original recording could indicate the existence of coherent phase arrivals even when they are not clear on a conventional record.

A digital format for the library would be preferable to f.m. on the grounds of reduced contamination of data with repeated transcription, together with ease of detection of such contamination as may occur. Since the system is to accept the original analogue tapes and transfer the data to computer tapes, this would appear to be the way to produce the library with a minimum of additional equipment. Unfortunately, the computer format requires approximately eight times as much tape as the 24-track f.m. format, but the computer standards are based on a far higher degree of freedom from drop-outs than is justified with seismic data; it is envisaged that a digital format could be evolved for more economical use of tape by techniques which have proved satisfactory in other fields of instrumentation (doubling the number of tracks and doubling the bit density) without any serious increase in drop-out troubles. A more important consideration is the need to start building the library at the earliest possible stage, i.e. before the complete digital system has been commissioned, and therefore the library in the initial stages will consist of f.m. tapes produced by direct re-recording (without demodulation). This requires only a second tape transport and a relatively simple amplifier for each track in addition to the normal playback system.

5.3. *Digital Computer Input*

The main analysis has been planned on the basis of using the *Atlas* computer at Manchester, sending the main data on magnetic tape and the program details either indirectly by posting punched tape or directly by the use of the land line data link which is already serving Edinburgh University.

One of the major drawbacks to the use of a digital computer for large data flows is the requirement that the data should be grouped into blocks on the computer input magnetic tape and separated by gaps. The equipment for buffering data into such blocks makes up a substantial proportion of the cost of a data laboratory, and there is a strong case for the view that this is an operation which should be handled by the computer. The technical problems of providing back-spacing operation of the computer tape handler are trivial, and this would permit the input of data in continuous digital form with only block markers and no inter-block gaps. No computer with such a facility is available in the U.K., although at least one has been in operation in the U.S.A. for several years. This is at Rice University, where a direct-digitizing seismometer system has been developed to take advantage of it.[1]

A further difficulty arises in the matter of checking of input. Normally a computer assumes the input to be of such high quality that even a single drop-out is unacceptable, and check-bits are provided for longitudinal or transverse parity (or both). If an error is detected by these checks, the input tape is re-read several times, and if the indication is still

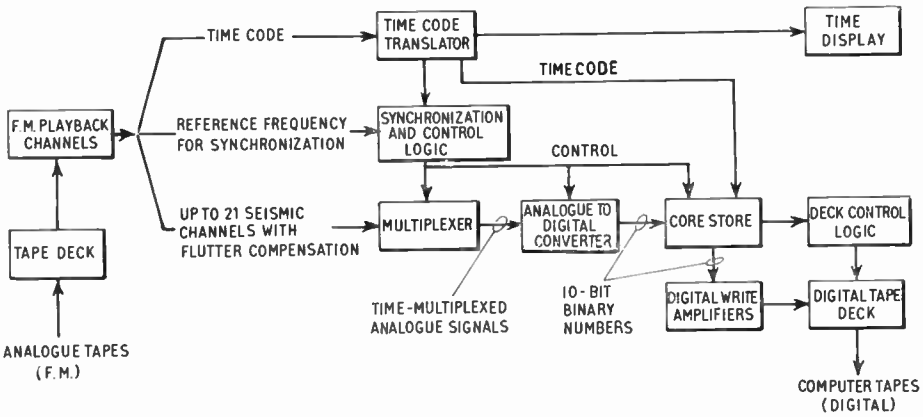

Fig. 3. Block diagram of digitization system.

unsatisfactory the entire input is rejected. In general, the seismic data are of much lower quality; the original ground motion picked up by the seismometer may contain such features as disturbances due to animals moving in the near vicinity of the seismometers, and the instrumentation system is liable to give rise to occasional spurious signals such as drop-outs in the f.m. tape record. Single drop-outs in the digital system would not seriously worsen the quality of the data, and elaborate checking of the input tape transfer is simply not worthwhile. The data could be accepted without check-bits, and a program applied to detect erroneous signal levels and to substitute more acceptable figures such as the mean of adjacent readings. Data containing errors should not be rejected outright but should only have the faulty portions tagged. What is needed, however, is a simple check to permit the detection of a continued equipment fault before a large amount of computer time has been used up, and a transverse parity check is incorporated for this purpose. The longitudinal parity check which would normally be written after each block in *Atlas* format (a 24-bit check-sum with end-around carry) is omitted, and the computer is programmed to proceed without it.

5.4. *Digitization*

The equipment for digitization comprises the 24-channel playback deck for f.m. tapes, a sampling switch, an analogue-to-digital converter, a magnetic-core store buffer, and a digital tape handler (Fig. 3). The maximum data rate is limited by the capacity of the digital tape handler to around 30 000 samples per second, and in this respect the 1-in format used on *Atlas* gives a rather higher data rate than the widely used ½-in IBM format. The maximum data rate used in practice is 20 000 samples per second, corresponding to a speed-up ratio of 28 for a 24-channel recording of signals up to 10 c/s.

Control is effected by a unit reading the time code, to start and stop the operation at pre-set time readings. It is not necessary to make use of the absolute time information during the processing operations, and it is sufficient to digitize the time-code in the same way as a seismometer channel, so that the time marks can be presented in the final output alongside the processed results. It is, however, most desirable that the sample rate should be synchronized by means of a reference frequency played back from the tape (such as the flutter-compensation signal) to minimize the tendency for irregularity in the sample rate resulting from the presence of flutter.

The special case when synchronization of the sample rate becomes essential is when data from two or more recorders is to be combined for summation or correlation. If the sample rates are not sufficiently close to remain in step throughout the portion of event being processed, a considerable amount of extra interpolation would be called for.

When data is to be assembled from several recorders to form an array, the procedure is to digitize each analogue tape separately to produce computer tapes. A preliminary run on the computer is then employed to match up the hourly time-checks and to sort the complete data on to a single digital tape by reference to the time-code.

5.5. *Computer Output*

For the basic velocity-filtering process, the computer is used simply for performing arithmetic operations on a large flow of data, and it is envisaged that the output will be required in the form of a paper chart record for visual interpretation. In this case the computer will provide the output on magnetic tape, and for playback of such tapes to give analogue output the core store is again used as a buffer, to feed a digital-to-analogue converter followed by a jet-pen recorder. For such purposes as contour mapping a cathode-ray tube and camera are provided.

5.6. *Simplified Processing*

For the operation of summation without lags, relatively simple equipment is sufficient, but the chief benefit of a spaced array lies in the velocity-filtering effect obtained by the insertion of lags, and this necessitates considerably more elaborate equipment. It is worth investigating array configurations which yield some improvement without the use of lags, especially for field work.

The simple three-component set is particularly rewarding: by summing the two horizontal components in appropriate ratio and sign to derive the radial component for a given event, and then cross-correlating the vertical component against this radial component, a clear indication of the type of particle motion is obtained. For the P waves the correlator gives a positive output, for the S waves a negative output, and for the surface waves an oscillating output. This opens up such possibilities as the recognition of converted phases, involving small arrivals of S waves in the presence of a strong P wave signal. Earlier work[5] has tended to concentrate on longer periods for such studies, on the assumption that the short-period waves are too greatly affected by local scattering near the seismometer, but preliminary experiments indicate that signals even in the region of 3 to 10 c/s contain usable directional characteristics. The playback facilities include an analogue multiplier and operational amplifiers for summation and integration to enable further investigation to be made of the potentialities of correlation techniques.

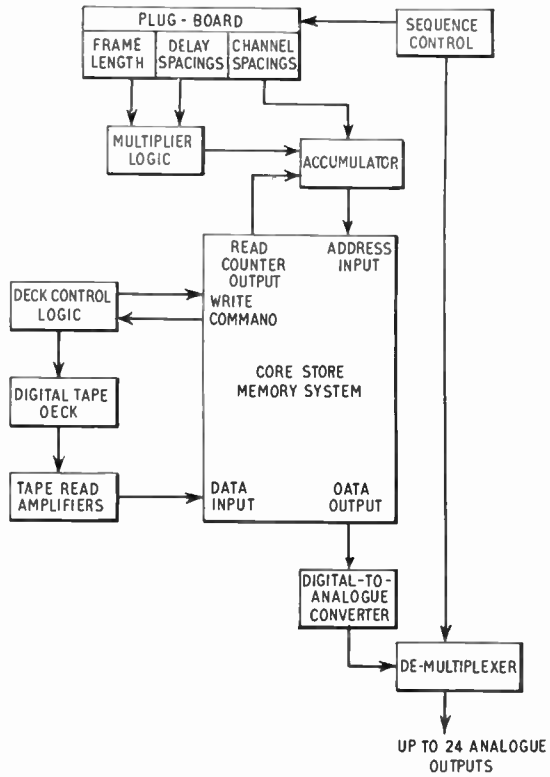

Fig. 4. Block diagram of digital processor.

5.7. *Special-purpose Digital Processor*

A design study has been carried out on a scheme for using the core store in conjunction with special addressing and read-out facilities to perform processing with lags (Fig. 4).

Given the data in time-multiplexed digital form on computer tape, the problem is chiefly one of addressing, provided that various limitations are accepted. The maximum time difference across the full array which can be handled conveniently corresponds to the time spanned by the data packed in a single block of 2048 samples. For 24 channels at signal frequencies up to 10 c/s the time per block is over 2 seconds, and this is in fact adequate for most purposes. For arrays of larger dimensions which may require time differences of more than a few seconds the signal frequencies involved are lower and a lower sampling rate can be employed, so that again a span of 2048 samples is adequate. To obtain the maximum benefit from the velocity-filtering process, interpolation should ideally be applied to give exact time lags, but for the sake of simplifying the equipment it would be acceptable to take the nearest sample instead.

The main use of such a special processor would not lie in running a general search for unknown events, but in studying selected events for which preliminary determinations of origin time and position are available, so that the theoretical arrival times and characteristics of particular phases can be predicted. It is therefore not too inconvenient to process for only a single velocity and azimuth at one pass and to have to change the input settings for each new velocity or azimuth. The scheme could, however, be extended to handle several velocities and azimuths simultaneously.

The capacity of the store is two complete *Atlas* blocks, so that while one block is being processed the other can be re-filled with fresh data. When the data are read into the store, it is required to present in sequence the outputs from a number of data points spaced apart by suitable intervals of time, i.e. spread over certain spans of address spacings. For any specified set of time lags there can be defined a corresponding set of address spacings, giving a movable frame which can be swept through the data in the store. The spacings are the sum of two terms: one giving the incremental delay, a spacing which is

an integer multiple of the number of data points in one complete scan; the other specifying the data point selected in terms of sequence within the scan.

Information set in by the operator on a simple plug-board or switch panel would define the array configuration and the incremental time lags required, and a special arithmetic unit would derive the spaced addresses from this information using the sequential read counter of the store to define a reference point for each scan. This arrangement would deal with arrays having uniform distances between elements, but for non-uniform distances it would be necessary to provide facilities for setting the individual address spacings separately.

Before summation, it is necessary to modify each channel output by a multiplying factor covering (i) reduction of all channels to a standard gain level, and (ii) relative weighting according to the position within the array.

Substantial reduction in the cost and complexity of the system may be achieved by conversion of the data back to analogue form after reading out from the store and before the summation and correlation operations.

The normal means of displaying the output is a four-channel jet-pen recorder, and a typical display would comprise the two summed signals before multiplication, the signal after multiplication and integration, and the time code. The same facilities would also serve the purpose of displaying any four channels from a time/multiplexed digital tape without additional processing.

6. Conclusion

The requirements of equipment for the acquisition and processing of seismic data have been discussed in some detail, together with the system design considerations.

The mobile equipment described is now ready for operation, and was used during the 1965 season for field-work in Ireland and Wales.

Data laboratory facilities for analogue playback and interpretation, and for copying tapes in f.m. format, are already in use. Facilities for operation in conjunction with a general-purpose digital computer are scheduled to be available during 1966.

7. References

1. J. Cl. de Bremaecker *et al.*, 'The Rice digital seismograph system', *J. Geophys. Res.*, **68**, No. 17, pp. 5029–34, 1st September 1963.
2. M. N. Hill (ed.), 'The Sea', Vol. 3, pp. 39–46. (Interscience, New York and London, 1963.)
3. J. D. Lebel and J. P. Gouyet, 'Earth science data acquisition in digital form using audio tape recorders', International Conference on Magnetic Recording, London 1964. (Institution of Electrical Engineers.)
4. C. G. Keen *et al.*, 'British seismometer array recording systems', *The Radio and Electronic Engineer*, **30**, No. 5, pp. 297–306, November 1965.
5. G. H. Sutton and P. W. Pomeroy, 'Analog analyses of seismograms recorded on magnetic tape', *J. Geophys. Res.*, **68**, No. 9, pp. 2791–815, 1st May 1963.
6. F. E. Whiteway, 'The recording and analysis of seismic body waves using linear cross arrays', *The Radio and Electronic Engineer*, **29**, No. 1, pp. 33–46, January 1965.
7. P. L. Willmore, 'Some properties of heavily damped electromagnetic seismographs', *Geophys. J. Roy. Astronom. Soc.*, **4**, pp. 389–404, 1961.

8. Bibliography

M. Shimshoni and S. W. Smith, 'Seismic Signal Enhancement with Three-component Detectors', California Institute of Technology, Division of Geological Sciences, Contribution No. 1244, 1964.

P. L. Willmore, 'A strategy for seismology', *Geophys. J. Roy. Astronom. Soc.*, **8**, No. 2, pp. 242–8, 1963.

P. L. Willmore, R. Parks, *et al.*, 'New methods in seismology', *Quart. J. Roy. Astronom. Soc.*, **4**, No. 4, pp. 391–405, December 1963.

Manuscript first received by the Institution on 19th June 1964, in revised form on 31st May 1965 and in final form on 11th October 1965. (Paper No. 1032/EA28.)

U.D.C. 621.376.233: 621.382.23

The Performance of Backward Diodes as Mixers and Detectors at Microwave Frequencies

By

T. OXLEY†

AND

F. HILSDEN†

Reprinted from the Proceedings of the Joint I.E.R.E.-I.E.E. Symposium on 'Microwave Applications of Semiconductors' held in London from 30th June to 2nd July 1965.

Summary: The physical properties of a backward diode, together with the parameters of a microwave mixer and low-level detector are briefly reviewed, indicating the choice of a bonded-contact structure and n-type germanium. The microwave performance of such a diode is discussed with particular emphasis on optimizing the diode for low-level detector and Doppler mixer applications.

Results of r.f. performance at X-band frequencies are illustrated. These show that bonded backward diodes may be fabricated with improved detector and Doppler mixer characteristics compared with conventional point-contact microwave diodes. Further, the desirability to optimize their characteristics for a particular application is examined. Zero-bias tangential sensitivities of −62 dBm (1 Mc/s video bandwidth) have been achieved. The low-frequency noise properties of the backward diode indicate a potential receiver noise figure performance of about 16 dB at 3 kc/s intermediate frequency. The ability of the bonded backward diode to operate satisfactorily as a mixer (i.f. = 45 Mc/s) with very low local-oscillator power is shown.

Finally, the performance of a bonded backward diode under development primarily as a detector is discussed. Measurements at zero bias indicate tangential sensitivities of −56 dBm (1 Mc/s video bandwidth) and video impedance about 800 Ω, whilst maintaining a mixer performance of about 8 dB. Further, this performance is shown to be substantially independent of temperature. The resistance of these devices to damage by electrical overloads is shown to be comparable with conventional point-contact microwave diodes.

1. Introduction

Until fairly recently, microwave mixer and detector diodes have been based upon the phenomena of majority carrier injection across the Schottky type barrier between a metal and semiconductor. However, the introduction of tunnel diodes by Esaki demonstrated that rectifying characteristics could be obtained based upon quantum-mechanical tunnelling of current carriers across a p–n junction. Such devices fabricated using alloyed-junction techniques can be unsatisfactory for microwave frequency performance due to the high junction capacitance associated with a heavily-doped semiconductor and large area junction. A method of fabricating diodes exhibiting the tunnelling phenomenon but restricting the capacitance was described by Eng,[1] who formed backward diodes by pulse-bonding contacts of gallium-plated gold wire to degenerate n-type germanium. Further work on this subject has been described by Burrus,[2] Oxley[3] and Shurmer,[4] and, as the results of recent advances in this field, this paper is intended to discuss the potential microwave applications of bonded backward diodes, with special attention to video detector and Doppler mixer aspects.

† Associated Semiconductor Manufacturers Ltd., Wembley Laboratories, Middlesex.

2. Rectification Efficiency at Microwave Frequencies

A diode rectifier may be represented by the simple equivalent circuit of the barrier resistance R_B, shunted by the barrier capacitance C_B, and this combination being in series with the spreading resistance r. For a mixer diode which normally operates under large-signal conditions (i.e. local-oscillator powers in the milliwatt region), the reverse resistance encountered is several kilohms, whilst the barrier capacitance is about 0·2 pF; thus at microwave frequencies the reverse impedance is effectively that of the capacitance alone. The rectification efficiency (and conversion loss) then is the ratio of conductance in the forward direction to the admittance in the reverse direction and may be given by[5]

$$\eta = 1 - j\frac{1}{\omega C_B r} \qquad \text{.....(1)}$$

In detector diodes, signal conditions are low (i.e. in the microwatt region) and the concept of front/back ratio for the mixer application has little significance and the equivalent circuit becomes a current generator shunted by the barrier admittance. At low level the diode operates as a square-law device, i.e. the current is approximately proportional to the square of the input voltage, or, the current is proportional to the input power. The diode sensitivity is measured by the short-circuit current and the microwave current sensitivity may be given by the relation[5]

$$\beta \simeq \frac{\beta_0}{1+\omega^2 C_B^2 R_B r} \qquad \ldots\ldots(2)$$

where β_0 is the low-frequency current sensitivity.

Thus for high efficiency, C_B and r must be minimized for mixer and detector considerations; however, detector sensitivity depends on the square of C_B in contrast to linear dependency for the mixer. These conditions are normally achieved using a point-contact structure and making the contact area as small as possible consistent with mechanical stability and resistance to electrical overloads. The pulse-bonded contact, however, does in fact differ from the conventional point contact in that the whisker wire is alloyed to the semiconductor rather than the pressure contact of the latter case, hence, slightly larger values of barrier capacitance may be expected for the same initial wire diameter.

3. The Backward Diode

The tunnel diode, or Esaki diode is a p–n junction diode exhibiting quantum mechanical tunnelling. The diode itself is made of heavily-doped semiconductor material and is an abrupt junction with an extremely narrow depletion layer. Much of the importance of the tunnel diode arises from its negative resistance property but, in the case of the backward diode, the tunnelling current is reduced from the high levels of a conventional diode to such levels that the negative resistance is almost non-existent.

Tunnel or backward diodes are normally fabricated by alloying techniques, hence the capacitance of such diodes may impose a limitation on the frequency at which the devices can be operated: so it is logical that a bonded structure (with its associated small contact area and low capacitance) is an attractive method to obtain the required capacitance for microwave frequencies. The performance of the diode is largely determined by the physical properties of the semiconductor and fabrication techniques employed. Carrier concentrations of about $10^{19}/cm^3$ are required and a high mobility is desired to minimize spreading resistance. Germanium, gallium antimonide and gallium arsenide all have acceptable properties. At present, however, investigation into the use of the latter two materials for bonded backward diodes, has not produced a more promising combination than n-type germanium with gallium as the acceptor source for the junction.

The fabrication of such devices, employing a gallium-plated gold whisker wire pulse-bonded to low-resistivity germanium, has been described fully in previous publications.[1–4] The diodes discussed in this paper were fabricated using similar techniques, and assembled in various existing encapsulations designed for mixer and detector applications in the frequency range of interest. These were, an X-band coaxial construction, a Q-band plug-in waveguide construction and a miniature double-ended capsule. However, in all cases, the whiskers were made from gold wire, about 0·002 inch diameter, and plated with gallium, and the semiconductor material was arsenic-doped n-type germanium of resistivity less than 1 mΩ cm. A mechanical contact was established between the whisker point and the germanium surface, the junction being formed using pulse-bonding techniques to alloy the tip of the whisker to the wafer.

4. Fabrication by Pulse Bonding

The tunnelling probability depends on the impurity concentration on both sides of the p–n junction. If in fabrication, one doping level is kept constant at some high level, then by adjusting the second impurity level the tunnelling process may be restricted. Control of this process for alloyed-junction backward diodes is usually achieved through the use of less heavily-doped semiconductor material. However, for bonded backward diodes, the semiconductor material is normally as heavily doped as possible and the tunnelling controlled to a certain extent by the pulse bonding process. The consequences of pulsing the junction to the desirable characteristics is illustrated in Fig. 1.

This shows examples of different forms of *I-V* characteristics which are controllably reproducible, as are intermediate forms, by bonding a gallium-plated wire to n-type germanium material of the same initial resistivity. The tunnelling process is produced by increasing the energy of the bonding pulse and therefore the extent to which the wire is alloyed to the semiconductor. Thus there is an associated enlargement in junction area, with consequent increase in barrier capacitance and decrease in spreading resistance as the peak current is increased. Diodes representative of characteristics with negligible peak current may be expected to have a junction capacitance of about 0·1 pF and spreading resistance about 10 Ω, characteristics with 30 μA peak current of about 0·2 pF and 5 Ω and characteristics with 250 μA peak current of about 0·5 pF and 2 Ω.

The *I-V* characteristics of a backward diode fabricated in this manner may therefore be adjusted to a

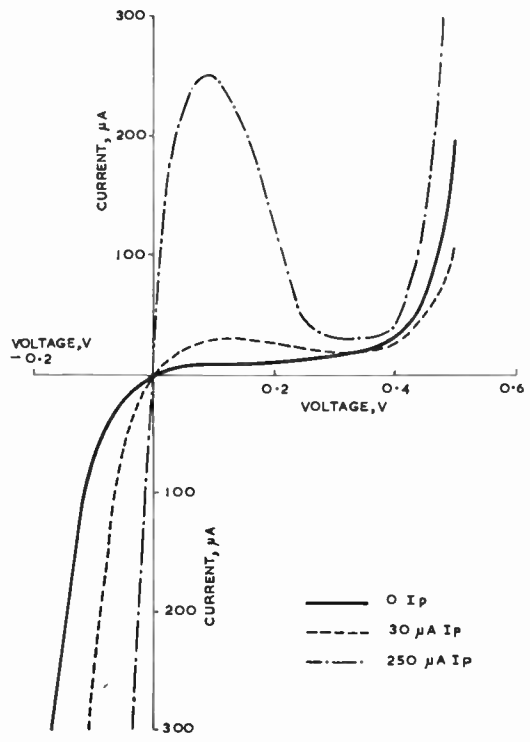

Fig. 1. *I-V* characteristics.

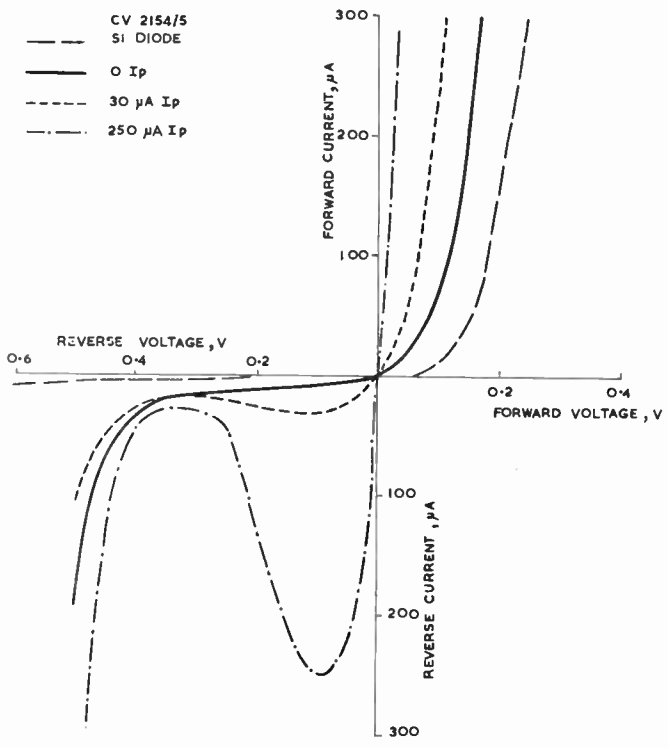

Fig. 2. *I-V* characteristics—detector level.

desirable shape, but with the usual compromise of barrier capacitance and spreading resistance to achieve optimum microwave performance for a particular application. However, due to the low value of spreading resistance encountered, larger values of barrier capacitance may be tolerated than are normally associated with conventional point-contact diodes.

5. Low Level Detector Application

The quality of the video crystal detector is normally expressed quantitatively in terms of current sensitivity and video impedance, known as the 'figure of merit'.

The 'figure of merit' is usually defined by

$$M = \frac{\beta R}{\sqrt{R+R_A}}$$

where β is the microwave current sensitivity,
R is the video impedance
and R_A is an arbitrary resistance used to represent the amplifier noise, defined as the equivalent noise resistance of the video amplifier.

However, the conventional sensitivity rating for video detectors is 'tangential sensitivity', which indicates the ability of the detector to detect a signal against a noise background. Tangential sensitivity may be defined as: the r.f. pulse power, below 1 mW reference level, necessary to display on an oscilloscope a signal exceeding the noise level by an amount equal to the width of the noise.

The relationship between 'figure of merit' and tangential sensitivity for a 1-Mc/s video bandwidth has been given by Frohmaier[6] and may be derived from the formula

$$T_s = \left(51 + 10\log_{10}\frac{M}{60}\right) - \text{dBm}$$

which implies that a tangential sensitivity of -51 dBm corresponds to a figure of merit of 60.

5.1. *D.C. Characteristics (Detector level)*

For detector applications, the best type of *I-V* characteristic is one with maximum curvature at the operating point and it is desirable that this should occur at zero bias, as the use of bias current may introduce some additional noise into the system. The *I-V* characteristics of backward diodes representative of those shown in Fig. 1 are reproduced in Fig. 2. To enable a direct comparison to be made with a conventional silicon point-contact diode, the backward diode characteristics have been reversed so that the direction of easy current flow is compatible with the conventional diode. Because of the greater curvature at the origin and steeper *I-V* characteristic, the backward diode may be expected to have a potentially higher current sensitivity than do conventional

detector diodes. In addition the backward diode exhibits lower values of video impedance than the conventional diode.

Video impedance is the slope of the *I-V* characteristic at the operating point and for zero bias operation it can be seen to be related to the diode peak current. The video impedances at zero bias of the backward diode characteristics shown are about 5000, 1000 and 100 Ω for devices with peak currents of zero, 30 μA and 250 μA respectively, compared with about 20 000 Ω for the conventional diode. The relation between curvature at the origin and video impedance will be noted, i.e. the curvature is reduced for very low values of video impedance, as it is for the high values found in conventional point contact diodes.

5.2. *Tangential Sensitivity*

The relationship between video impedance and tangential sensitivity (1 Mc/s video bandwidth) for a zero bias backward diode detector has been given by Shurmer,[4] from a theoretically derived low-frequency sensitivity of 12 μA/μW. Figure 3 examines experimental evidence obtained at X and Q-band frequencies for zero-bias tangential sensitivity as a function of video impedance and comparison is made with these theoretical values. It is of interest to note that microwave sensitivities approaching the theoretical low-frequency values are obtained at X-band frequencies and thus it is apparent that the reduction term $\omega^2 C^2 R_B r$ is one or less and does not therefore degrade the low-frequency values. However, this is not the case at Q-band frequencies, where the low-frequency sensitivity is degraded to an extent dependent on the barrier capacitance, i.e. the loss in sensitivity is about 9 dB for a video impedance of about 1000 Ω and about 6 dB for a video impedance of about 5000 Ω. This does in fact reduce to about 5 dB for 8000 Ω.

The best conventional point-contact detectors, biased for optimum sensitivity, achieve values of tangential sensitivity for a 1-Mc/s video bandwidth of about −52 dBm at X-band and −47 dBm at Q-band frequencies. It will be apparent then that the backward diode can offer a substantial improvement in sensitivity of about 5 dB at X-band and about 8 dB at Q-band frequencies, and this may be obtained without the complications of bias. Further, the video impedance may be optimized to a certain extent for a particular application.

5.3. *R.F. Bandwidth*

The microwave bandwidth of a detector diode is also of importance for many applications and a compromise of sensitivity may be required to achieve the best overall performance. It is reasonable to expect better bandwidths for low values of video

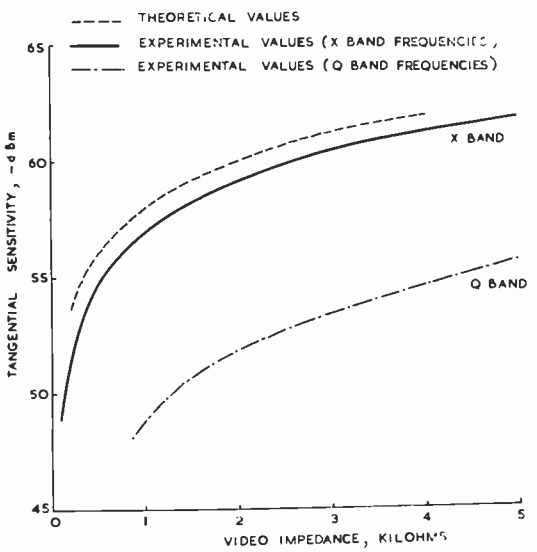

Fig. 3. Tangential sensitivity as a function of video impedance. (1 Mc/s video bandwidth).

impedance as the relative effect of the barrier capacitance is reduced, provided of course that the capacitance does not increase in proportion to the decrease in video impedance. Conventional detector diodes are, in fact, often biased in the forward direction, not only to take advantage of any improvement in sensitivity, but also to reduce their video impedance with a consequent improvement in bandwidth. Due, therefore, to the low values of video impedance obtainable for the backward diode detector, it may be expected that such a device should have potential broadband properties. However, as already discussed, the barrier capacitance of the bonded backward diode increases in relation to the decrease in the zero-bias video impedance, and a compromise of these parameters may become necessary for zero-bias operation and broadband applications extending into X-band frequencies. As for conventional detectors then another approach for further improvements in the bandwidth characteristics of the bonded backward diode may be the use of a small forward bias, and it may therefore be of interest to consider very briefly the performance of a biased backward diode.

5.4. *Bias*

At present there is no evidence of a practical improvement in tangential sensitivity by biasing the backward diode. High values of sensitivity may be achieved by correct biasing of tunnel diodes to the peak or valley regions, however, the video impedance is likely to be objectionally high and stability problems are encountered.

The effect of applying bias in the direction of easy current flow is illustrated in Fig. 4. This examines

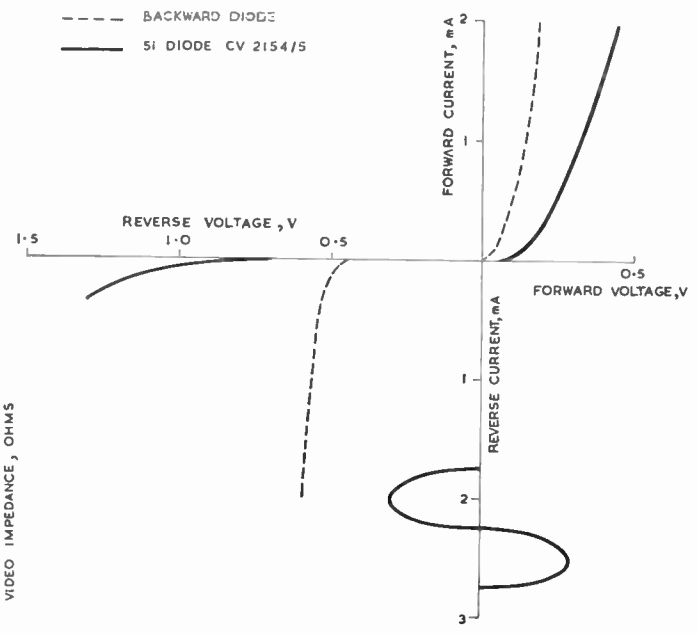

Fig. 5. *I-V* characteristics—mixer level.

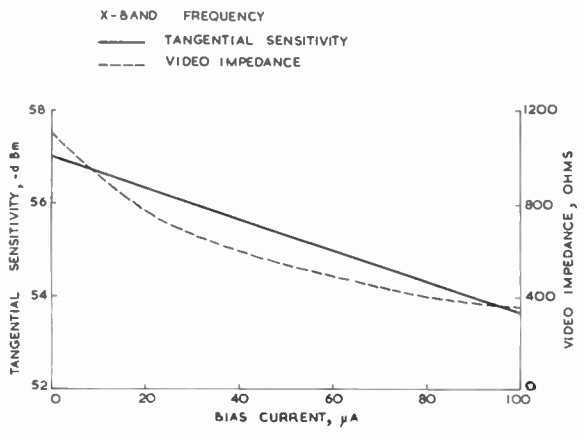

Fig. 4. Tangential sensitivity and video impedance as a function of bias current (X-band frequency) (1 Mc/s video bandwidth).

tangential sensitivity and video impedance as a function of bias current for an X-band diode with a zero-bias impedance of about 1000 Ω. The reduction in video impedance shown without serious loss in sensitivity is typical of a forward-biased bonded backward-diode detector. The evidence indicates that by correct choice of *I-V* characteristic, i.e. zero-bias video impedance and barrier capacitance, a biased backward diode has possibilities for broadband requirements and for applications at millimetre wavelengths. For example, at Q-band frequencies (i.e. frequencies about 35 Gc/s), an 8000 Ω zero-bias video impedance diode may be biased to reduce the impedance to less than that of 1000 ohms and still achieve a tangential sensitivity (1 Mc/s video bandwidth) of about −56 dBm.

6. Mixer Applications

A convenient way of expressing the performance of a microwave mixer diode is in terms of the overall noise figure F_0, of the receiver.

It can be shown that

$$F_0 = L_c(N_r + F_{i.f.} + 1)$$

assuming any local-oscillator noise is adequately suppressed, where L_c is the conversion loss of the mixer diode, N_r is the noise temperature ratio of the mixer diode and $F_{i.f.}$ is the noise figure of the i.f. amplifier.

As already discussed, the conversion loss of the diode is dependent on the product $C_B r$ and this must be minimized for optimum performance.

Noise temperature ratio, on the other hand, must also be considered; the contributions here are thermal, shot and flicker noise. For conventional point-contact mixer diodes, the noise temperature ratio is associated with the semiconductor surface preparation, fabrication techniques and reverse current leakage of the diode. At intermediate frequencies of about 45 Mc/s, the major contribution is usually shot noise, but at lower frequencies flicker noise predominates. However, the rectifying characteristics of the backward diode are based upon a different mechanism from the conventional diode, and the noise behaviour is not the same. In fact, examination of noise under d.c. bias conditions has indicated that the tunnelling mechanism does not produce flicker noise to the same extent as the usual point-contact junction. Further, the tunnelling phenomenon is only feasible for abrupt junctions in heavily doped semiconductors, thus the surface contribution should be reduced compared with conventional mixer diodes. Also, the larger area junctions permissible as the spreading resistance is reduced, suggest decreased current density at the contact and imply improved flicker noise properties.

6.1. *I-V Characteristics* (*Mixer level*)

A brief re-examination of the *I-V* characteristics of the bonded backward diode related to mixer applications is worthwhile considering. For this purpose a typical characteristic only is reproduced in Fig. 5. However, in the following discussion the r.f. performance of backward diodes exhibiting different

values of peak currents is considered. Figure 5 compares the characteristics of a bonded backward diode with a conventional silicon point-contact diode. A local-oscillator swing is shown diagrammatically at zero bias. The characteristics show very clearly the advantages of the backward diode compared with a conventional mixer as regards conduction in the forward direction, thus indicating the ability of the backward diode to rectify efficiently, with consequent high conversion efficiency, at smaller input powers than a conventional diode, provided of course that the product $C_B r$ is of the right order for microwave frequencies. However, by examination of the reverse characteristic, limitation on dynamic range for the backward diode is also clearly indicated. Too large an increase in local-oscillator power will result in excessive reverse-current leakage and consequently an increase in the noise temperature ratio characteristic coupled with degradation in conversion loss.

The backward-diode characteristic also reveals that no extensive benefit may be derived from the use of bias. Forward bias at constant local-oscillator power will result in power being dissipated in the spreading resistance, thus degrading the conversion loss, and a large reverse bias will result in excessive reverse-current leakage. Optimum performance thus occurs at about zero bias conditions.

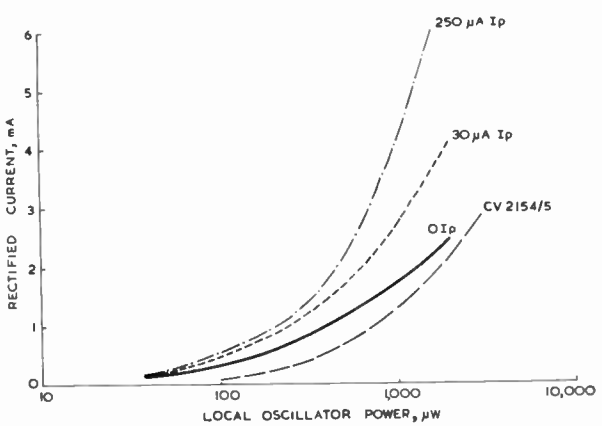

Fig. 6. Rectified current as a function of local-oscillator power.

6.2. *R.F. Performance*

The r.f. performance of the bonded backward diode for mixer applications is next illustrated. The relative merits of backward diodes representative of negligible peak current (0 I_p), 30 μA peak current (30 μA I_p) and 250 μA peak current (250 μA I_p) devices are considered and where possible comparison is made with a conventional silicon mixer diode, of the CV2154/5 type.

6.2.1. Rectification efficiency

Figure 6 compares the relative rectification efficiencies at X-band frequencies. The ability of the backward diode to rectify more efficiently at low r.f. powers compared with the conventional diode is clearly shown. Comparing the backward diodes, the improved rectification efficiency at high power levels in relation to the diode peak current is of interest and in accordance with their *I-V* characteristics (Fig. 1).

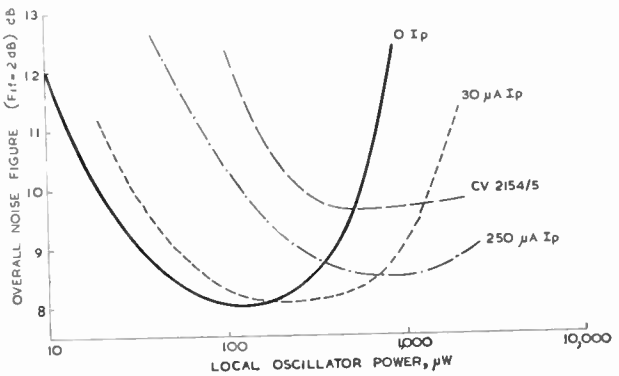

Fig. 7. Overall noise figure as a function of local-oscillator power (i.f. = 45 Mc/s).

6.2.2. Overall noise figure (i.f. = 45 Mc/s)

Figure 7 shows the overall noise figure performance at an intermediate frequency of 45 Mc/s as a function of local-oscillator power. Overall noise figure is quoted at X-band frequencies in conjunction with a 45-Mc/s i.f. amplifier with a noise figure of 2 dB. The superiority of the backward diode compared with the conventional diode under conditions of limited local-oscillator power is clearly shown. Further, the noise figure performance of about 8 dB at optimum conditions is comparable with the majority of present low-noise X-band mixer diodes. Comparing the performance of the backward diodes, the better dynamic range of a high peak current diode, but greater ability of a low peak current diode to operate with limited local-oscillator power is demonstrated. This relation between optimum local-oscillator power, dynamic range and diode peak current is of great interest and shows the necessity for optimizing the backward diode characteristics for a particular application. Typical values of conversion loss at optimum local-oscillator drive are similar for the three types of backward diode characteristics, i.e. about 5 dB. Values of noise temperature ratio at the intermediate frequency of 45 Mc/s are about 1·2, 1·4 and 1·8 for the 0 I_p, 30 μA I_p and 250 μA I_p diodes respectively.

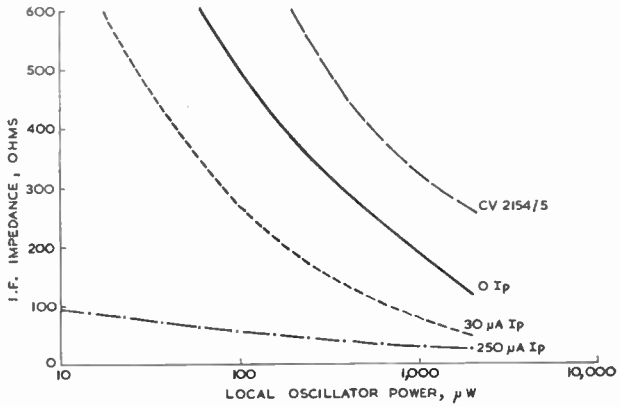

Fig. 8. I.f. impedance as a function of local-oscillator power.

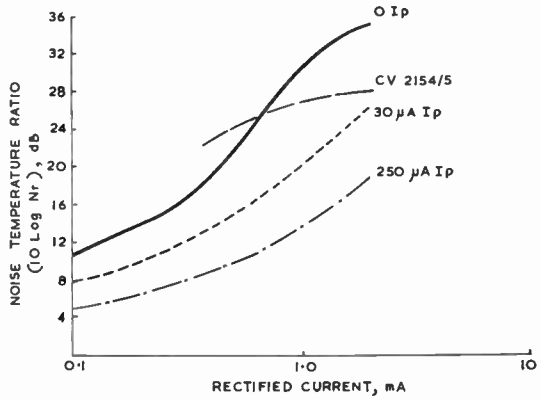

Fig. 9. Noise temperature ratio (i.f. = 3 kc/s) as a function of diode rectified current.

6.2.3. I.F. impedance

Figure 8 shows the i.f. impedance of these devices as a function of local-oscillator drive. The lower i.f. impedance of the backward diodes compared with a conventional diode is emphasized by the high peak current device, which would certainly necessitate a modified i.f. amplifier input design compared with conventional mixer diodes.

6.2.4. Doppler performance

These diodes are next assessed for Doppler applications where performance at audio intermediate frequencies is of interest. Figure 9 examines noise temperature ratio measured at 3 kc/s as a function of rectified current. The results illustrate the potential low flicker-noise properties obtainable with the backward diode compared with a conventional silicon mixer diode of the CV2154/5 type, and indicate the relation between these properties and the peak current of the backward diode. Further, the dependency of low-frequency noise on rectified current is shown, illustrating the necessity of low drive to take full advantage of the flicker noise properties of the backward diode, which may be accomplished in the case of the backward diode and still preserve a high conversion efficiency. However, this does of course imply a poor dynamic range, which is demonstrated more effectively in Fig. 10, where conversion loss at X-band frequencies has been taken into account and receiver noise figure as a function of local-oscillator power is shown. The results show that optimum performance is obtained at about 50 μW local oscillator power for the three types of backward diode, but substantiate the superiority of the high peak current device, especially as regards dynamic range.

The performance of these devices is finally summarized in Fig. 11, by illustrating receiver noise figure at X-band frequencies as a function of intermediate frequency. In general, the conversion loss of mixer diodes is independent of receiver intermediate

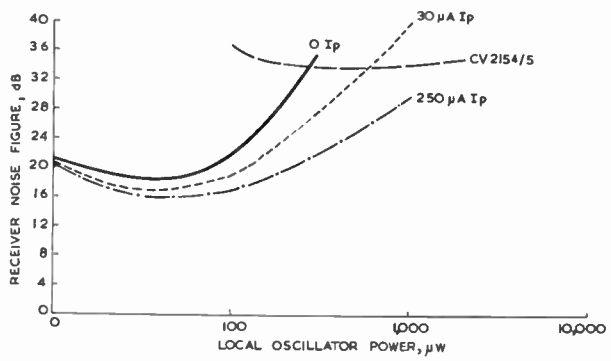

Fig. 10. Noise figure performance (i.f. = 3 kc/s) as a function of local-oscillator power.

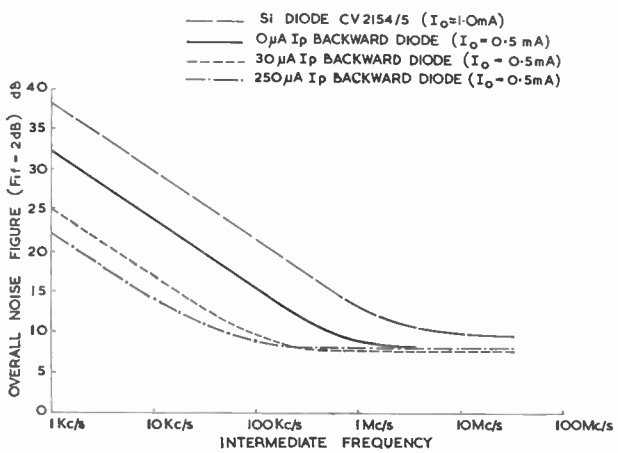

Fig. 11. X-band receiver overall noise figure performance as a function of intermediate frequency.

frequency, but due to the flicker noise contribution to the noise temperature characteristic, the overall noise figure of the receiver deteriorates as the intermediate frequency is reduced. The diodes were assessed at a constant rectified current of 0·5 mA. A significant improvement is thus obtained in performance at audio frequencies with use of the backward diode. In fact, a potential improvement in some Doppler systems of almost 20 dB is likely. It is also of interest to note the improved performance of the high peak current diode, which is only degraded by about 9 dB at 3 kc/s compared with 45 Mc/s intermediate frequencies.

The experimental evidence is of sufficient interest to suggest future work to explore the potential of backward diodes with increased values of peak current. Thus the possibilities of an alloyed junction should not be excluded for this particular application. As already implied, a larger capacitance may be tolerated for mixer applications of a backward diode due to the inherent low spreading resistance. The larger area junction suggests decreased current density and thus flicker noise and, although the associated capacitance will certainly imply an increase in conversion loss, this may well be compensated by a decrease in noise temperature ratio. However, the disadvantage of an alloyed structure is the control of the parameters of the equivalent circuit, i.e. barrier capacitance, barrier resistance, case inductance etc. Control of these is essential to achieve an r.f. impedance compatible with a particular application, e.g. waveguide, coaxial or stripline, and to maintain a close spread in r.f. impedance between units, for use with pre-tuned mounts of the modern radar system.

7. Broadband Detector VX6507

The VX6507 is an example of a bonded backward diode under development primarily for use as a low-level detector at X-band frequencies. The specific requirements for this device favoured the coaxial-type construction and zero-bias operation. This final section is intended to illustrate the performance of this device for detector and mixer applications.

The VX6507 is representative of a 30 μA peak current device already discussed in this paper.

7.1. *Video Detector Performance*

The histogram of Fig. 12 shows the result of measurements at X-band frequencies of tangential sensitivity for a 1-Mc/s video bandwidth and comparison is made with a biased conventional detector. An improvement of about 5 dB is achieved by use of the VX6507. Typical values of current sensitivity, video impedance and 'figure of merit' are 10 μA/μW, 800 Ω and 250 respectively.

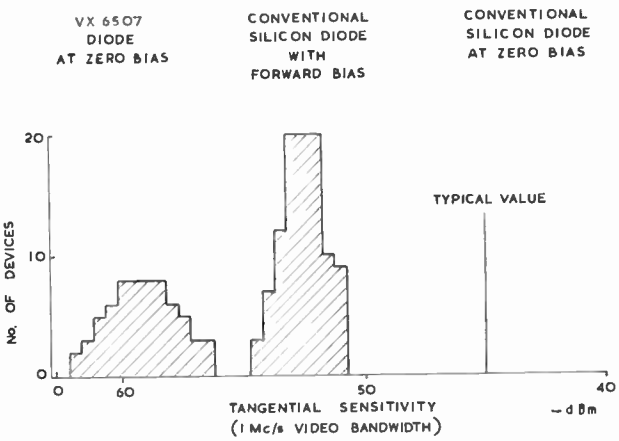

Fig. 12. Histogram of tangential sensitivity performance. VX6507. (f = 9375 Mc/s. Video bandwidth = 1 Mc/s).

The broadband characteristics are demonstrated in Fig. 13, which shows the r.f. admittance with respect to 1/68 mhos for a frequency range up to 10·7 Gc/s, at zero bias and with a forward bias current of 60 μA.

7.2. *Mixer Performance*

The design of the VX6507 is such that at mixer level at X-band frequencies, a similar r.f. admittance to that of the CV2154/5 and CV7108/9 type coaxial mixer diodes is achieved. This ensures interchangeability with conventional coaxial mixer diodes in existing equipments. The histogram of Fig. 14 shows the results of measurements at X-band frequencies of overall noise figure in conjunction with a 45-Mc/s i.f. amplifier with a noise figure of 2 dB. The test mount was a standard CV2154/5 type and the VX6507 diodes were measured at a rectified current of 0·6 mA, which corresponds to about 150 μW local oscillator power. The noise figure performance of 8·0 dB typical is about 1·5 dB better than that obtained for the CV2154/5 and comparable with the low noise types CV7108/9. The typical i.f. impedance is about 250 Ω under these conditions of local oscillator drive.

For Doppler applications, the overall noise figure performance at X-band frequencies with a 3 kc/s i.f. amplifier is about 20 dB at 0·5 mA drive, i.e. an improvement of about 15 dB compared with the CV2154/5.

7.3. *Temperature Dependency*

The VX6507 has a design operation temperature range of −55°C to 150°C. The dependency of mixer performance on temperature is shown in Fig. 15 which illustrates overall noise figure performance over the temperature range −60°C to 100°C. Comparison is made with the CV2154/5 and the improved temperature performance of the VX6507 is clearly indicated. The dependency of detector performance

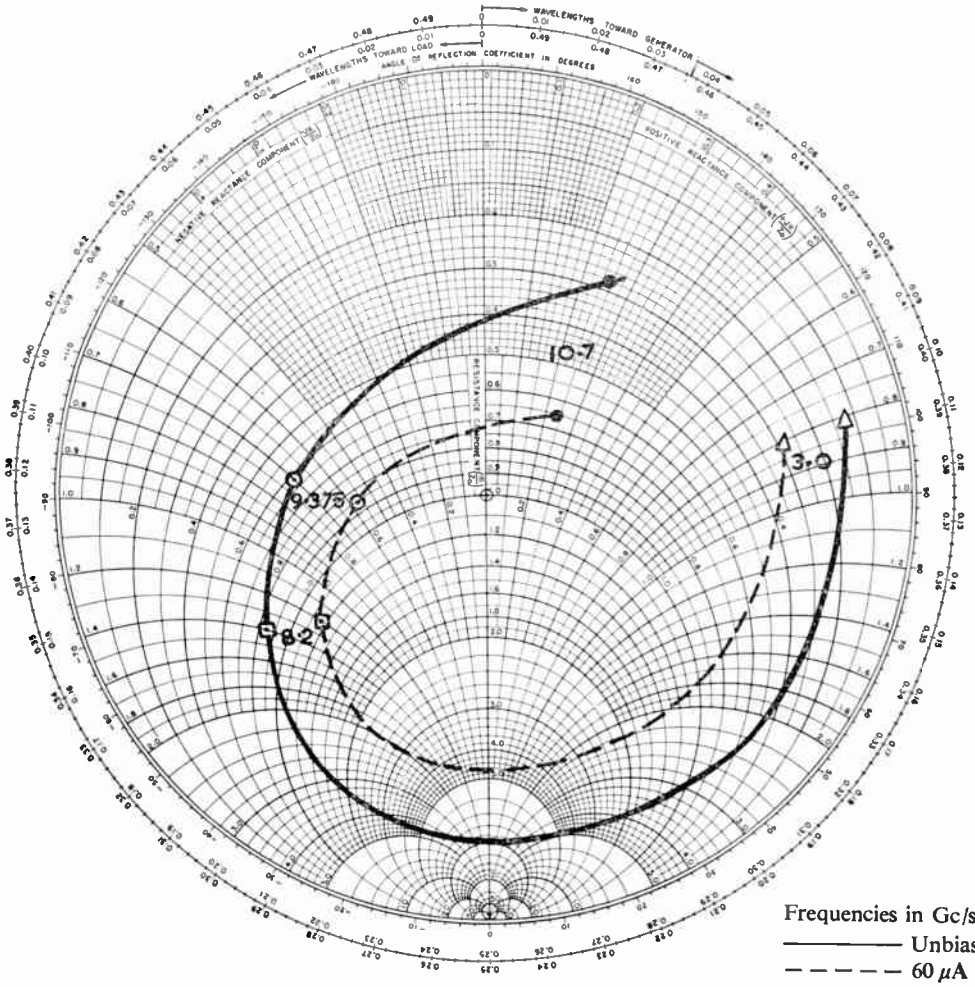

Fig. 13. R.f. admittance as a function of frequency. VX6507.

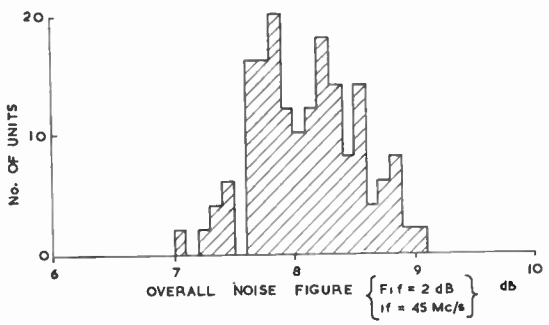

Fig. 14. Histogram of overall noise figure performance. VX6507. ($F_{i.f.}$ = 3·4 dB).

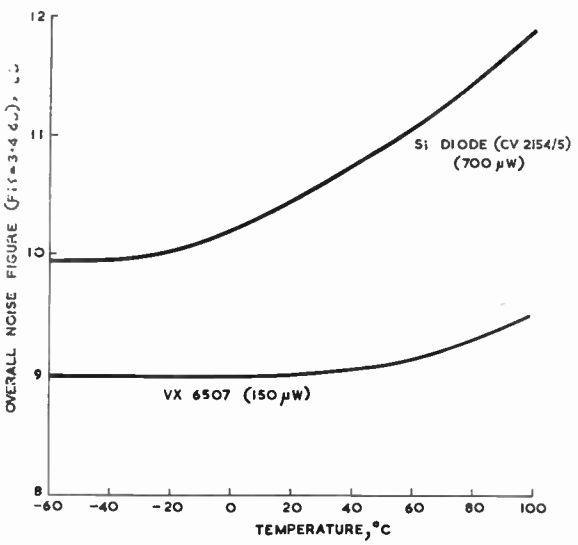

Fig. 15. Overall noise figure as a function of temperature. VX6507.

is shown in Fig. 16, which shows zero-bias video impedance in the temperature range 20°C to 150°C and indicates a deterioration in tangential sensitivity of about 2 dB at 150°C compared with room temperature (Fig. 3).

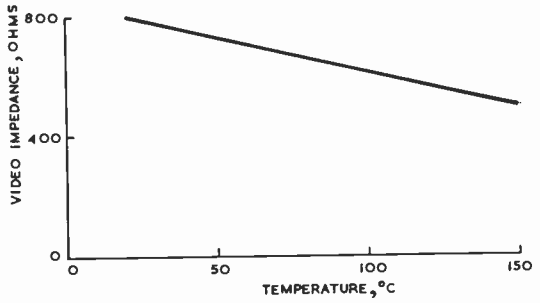

Fig. 16. Video impedance as a function of temperature. VX6507.

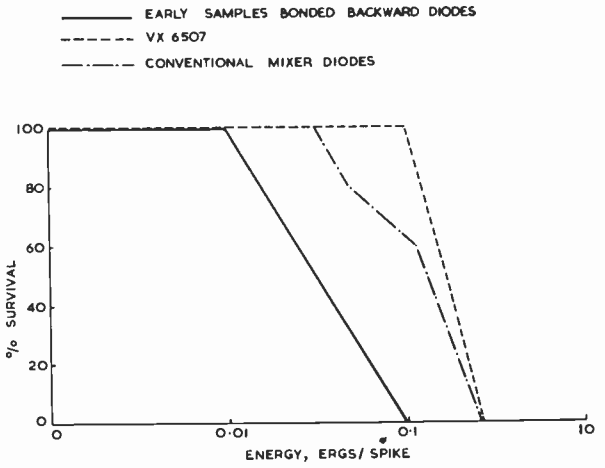

Fig. 17. Burn-out performance. VX6507. Multiple d.c. spikes. Survival curves.

7.4. *Burn-out Performance*

The principal requirement for resistance to burn-out of mixer diodes is the ability to withstand spike leakage from a t/r cell, and Fig. 17 examines the burn-out performance of the VX6507 as assessed by d.c. spikes. The results are presented as survival curves for multiple d.c. spike tests normally specified for mixer diodes, i.e. 5000 spikes at increasing energy levels, the criterion for burn-out being a deterioration in noise figure performance of 1 dB or greater. Comparison is made with conventional X-band mixer diodes and results obtained with earlier types of bonded backward diodes are included. As shown, earlier work[3] had suggested that bonded backward diodes were inferior to conventional mixer diodes in this respect. However, improvements in fabrication processes and production of larger junction area devices have increased their resistance to burn-out and the VX6507 is considered at least comparable with conventional diodes. Further, long-duration d.c. tests have shown no change in parameters for number of spikes in excess of 10^6 at a level of 0·1 ergs/spike, which again compares very favourably with conventional mixer diodes.

For microwave diodes not protected by t/r switches, such as video detectors, overloads encountered consist of microsecond pulses and it is the pulse peak power rather than the pulse energy that determines the extent of burn-out. In the case of detectors it is normally the change in r.f. admittance that is specified as the criterion for burn-out. Tests with 0·5 μs pulses at a repetition rate of 1000 pulses/second have indicated a burn-out level for the VX6507 of about 0·6 W peak, with a safe design limit of about 100 mW peak.

7.5. *Mechanical Performance*

The VX6507 will meet normal environmental and mechanical requirements specified for conventional microwave diodes. Although earlier samples of bonded backward diodes exhibited poor mechanical stability characteristics,[3] improvements in fabrication technology and mechanical design have resulted in successful fabrication of rugged backward diodes of this type.

8. Conclusions

It has been shown that pulse-bonded germanium backward diodes may be fabricated which achieve substantial improvements in performance compared with conventional point-contact diodes for such microwave applications as low-level detectors, mixers under conditions of limited local-oscillator power, and Doppler mixers. A relation between r.f. performance for these different applications and the diode characteristics has been illustrated, also the diode may be optimized during the fabrication process for a given requirement. It has been shown that, although higher values of capacitance can be tolerated which, due to the low spreading resistance, may be of benefit for burn-out considerations and Doppler mixers, in detector applications, a low barrier capacitance is required for high sensitivity and bandwidth requirements. This implies the necessity for optimizing a backward diode for a particular application. The optimum characteristics substantially agree for both detector and low-power mixers and a backward diode under development primarily as a detector has substantiated this work.

The backward diode has been shown to exhibit potential low flicker noise properties, and improvements, coupled with increased dynamic range, may be

achieved by optimizing the diode for these aspects. However, further investigation here is needed to establish its full potential as a Doppler mixer diode, with more attention to diodes having higher peak currents than those discussed in this paper. With these devices it will be possible to examine the effect of the valley current which has not yet been considered.

The resistance to a spike burn-out of the bonded backward diode is considered to be comparable with conventional mixer diodes as assessed by d.c. spike tests.

9. References

1. S. T. Eng, 'Low-noise properties of microwave backward diodes', *Trans. Inst. Radio Engrs on Microwave Theory and Techniques*, **MTT-9**, No. 5, pp. 419–24, September 1961.
2. C. A. Burns, Jr., 'Backward diodes for low-level millimeter-wave detection', *Trans. Inst. Elect. Electronics Engrs on Microwave Theory and Techniques*, **MTT-11**, No. 5, pp. 357–62, September 1963.
3. T. H. Oxley, 'Backward diodes as mixers at microwave frequencies', *J. Electronics Control*, **17**, No. 1, pp. 1–17, July 1964.
4. H. V. Shurmer, 'Backward diodes as microwave detectors', *Proc. Instn Elect. Engrs*, **111**, No. 9, pp. 1511–16, September 1964. (I.E.E. Paper No. 4536E.)
5. H. C. Torrey and C. A. Whitmer, 'Crystal Rectifiers', (McGraw-Hill, New York, 1948.)
6. J. H. Frohmaier, 'Noise performance of a three-stage microwave receiver', *Electronic Technology*, **37**, p. 245, June 1960. (Letter.)

Manuscript received by the Institution on 17th May 1965. (Paper No. 1033.)

STANDARD FREQUENCY TRANSMISSIONS

(Communication from the National Physical Laboratory)

Deviations, in parts in 10^{10}, from nominal frequency for **February 1966**

February 1966	GBZ 19·6 kc/s 24-hour mean centred on 0300 U.T.	MSF 60 kc/s 1430–1530 U.T.	Droitwich 200 kc/s 24-hour mean centred on 0300 U.T.	February 1966	GBZ 19·6 kc/s 24-hour mean centred on 0300 U.T.	MSF 60 kc/s 1430–1530 U.T.	Droitwich 200 kc/s 24-hour mean centred on 0300 U.T.
1	—	− 301·2	—	15	− 300·5	− 300·1	+ 0·7
2	− 297·7	− 301·1	—	16	− 293·8	− 299·8	+ 0·5
3	− 299 5	− 301·4	+ 0·3	17	− 300·1	− 300·2	+ 0·3
4	− 298·7	− 301·2	+ 0·5	18	− 300 0	− 300·2	+ 0·3
5	− 299·4	− 300·9	+ 0·4	19	− 298 9	− 300·5	+ 0·1
6	− 298·5	− 300·9	0	20	− 299 0	− 300 7	− 0·9
7	− 298·6	− 300·7	− 0·1	21	− 301 0	− 301·8	− 1·1
8	− 299·4	− 301·3	+ 0·1	22	− 299·5	− 301·3	− 1·1
9	− 300·4	− 301·6	+ 0·1	23	− 301 9	− 299 6	− 0·5
10	− 298·6	− 299 2	+ 0·2	24	− 300·1	− 299·7	− 0·4
11	− 299·5	− 300·4	+ 0·9	25	− 298 5	− 299·4	− 0·5
12	− 298·9	—	+ 1·2	26	− 300 7	− 300·4	− 1·1
13	− 299·5	—	+ 0·9	27	− 301·4	− 300·7	− 1·0
14	− 300·0	− 299·9	+ 0·9	28	300·6	− 300·7	− 1·2

Nominal frequency corresponds to a value of 9 192 631 770·0 c/s for the caesium $F,m\ (4,0)$–$F,m\ (3,0)$ transition at zero field.

Note: GBR Rugby has been replaced temporarily by GBZ Criggion.

Radio Engineering Overseas . . .

The following abstracts are taken from Commonwealth, European and Asian journals received by the Institution's Library. Abstracts of papers published in American journals are not included because they are available in many other publications. Members who wish to consult any of the papers quoted should apply to the Librarian, giving full bibliographical details, i.e. title, author, journal and date, of the paper required. All papers are in the language of the country of origin of the journal unless otherwise stated. Translations cannot be supplied.

MICROWAVE REFRACTOMETER

The author of a German paper describes a microwave refractometer which permits a digital measurement of the complex refractive index of gases with a high sensitivity, stability, and time resolution. It is used in the frequency range 3 to 14 Gc/s for the investigation of quasi-tropospheric mixtures of air and water vapour. Results are obtained which cover the relationship between the refractive index and the density, the interfering effect of water vapour adsorption at the boundaries of the waveguide resonator indicator, and the diffusion by mixing polar water vapour with apolar components of the air.

Special measures are required (such as pressure-time control) for the determination of the gas pressure with the accuracy appropriate to the resonance resolution.

'A digital microwave refractometer for gases', H. J. Liebe, *Nachrichtentechnische Zeitschrift*, **18**, No. 9, pp. 510–18, September 1965.

FRENCH NETWORK OF STATIONS FOR SATELLITE TRACKING

The French electronics industry in 1965 completed the task of producing a network of stations (named *Diane*) concerned with tracking, telemetry and remote control of satellites. A series of papers published in the January 1966 issue of *L'Onde Electrique* describes the various aspects of the work.

The reasons for the choice of frequency range 136–138 Mc/s and interferometry as a method of tracking are first explained.[1] The second paper examines the problems which must be met in a satellite tracking station and describes the basis of the measurements which are made and the reasons for the choice of technical methods used.[2]

Further, an account of the special technical requirements arising in connection with interferometry antennas for the stations is given and the choice of polarization determined by the problem of ground reflections is explained.[3] The necessity for the use of slots is mentioned, their operation is examined qualitatively and the effect of the dimensional parameters is considered experimentally. The design of the auxiliary antennas intended to remove the inherent ambiguity of this type of interferometry measurements is described.

The network of coaxial cables some 2000 metres in length forms the subject of a further paper.[4] These cables are used to convey information to the intelligence centre from incoming aerial signals received from a satellite. In order that the position of a satellite at any instant should be precisely defined, it is necessary that there should be no risk of phase-shift in the received signals. The article describes the specification of the coaxial cable which has been used in the stations of the *Diane* network. Emphasis is placed on the very high accuracy of manufacture and of measurement and on the self-compensatory characteristics of the phase coefficient in these cables as a function of temperature variation.

1. 'Principles and general characteristics of ground stations' by J. Saint-Etienne. (pp. 8–13.)

2. '*Diane* satellite tracking stations' by C. Michaud. (pp. 14–19.)

3. 'Interferometry antennas in the *Diane* stations' by C. Ancona. (pp. 20–29.)

4. 'Phase compensated coaxial cable for an interferometer goniometer' by J. Orsini and R. Jocteur. (pp. 30–41.)

L'Onde Electrique, **46**, No. 466, January 1966.

A NEW COLOUR TELEVISION SYSTEM

The author of a Czechoslovakian paper states the basic principles, arrangements and advantages of the new DST (dot sequential transmission) system of colour television, as designed and experimentally verified in the Research Institute for Broadcasting and Television in Prague. The DST system uses frequency modulation for the transmission of colour information, thus rendering the system insensitive towards non-linear distortion originating from differential gain and differential phase. In contrast to the SECAM system the present one does not need an ultrasonic delay line in the colour television receiver decoder.

'The DST colour television system', M. Ptáček, *Slaboproudy Obzor*, **26**, No. 9, pp. 505–13, 1965.

ELECTRON PATH PLOTTING

The author of this German paper describes equipment which permits automatic calculation of electron paths, field lines, and equipotential lines in rotary symmetrical electrostatic fields. The field distribution is simulated by a network of resistances. The equipment addresses individual points of the resistance network while being controlled by progressing co-ordinate values; it measures the field strength components at these points, and integrates these components by digital methods.

Tests with a homogeneous and centralized field have yielded an error of approximately 0·1% with reference to the length of the calculated curve.

'Novel equipment for the calculation of electron paths by means of a resistance network and a virtual probe', T. Onciul, *Nachrichtentechnische Zeitschrift*, **18**, No. 3, pp. 124–29, March 1965.